USER'S GUIDE

of

TOUGH2-EGS-MP: A Massively Parallel Simulator with Coupled Geomechanics for Fluid and Heat Flow in Enhanced Geothermal Systems

VERSION 1.0

Yi Xiong

Perapon Fakcharoenphol

Shihao Wang

Philip H. Winterfeld

Keni Zhang

Yu-Shu Wu

Petroleum Engineering Department

Colorado School of Mines,

1500 Illinois Street,

Golden, CO 80401 USA

December 2013

This work was supported by the U.S. Department of Energy "Development of Advanced Thermal-Hydrological-Mechanical-Chemical (THMC) Modeling Capabilities for Enhanced Geothermal Systems" under Contract No. DE-EE0002762 and by Foundation CMG.

ABSTRACT

TOUGH2-EGS-MP is a parallel numerical simulation program coupling geomechanics with fluid and heat flow in fractured and porous media, and is applicable for simulation of enhanced geothermal systems (EGS). TOUGH2-EGS-MP is based on the TOUGH2-MP code, the massively parallel version of TOUGH2. In TOUGH2-EGS-MP, the fully-coupled flow-geomechanics model is developed from linear elastic theory for thermo-poro-elastic systems and is formulated in terms of mean normal stress as well as pore pressure and temperature. Reservoir rock properties such as porosity and permeability depend on rock deformation, and the relationships between these two, obtained from poro-elasticity theories and empirical correlations, are incorporated into the simulation.

This report provides the user with detailed information on the TOUGH2-EGS-MP mathematical model and instructions for using it for Thermal-Hydrological-Mechanical (THM) simulations. The mathematical model includes the fluid and heat flow equations, geomechanical equation, and discretization of those equations. In addition, the parallel aspects of the code, such as domain partitioning and communication between processors, are also included. Although TOUGH2-EGS-MP has the capability for simulating fluid and heat flows coupled with geomechanical effects, it is up to the user to select the specific coupling process, such as THM or only TH, in a simulation.

There are several example problems illustrating applications of this program. These example problems are described in detail and their input data are presented. Their results demonstrate that this program can be used for field-scale geothermal reservoir simulation in porous and fractured media with fluid and heat flow coupled with geomechanical effects.

TABLE OF CONTENTS

LIST OF FIGURES

LIST OF TABLES

1 INTRODUCTION

The geomechanical behavior of fractured and porous media reservoirs is important for understanding fluid and heat flow coupled with stress induced phenomena, such as formation subsidence, stress induced change in reservoir properties, and borehole failure. Numerical modeling of efficient coupled fluid flow and geomechanics is complex, and has been carried out historically in three separate areas: geomechanical modeling, reservoir simulation, and fracture mechanics (Setari et al., 2000; Setari and Walters, 2001; Longuemare et al., 2002).

Most geothermal reservoir simulation studies have involved solving fluid and heat flow equations (e.g., Mercer et al. 1974; Thomas and Pierson, 1978; Pruess, 1991) but had little coupling with geomechanical effects. TOUGH2 (Pruess et al., 1999) is a general-purpose numerical simulator for multi-dimensional fluid and heat flow of multiphase, multi-component fluid mixtures in porous and fractured media. It provides a flexible and comprehensive framework for EGS reservoir simulation. TOUGH2-MP (Zhang et al., 2008) is the massively parallel version of TOUGH2; it provides both TOUGH2 simulation and parallel computing capabilities. Based on the framework of TOUGH2-MP, TOUGH2-EGS-MP has been developed and it couples geomechanical effects with fluid and heat flow for EGS reservoirs. The massively parallel computing has been implemented with Message Passing Interface (MPI; Message Passing Forum,1994) technology, which enables multiple processors to simultaneously solve the equations and achieve higher performance. TOUGH2-EGS-MP is programmed with standard Fortran90, and can be compiled and run on different platforms and operating systems, including desktop Windows PCs and clusters with Linux. Although TOUGH2-EGS-MP was designed for parallel computing with multiple processors, the code can still provide gains in computational efficiency for single processor machines by executing multiple MPI processes. The code has been tested on both desktop Windows PCs and Linux clusters; the results demonstrated significant gains in computing efficiency for multi-core PCs and Linux clusters with several tens to hundreds of processors.

This report provides a comprehensive description of the mathematical formulation, numerical methods, parallel computing environment and specifications for preparing input data for TOUGH2-EGS-MP, along with illustrative sample problems. Section 2 covers the mathematical model including the derivation and discussion of the governing mass, energy

and stress equations. Section 3 discusses the numerical discretization, the simulation procedures, the parallel computing and organization of thermo-physical and stress arrays, in order to assist the user for understanding the program implementation. Section 4 provides the instructions for building and running TOUGH2-EGS-MP on PCs and clusters. Section 5 contains the detailed description of TOUGH2-EGS-MP input data and input files. Section 6 presents example problems, including analytical verification for the geomechanical model, applications for EGS reservoirs and computing performance analysis.

2 MATHEMATICAL MODEL

2.1 Formulation of fluid and heat flow

The TOUGH2-EGS-MP simulator is based on a general mathematical and numerical framework, and solves mass and energy balance equations describing fluid and heat flow in multiphase, multi-component systems coupled with geomechanics. Fluid flow is described with a multiphase extension of Darcy's law; in addition, there is diffusive mass transport in all phases. Heat flow is governed by conduction and convection, also including sensible as well as latent heat effects. Following Pruess et al. (1999), the governing mass and heat balance equations in each subdomain or REV (Representative Elementary Volume) of an EGS reservoir can be written in the form:

$$\frac{d}{dt}\int_{V_n}\mathbf{M}^{\kappa}dV_n = \int_{\Gamma_n}\mathbf{F}^{\kappa}\bullet\mathbf{n}d\Gamma_n + \int_{V_n}q^{\kappa}dV_n \qquad (2.1)$$

where κ = 1, ..., NK (total number of components) and n =1,…, NEL (total number of grid blocks).

The integration in Equation 2.1 is over an arbitrary subdomain V_n of the flow system under study, bounded by the closed surface Γ_n. The quantity $\boldsymbol{M}$ appearing in the accumulation term (left hand side) represents mass or energy per volume, $\boldsymbol{F}$ denotes mass or heat flux, and q denotes sinks and sources. $\boldsymbol{n}$ is a normal vector on surface element $d\Gamma_n$, pointing inward into V_n.

The terms in Equation 2.1, mass accumulation, flux, source, and sink are calculated at each Newton iteration step. The general form of the mass accumulation term is:

$$M^{\kappa} = \sum \phi S_{\beta}\rho_{\beta}X_{\beta}^{\kappa} \qquad (2.2)$$

where κ = 1, ..., *NK*, and β=*1, …NPH* (total number of phases). ϕ is effective porosity, ρ_{β} is density of phase β, S_{β} is the saturation of phase β, and X_{β}^{κ} is the mass fraction of component κ in phase β. Before the calculation of mass accumulation, the parameters on the right hand side of Equation 2.2 are calculated as functions of primary and secondary variables.

The heat accumulation term includes contributions from the rock matrix, aqueous and gaseous phases, and is given by:

$$M^{\kappa} = (1-\phi)\rho_R C_R T + \phi \sum_{\beta} S_{\beta}\rho_{\beta} u_{\beta} \tag{2.3}$$

$\kappa = NK+1$ (NK+1 denotes the heat component) and β=1,…, NPH. Here ρ_R and C_R are grain density and specific heat of the host rock, respectively, T is temperature, and u_{β} is specific internal energy in phase β.

The mass fluxes of aqueous and gaseous phases are determined by a multiphase version of Darcy's law, written in the form:

$$F_{\beta} = -k_0\left(1+\frac{b}{P_{\beta}}\right)\frac{k_{r\beta}\rho_{\beta}}{\mu_{\beta}}(\nabla P_{\beta} - \rho_{\beta}\boldsymbol{g}) \tag{2.4}$$

$$\beta = 1,\ldots, NPH$$

Advective mass flux is a sum over phases:

$$F^{\kappa}\Big|_{adv} = \sum_{\beta} X_{\beta}^{\kappa} F_{\beta} \tag{2.5}$$

where k_0 is absolute permeability, b is the Klinkenberg factor (Klinkenberg, 1941) for gas slippage effect (b=0 when β=aqueous phase), $k_{r\beta}$ is relative permeability to phase β, μ_{β} is viscosity, P_{β} is pressure in the β phase, and $\boldsymbol{g}$ is the vector of gravitational acceleration. The diffusive fluxes are evaluated by the formulation:

$$J_{\beta}^{\kappa} = -\phi\tau_{\beta}\rho_{\beta} d_{\beta}^{\kappa} \nabla X_{\beta}^{\kappa} \tag{2.6}$$

where d_{β}^{κ} is the molecular diffusion coefficient for component κ in phase β, τ_{β} is the tortuosity which is a function of rock property and phase saturation, and X_{β}^{κ} is mass fraction of component κ in phase β.

The heat flux term accounts for conduction, advection and heat transfer by radiation, and is given by:

$$F^{\kappa} = -[(1-\phi)K_R + \phi \sum_{\beta=1,2,3} S_\beta K_\beta]\nabla T + f_\sigma \sigma_0 \nabla T^4 + \sum_{\beta=1,2} h_\beta F_\beta \quad (2.7)$$

where K_R is thermal conductivity of the rock, K_β is thermal conductivity of phase β, T is temperature, h_β is specific enthalpy of phase β, f_σ is radiant emittance factor, and σ_0 is the Stefan-Boltzmann constant.

2.2 Formulation of geomechanics in porous medium

This new coupling method assumes that boundaries of each block element can move as an elastic material and obey the generalized Hooke's law. The mean normal stress is selected as an additional primary variable in the model.

Under the assumption of linear elasticity with small strains in a thermo-poro-elastic system, Hooke's law can be expressed in three dimensionals as follows (Jaeger et al., 2007)

$$\sigma_{kk} - \left[\alpha P + 3\beta K(T - T_{ref})\right] = 2G\varepsilon_{kk} + \lambda(\varepsilon_{xx} + \varepsilon_{yy} + \varepsilon_{zz}), k = x, y, z \quad (2.8)$$

where σ is the normal stress, α is the Biot's coefficient, β is the linear thermal expansion coefficient, K is the bulk modulus, λ is the Lame's constant, G is the shear modulus, and ε is the strain. The subscript k stands for the directions. Summing over the x, y and z components of Equation 2.8 gives the following:

$$\frac{\sigma_{xx} + \sigma_{yy} + \sigma_{zz}}{3} - \alpha P - 3\beta K\left(T - T_{ref}\right) = \left(\lambda + \frac{2}{3}G\right)\left(\varepsilon_{xx} + \varepsilon_{yy} + \varepsilon_{zz}\right) \quad (2.9)$$

Rewriting Equation 2.9 with mean normal stress and volumetric strain yields:

$$\sigma_m - \alpha P - 3\beta K\left(T - T_{ref}\right) = \left(\lambda + \frac{2}{3}G\right)\varepsilon_v \quad (2.10)$$

where σ_m and ε_v are the mean normal stress and volumetric strain, respectively.

One fundamental relation in linear elasticity theory is that between strain and displacement

vector, *u*. The displacement vector points from the new position of a volume element to its previous one. The strain tensor is related to the displacement vector by:

$$\overline{\overline{\varepsilon}} = \frac{1}{2}\left[\nabla\bar{u} + (\nabla\bar{u})^T\right] \tag{2.11}$$

which can be also written as:

$$\varepsilon_{jk} = \frac{1}{2}\left[\frac{\partial u_k}{\partial x_j} + \frac{\partial u_j}{\partial x_k}\right], (k, j) = x, y, z; x_l = x, y, z \tag{2.12}$$

Another fundamental relation is the static equilibrium condition:

$$\nabla \cdot \overline{\overline{\sigma}} + \bar{F} = 0 \tag{2.13}$$

where $\overline{\overline{\sigma}}$ is the stress tensor and $\bar{F}$ is the body force vector.

Substituting Equation 2.8 into Equation 2.12 leading to the three explicit equations:

$$\alpha\frac{\partial P}{\partial x} + 3\beta K\frac{\partial T}{\partial x} + 2G\frac{\partial \varepsilon_{xx}}{\partial x} + \lambda\frac{\partial(\varepsilon_{xx}+\varepsilon_{yy}+\varepsilon_{zz})}{\partial x} + 2G\frac{\partial \varepsilon_{yx}}{\partial y} + 2G\frac{\partial \varepsilon_{zx}}{\partial z} + F_x = 0 \tag{2.14}$$

$$\alpha\frac{\partial P}{\partial y} + 3\beta K\frac{\partial T}{\partial y} + 2G\frac{\partial \varepsilon_{yy}}{\partial y} + \lambda\frac{\partial(\varepsilon_{xx}+\varepsilon_{yy}+\varepsilon_{zz})}{\partial y} + 2G\frac{\partial \varepsilon_{yx}}{\partial x} + 2G\frac{\partial \varepsilon_{yz}}{\partial z} + F_y = 0 \tag{2.15}$$

$$\alpha\frac{\partial P}{\partial z} + 3\beta K\frac{\partial T}{\partial z} + 2G\frac{\partial \varepsilon_{zz}}{\partial z} + \lambda\frac{\partial(\varepsilon_{xx}+\varepsilon_{yy}+\varepsilon_{zz})}{\partial z} + 2G\frac{\partial \varepsilon_{yz}}{\partial y} + 2G\frac{\partial \varepsilon_{xz}}{\partial x} + F_z = 0 \tag{2.16}$$

Using Equation 2.11 and Equations 2.14-16, the following equations in terms of the displacement vector are obtained:

$$\alpha\frac{\partial P}{\partial x} + 3\beta K\frac{\partial T}{\partial x} + (2G+\lambda)\frac{\partial^2 u_x}{\partial x^2} + \lambda\frac{\partial^2 u_y}{\partial x\partial y} + \lambda\frac{\partial^2 u_z}{\partial x\partial z} + G\left(\frac{\partial^2 u_x}{\partial y^2} + \frac{\partial^2 u_y}{\partial x\partial y}\right) + G\left(\frac{\partial^2 u_x}{\partial z^2} + \frac{\partial^2 u_z}{\partial x\partial z}\right) + F_x = 0 \tag{2.17}$$

$$\alpha\frac{\partial P}{\partial y} + 3\beta K\frac{\partial T}{\partial y} + (2G+\lambda)\frac{\partial^2 u_y}{\partial y^2} + \lambda\frac{\partial^2 u_x}{\partial x\partial y} + \lambda\frac{\partial^2 u_z}{\partial y\partial z} + G\left(\frac{\partial^2 u_y}{\partial x^2} + \frac{\partial^2 u_x}{\partial x\partial y}\right) + G\left(\frac{\partial^2 u_y}{\partial z^2} + \frac{\partial^2 u_z}{\partial y\partial z}\right) + F_y = 0 \tag{2.18}$$

$$\alpha\frac{\partial P}{\partial z} + 3\beta K\frac{\partial T}{\partial z} + (2G+\lambda)\frac{\partial^2 u_z}{\partial z^2} + \lambda\frac{\partial^2 u_y}{\partial z\partial y} + \lambda\frac{\partial^2 u_x}{\partial x\partial z} + G\left(\frac{\partial^2 u_z}{\partial x^2} + \frac{\partial^2 u_x}{\partial x\partial z}\right) + G\left(\frac{\partial^2 u_z}{\partial y^2} + \frac{\partial^2 u_y}{\partial y\partial z}\right) + F_z = 0 \tag{2.19}$$

Equations 2.17-2.18 can be rearranged as

$$\alpha\frac{\partial P}{\partial x}+3\beta K\frac{\partial T}{\partial x}+(G+\lambda)(\frac{\partial^2 u_x}{\partial x^2}+\frac{\partial^2 u_y}{\partial x\partial y}+\frac{\partial^2 u_z}{\partial x\partial z})+G(\frac{\partial^2 u_x}{\partial x^2}+\frac{\partial^2 u_x}{\partial y^2}+\frac{\partial^2 u_x}{\partial z^2})+F_x=0 \tag{2.20}$$

$$\alpha\frac{\partial P}{\partial y}+3\beta K\frac{\partial T}{\partial y}+(G+\lambda)(\frac{\partial^2 u_x}{\partial x\partial y}+\frac{\partial^2 u_y}{\partial y^2}+\frac{\partial^2 u_z}{\partial y\partial z})+G(\frac{\partial^2 u_y}{\partial x^2}+\frac{\partial^2 u_y}{\partial y^2}+\frac{\partial^2 u_y}{\partial z^2})+F_y=0 \tag{2.21}$$

$$\alpha\frac{\partial P}{\partial z}+3\beta K\frac{\partial T}{\partial z}+(G+\lambda)(\frac{\partial^2 u_x}{\partial x\partial z}+\frac{\partial^2 u_y}{\partial y\partial z}+\frac{\partial^2 u_z}{\partial z^2})+G(\frac{\partial^2 u_z}{\partial x^2}+\frac{\partial^2 u_z}{\partial y^2}+\frac{\partial^2 u_z}{\partial z^2})+F_z=0 \tag{2.22}$$

Equations 2.20-2.22 can be expressed in vector form as:

$$\alpha\nabla P+3\beta K\alpha\nabla T+(\lambda+G)\nabla(\nabla\bullet\bar{u})+G\nabla^2\bar{u}+\bar{F}=0 \tag{2.23}$$

which is the thermo-poro-elastic Navier equation.

Equation 2.23 has two terms containing the displacement vector and taking the divergence of it results in the following explicit equations

$$\alpha\frac{\partial^2 P}{\partial x^2}+3\beta K\frac{\partial^2 T}{\partial x^2}+(G+\lambda)\frac{\partial}{\partial x}(\frac{\partial^2 u_x}{\partial x^2}+\frac{\partial^2 u_y}{\partial x\partial y}+\frac{\partial^2 u_z}{\partial x\partial z})+G\frac{\partial}{\partial x}(\frac{\partial^2 u_x}{\partial x^2}+\frac{\partial^2 u_x}{\partial y^2}+\frac{\partial^2 u_x}{\partial z^2})+\frac{\partial F_x}{\partial x}=0 \tag{2.24}$$

$$\alpha\frac{\partial^2 P}{\partial y^2}+3\beta K\frac{\partial^2 T}{\partial y^2}+(G+\lambda)\frac{\partial}{\partial x}(\frac{\partial^2 u_x}{\partial x\partial y}+\frac{\partial^2 u_y}{\partial y^2}+\frac{\partial^2 u_z}{\partial y\partial z})+G\frac{\partial}{\partial x}(\frac{\partial^2 u_y}{\partial x^2}+\frac{\partial^2 u_y}{\partial y^2}+\frac{\partial^2 u_y}{\partial z^2})+\frac{\partial F_y}{\partial x}=0 \tag{2.25}$$

$$\alpha\frac{\partial^2 P}{\partial z^2}+3\beta K\frac{\partial^2 T}{\partial z^2}+(G+\lambda)\frac{\partial}{\partial z}(\frac{\partial^2 u_x}{\partial x\partial z}+\frac{\partial^2 u_y}{\partial y\partial z}+\frac{\partial^2 u_z}{\partial z^2})+G\frac{\partial}{\partial z}(\frac{\partial^2 u_z}{\partial x^2}+\frac{\partial^2 u_z}{\partial y^2}+\frac{\partial^2 u_z}{\partial z^2})+\frac{\partial F_z}{\partial z}=0 \tag{2.26}$$

Adding Equations 2.23-2.25 together and changing the order of differentiation:

$$\begin{aligned}&\alpha(\frac{\partial^2 P}{\partial x^2}+\frac{\partial^2 P}{\partial y^2}+\frac{\partial^2 P}{\partial z^2})+\frac{\partial F_x}{\partial x}+\frac{\partial F_y}{\partial y}+\frac{\partial F_z}{\partial z}+3\beta K(\frac{\partial^2 T}{\partial x^2}+\frac{\partial^2 T}{\partial y^2}+\frac{\partial^2 T}{\partial z^2})+\\&(G+\lambda)\frac{\partial^2}{\partial x^2}(\frac{\partial u_x}{\partial x}+\frac{\partial u_y}{\partial y}+\frac{\partial u_z}{\partial z})+G(\frac{\partial^2}{\partial x^2}+\frac{\partial^2}{\partial y^2}+\frac{\partial^2}{\partial z^2})\frac{\partial u_x}{\partial x}+\\&(G+\lambda)\frac{\partial^2}{\partial y^2}(\frac{\partial u_x}{\partial x}+\frac{\partial u_y}{\partial y}+\frac{\partial u_z}{\partial z})+G(\frac{\partial^2}{\partial x^2}+\frac{\partial^2}{\partial y^2}+\frac{\partial^2}{\partial z^2})\frac{\partial u_y}{\partial y}+\\&(G+\lambda)\frac{\partial^2}{\partial z^2}(\frac{\partial u_x}{\partial x}+\frac{\partial u_y}{\partial y}+\frac{\partial u_z}{\partial z})+G(\frac{\partial^2}{\partial x^2}+\frac{\partial^2}{\partial y^2}+\frac{\partial^2}{\partial z^2})\frac{\partial u_z}{\partial z}=0\end{aligned} \tag{2.27}$$

Equation 2.27 may be written in vector form with only one term containing the displacement vector:

$$\alpha\nabla^2 P + 3\beta K\nabla^2 T + (\lambda + 2G)\nabla^2(\nabla\bullet\bar{u}) + \nabla\bullet\bar{F} = 0 \tag{2.28}$$

The divergence of the displacement vector is the volumetric strain:

$$\nabla\bullet\bar{u} = \frac{\partial u_x}{\partial x} + \frac{\partial u_y}{\partial y} + \frac{\partial u_z}{\partial z} = \varepsilon_{xx} + \varepsilon_{yy} + \varepsilon_{zz} = \varepsilon_v \tag{2.29}$$

Combining Equations 2.29 and 2.10 yields:

$$\nabla\bullet\bar{u} = \varepsilon_v = \frac{\sigma_m - \alpha P - 3\beta K\left(T - T_{ref}\right)}{\left(\lambda + \frac{2}{3}G\right)} \tag{2.30}$$

Substituting Equation 2.30 in 2.28 yields:

$$\alpha\nabla^2 P + 3\beta K\nabla^2 T + \frac{\lambda + 2G}{\lambda + \frac{2}{3}G}\nabla^2(\sigma_m - \alpha P - 3\beta K(T - T_{ref})) + \nabla\bullet\bar{F} = 0 \tag{2.31}$$

The coefficient of the third term in Equation 2.31 is only a function of Poisson's ratio υ:

$$\frac{\lambda + 2G}{\lambda + \frac{2}{3}G} = \frac{3(1-\upsilon)}{(1+\upsilon)} \tag{2.32}$$

Equation 2.31 then becomes:

$$\frac{3(1-\nu)}{(1+\nu)}\nabla^2\sigma_m + \nabla\bullet\bar{F} - \frac{2(1-2\nu)}{(1+\nu)}(\alpha\nabla^2 P + 3\beta K\nabla^2 T) = 0 \tag{2.33}$$

Equation 2.33 is the governing geomechanical equation for TOUGH2-EGS-MP and the mean normal stress is an additional primary variable besides pore pressure and temperature. The volumetric strain is another geomechanical variable, which can be solved with the relationship for using Equation 2.30.

Finally, for the multi-porosity medium represented by multiple interacting continua (MINC) (Pruess and Narasimhan, 1982, 1985; Pruess, 1991), the governing geomechanical equation may be written as

$$\frac{3(1-\nu)}{(1+\nu)}\nabla^2\sigma_m + \nabla\bullet\bar{F} - \sum_j \frac{2(1-2\nu)}{(1+\nu)}(\alpha_j\nabla^2 P_j + 3\beta_j K_j \nabla^2 T_j) = 0 \qquad (2.34)$$

where subscript *j* refers to a multi-porosity continuum or one MINC block in MINC-method.

2.3 Hydraulic properties correlations

The hydraulic properties of EGS reservoirs, such as porosity, permeability, and capillary pressure, are dependent on geomechanics.

2.3.1 Stress dependent correlations

The correlation between hydraulic properties, such as porosity/permeability and stress has been intensively investigated. We describe the dependence of permeability and porosity on effective stress in TOUGH2-EGS-MP in this section. Effective stress was initially defined as the difference between the normal stress and the pore pressure by Terzaghi (1936) and was generalized by Biot and Willis (1957) as:

$$\sigma' = \sigma - \alpha P \qquad (2.35)$$

where α is the Biot or effective stress coefficient. Some widely accepted correlations between effective stress and hydraulic properties have been incorporated into TOUGH2-EGS-MP.

Rutqvist et al. (2002b) presented the following function for porosity, obtained from laboratory experiments on sedimentary rock by Davies and Davies (1999)

$$\phi = \phi_r + (\phi_0 - \phi_r)e^{-a\sigma'} \qquad (2.36)$$

where ϕ_0 is zero effective stress porosity, ϕ_r is high effective stress porosity, and the exponent *a* is a parameter related specifically to the rock. An associated correlation for permeability in terms of porosity also has been presented

$$k = k_0 e^{c(\frac{\phi}{\phi_0} - 1)} \tag{2.37}$$

where c is also rock specific parameter. For fractured media, Rutqvist et al. (2002b) defined the aperture width b_i in the direction i as function of effective stress

$$b_i = b_{0,i} + \Delta b_i = b_i + b_{\max}(e^{-d\sigma'} - e^{-d\sigma_0'}) \tag{2.38}$$

where subscript *0* refers to initial conditions, Δb_i is the aperture change, which is function of maximum "mechanical" aperture b_{max}, initial and current effective stress σ_0' and σ', and a fracture specific parameter d. Fracture porosity is correlated to the aperture b_i as:

$$\phi = \phi_0 \frac{b_1 + b_2 + b_3}{b_{1,0} + b_{2,0} + b_{3,0}} \tag{2.39}$$

and permeability in direction i is correlated to fracture aperture of other directions j and k as:

$$k_i = k_{i,0} \frac{b_j^3 + b_k^3}{b_{j,0}^3 + b_{k,0}^3} \tag{2.40}$$

McKee et al. (1988) derived a relationship between porosity and effective stress from poro-elasticity theory for incompressible rock grains:

$$\phi = \phi_0 \frac{e^{-c_p(\sigma' - \sigma_0')}}{1 - \phi_0(1 - e^{-c_p(\sigma' - \sigma_0')})} \tag{2.41}$$

where c_p is average pore compressibility. They also related permeability and porosity with the Carman-Kozeny equation:

$$k = k_i \frac{(1-\phi_i)^2}{(1-\phi)^2}\left(\frac{\phi}{\phi_i}\right)^3 \tag{2.42}$$

These relationships fit laboratory and field data for granite, sandstone, clay and coal. Ostensen (1986) studied the relationship between effective stress and permeability for tight gas sands:

$$k^n = D \ln\left[1+\left(\frac{\sigma'^*}{\sigma'}\right)^2\right] \tag{2.43}$$

where exponent n is 0.5, D is a parameter, and σ'^* is effective stress for zero permeability, obtained by extrapolating measured square root permeability versus effective stress on a semi-log plot.

Verma and Pruess (1988) presented a power law expression relating permeability to porosity:

$$\frac{k-k_c}{k_0-k_c} = \left(\frac{\phi-\phi_c}{\phi_0-\phi_c}\right)^n \tag{2.44}$$

where k_c and ϕ_c are asymptotic values of permeability and porosity, respectively, and exponent n is a parameter.

Gutierrez and Lewis (2001) presented expressions for solid volume change with pressure and effective stress. These expressions can be integrated to yield an expression for solid volume:

$$V_s(P,\sigma) = V_{s,r}\left[1+\frac{1-\phi_r}{K_s}(P-P_r)-\frac{1}{K_s}(\sigma-\sigma_r)\right] \tag{2.45}$$

where subscript r refers to reference conditions. Bulk volume is related to the volumetric strain as follows:

$$V = V_r(1-\varepsilon_v) \tag{2.46}$$

where V is the bulk volume. The definition of porosity relates to solid volume and bulk volume as:

$$\phi = 1-\frac{V_s}{V} \tag{2.47}$$

Combining above three equations yield porosity as a function of pressure, temperature and effective stress:

$$\phi = 1 - \frac{\left(1-\phi_r\right)\left[1+\frac{1-\phi_r}{K_s}\left(P-P_r\right)-\frac{1}{K_s}\left(\sigma-\sigma_r\right)\right]}{\frac{1-\varepsilon_v}{1-\varepsilon_{v,r}}} \tag{2.48}$$

The above correlations have been incorporated into TOUGH2-EGS-MP, and the user can choose the appropriate one for the simulation.

3 NUMERICAL MODEL AND CODE ARCHITECTURE

3.1 Space and times discretization

The continuous space and time variables are discretized for numerical simulation. We use the integral finite difference method (IFDM) (Edwards, 1972; Narasimhan and Witherspoon, 1976) for this. IFDM avoids any reference to a global system of coordinates, and thus offers the advantage of being applicable to regular or irregular discretization in one, two, and three dimensions. The IFDM also makes it possible, by means of simple preprocessing of geometric data, to implement double- and multiple-porosity methods for modeling flow in fractured media. Time is discretized fully implicitly as a first-order backward finite difference. Parameters associated with the IFDM are shown in Figure 3.1.

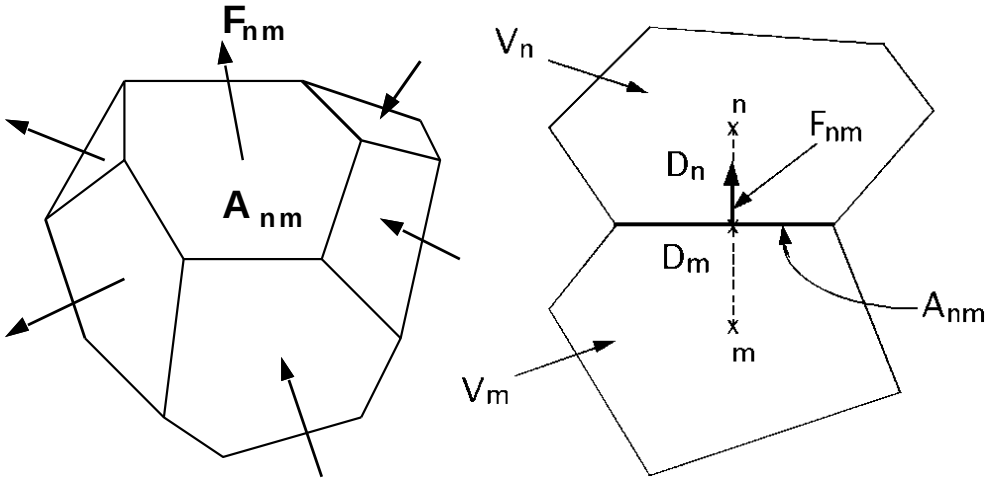

Figure 3.1 Space discretization for the integral finite difference method (Pruess et al., 1999)

Time and space discretization of Equation 2.1 results in a set of coupled non-linear equations, which can be written in residual form as follows (Pruess et al., 1999):

$$R_n^{\kappa}(x^{t+1}) = M_n^{\kappa}(x^{t+1}) - M_n^{\kappa}(x^t) - \frac{\Delta t}{V_n}\{\sum_m A_{nm} F_{nm}^{\kappa}(x^{t+1}) + V_n q_n^{\kappa,t+1}\} = 0, \kappa = 1,2,3 \qquad (3.1)$$

where the vector x^t consists of primary variables at time t, R_n^k is the residual of component k (component *1* is water, *2* is air and *3* is the energy) for grid block n, M denotes mass or thermal energy per unit volume for a component, V_n is the volume of the block n, q denotes sinks and sources of mass or energy, Δt denotes the current time step size, $t+1$ denotes the

current time, A_{nm} is the interface area between neighboring blocks n and m, and F_{nm} is the "flow" term (fluid flow, heat transfer, and advective and diffusive mass transport) between them.

Equation 2.33 expresses the mean stress in terms of the pore pressure and body forces. It is also discretized using the Integral Finite Difference method over volume element, V, with outer surface, Γ. Applying the divergence theorem to the Laplacian operators in Equation 2.33 gives

$$\int (\frac{3(1-\nu)}{(1+\nu)} \nabla \sigma_m + \bar{F} - \frac{2(1-2\nu)}{(1+\nu)} (\alpha \nabla P + 3\beta K \nabla T)) \cdot \hat{n} d\Gamma = 0 \tag{3.2}$$

The surface integral can be expressed as a discrete sum of averages over surface segments

$$\sum_j (\frac{3(1-\nu)}{(1+\nu)} \nabla \sigma_m + \bar{F} - \frac{2(1-2\nu)}{(1+\nu)} (\alpha \nabla P + 3\beta K \nabla T))_j A_j = 0 \tag{3.3}$$

where j is the neighboring grid blocks. The boundary conditions for Equation 3.3 are a reference temperature, pressure, and mean normal stress at some distance from a given grid block.

The finite difference approximation for Equation 3.3 in residual form is

$$R_n^4(x^{t+1}) = \sum_j (\frac{3(1-\nu)}{(1+\nu)} \frac{\sigma_j - \sigma_i}{s_{ij}} - \frac{2(1-2\nu)}{(1+\nu)} \alpha \frac{p_j - p_i}{s_{ij}} - \frac{2E}{(1+\nu)} \beta \frac{T_j - T_i}{s_{ij}} + \rho_{tot} g \hat{k} \cdot \hat{n})_{ij} A_{ij} = 0 \tag{3.4}$$

The model solves four equations (Equation 3.1 for three components and Equation 3.4) simultaneously for four primary variables for each grid block. The Newton/Raphson method is used for solving the equations, and is the following:

$$-\sum_i \left. \frac{\partial R_n^{\kappa,t+1}}{\partial x_i} \right|_p (x_{i,p+1} - x_{i,p}) = R_n^{\kappa,t+1}(x_{i,p}), \kappa = 1,2,3,4 \tag{3.5}$$

where $x_{i,p}$ represents the value of i^{th} primary variable at the p^{th} iteration step.

The four primary variables in the system depend on which phases are present. The possible phase conditions and the corresponding primary variables are summarized as Table 3.1.

Table 3.1 Phase conditions and primary variables for solving Equation 3.5

Phase Condition	**Primary Variables**			
	1	2	3	4
Single Phase Liquid	Liquid pressure P_l	Air mass fraction X	Temperature T	Stress σ
Single Phase Gas	Gas pressure P_g	Air mass fraction X	Temperature T	Stress σ
Two phase	Gas pressure P_g	Gas saturation plus 10 $S_g + 10$	Temperature T	Stress σ

The accumulation term of the component *k* mass balance has the general form:

$$\frac{d}{dt}\int_0^{V(t)} M_k dV \tag{3.6}$$

The upper limit in the integral indicates that grid block volume changes with time. The finite difference approximation for Equation 3.6 is:

$$\frac{((VM_k)^{n+1} - (VM_k)^n)}{\Delta t} \tag{3.7}$$

With grid block volume and bulk strain are related by:

$$V = V_0(1 - \varepsilon_v) \tag{3.8}$$

where V_0 is initial grid block volume.

3.2 Multi-porosity flow model

Figure 3.2 illustrates the classical double-porosity concept for modeling flow in fractured porous media as developed by Warren and Root (1963). The flow domain is composed of matrix blocks of low permeability, embedded in a network of interconnected fractures. In these reservoirs, the fractures have larger permeability and smaller porosity relative to those of the porous rock matrix. As a result, a pressure change in the reservoir would travel through fracture much faster than through the rock matrix. The classical double-porosity approach assumes that global fluid flow occurs mostly through the fractures with pseudo-steady

exchange between the fractures and matrix, which is dependent on pressure and temperature differences between them.

However, the assumption of pseudo-steady exchange between fracture and matrix is not valid for many systems, such as those with complex, multiphase flow or large matrix volumes (Wu and Pruess, 1988), because the time scale associated with flow through the matrix is too large. We model those situations with the Multiple Interacting Continua (MINC) approach (Pruess and Narasimhan, 1982, 1985; Pruess, 1991). In the MINC conceptual model, flow within the matrix is described more accurately by subdividing the matrix into nested volumes, as shown in Figure 3.3, with flow occurring between adjacent nested matrix volumes, as well as between the fractures and the outer matrix volume. The idea behind the MINC approach is that the local changes in matrix conditions depend on the distance from the fractures, and the construction of MINC blocks reflects this. Flow within the matrix is one-dimensional transient flow, and MINC approach reduces to the classical double porosity model if there is only one matrix subdivision.

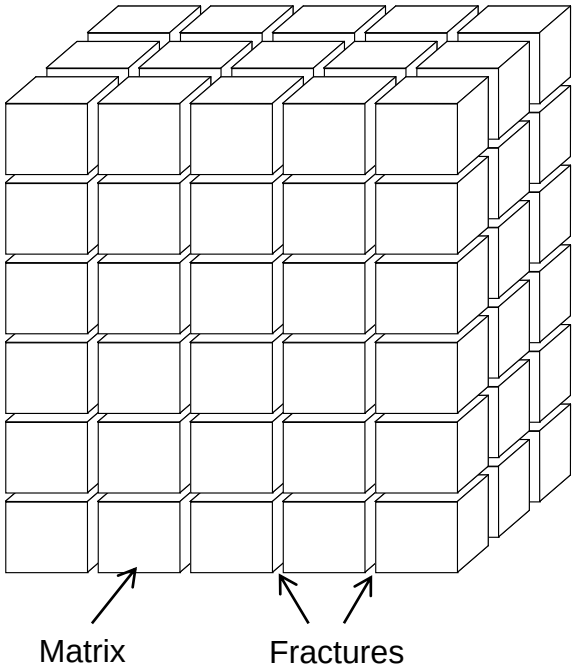

Figure 3.2 Schematic of "double porosity" model for a fractured porous medium (Warren and Root, 1963).

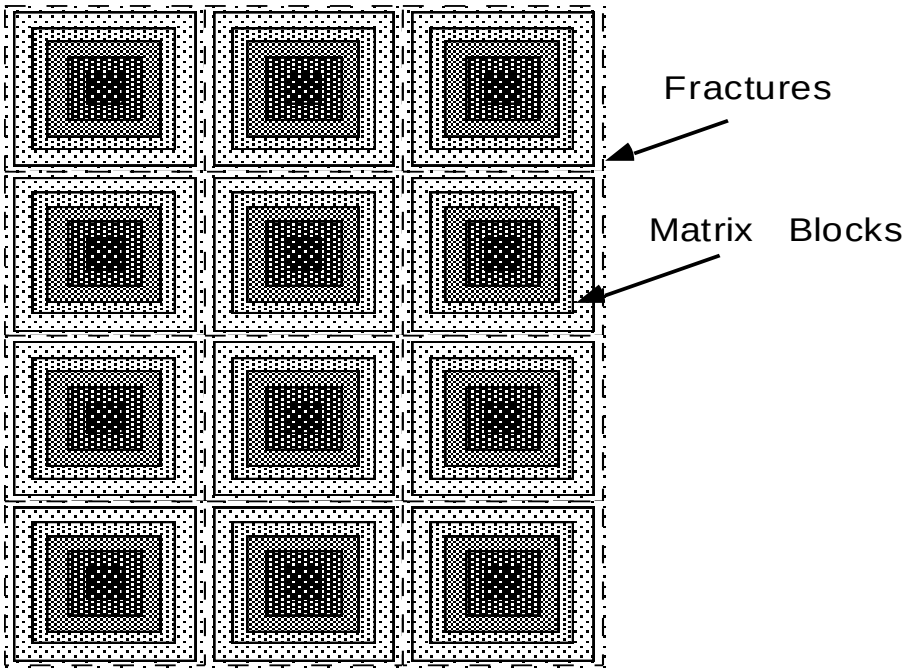

Figure 3.3 Subgridding in the approach of "multiple interacting continua" (MINC) (Pruess, 1991).

The MINC grid blocks can be generated with the MESHMAKER module in our code. For a given fractured reservoir, flow problem, selection of the most appropriate gridding scheme must be based on a careful consideration of the physical and geometric conditions of flow. The MINC approach may not be applicable to systems in which fracturing is so sparse that the fractures cannot be approximated as a continuum.

Considering a simulation domain discretized into N_v grid blocks with N_k components. For the single-porosity approach, there are N_k+2 equations, N_k mass conservation equations, one momentum conservation equation and one energy equation, associated with each grid block, and total $N_v(N_k+2)$ equations for the entire simulation domain. For MINC approach with N_ϕ multi-porous continua in each grid block, there are N_k+1 equations, N_k mass conservation equations, one energy equation for each porous continuum, and one momentum equation for the entire grid block, therefore total $N_v(1+N_\phi(1+N_k))$ equations for the entire simulation domain. The number of equations for single and multi-porosity medium are summarized as Table 3.2.

Table 3.2 Summary of equations for single and multi-porosity medium

Porosity System	Number of Global Grid Blocks (GGB)	Local Grid Block (LGB)	Mass and Energy Conservation Equations/LGB	Momentum Conservation Equations/LGB	Total Equations/LGB	Total Equations
Single	N_v	*1*	$1+N_k$	*1*	$2+N_k$	$(2+N_k)N_v$
Multi	N_v	N_ϕ	$(1+N_k)N_\phi$	*1*	$(1+N_k)N_\phi+1$	$[(1+N_k)N_\phi+1]N_v$

3.3 Methodology of parallel computing

The TOUGH2-EGS-MP code is a parallel computer program, which solves a problem by subdividing the problem into a number of smaller ones, solving those smaller ones concurrently, and then assembling the overall solution from those of the subdivisions. Solving a problem in parallel is often faster than solving it serially. Amdahl's law gives a theoretical upper limit, *S*, for the speedup of a parallel program in which *A* is the fraction of the program's running time spent on non-parallelizable parts and *P* is the number of problem subdivisions (or processors):

$$S = \frac{1}{A + \frac{1-A}{P}} \tag{3.9}$$

One deficiency in Amdahl's law is the assumption that the parallelizable part scales linearly with the number of problem subdivisions. Parallel programs often require problem subdivisions to communicate with each other, and the overhead associated with this communication could severely diminish the speedup factor as the number of problem subdivisions becomes large. In addition, the computational work needs to be evenly distributed among subdivisions in order for this speedup to occur.

For a typical TOUGH2-EGS-MP simulation, most of the computation time is spent in three parts: updating thermophysical parameters, assembling the Jacobian matrix, and solving the algebraic equations, with the latter dominating for extremely large problems. The algebraic equations are solved in parallel using the AZTEC package (Tuminaro et al., 1999). AZTEC includes a number of Krylov iterative methods, such as conjugate gradient (CG), generalized minimum residual (GMRES) and stabilized biconjugate gradient (BiCGSTAB). In order to maximize computational speed and efficiency, a parallel simulation needs to distribute computational time uniformly for these three parts. In order to do that, a parallel scheme must take into account domain decomposition, grid block reordering, and efficient message exchange between processors. These important parallel computing strategies and implementation procedures are discussed below.

3.4 Domain partitioning and grid block reordering

A successful parallel computing scheme requires an efficient and effective method for partitioning grids. Such a scheme would distribute grid blocks evenly to different processors and minimize the number of connections common to different processors. This distribution would balance computational work among the processors and minimize the time consumed in communication between processors.

In TOUGH2-EGS-MP, the simulation domain is subdivided into grid blocks and communication between grid blocks occurs at the interfaces between them. This can be represented as a grid with each grid block as a node and grid block interfaces as connections. The grid configuration is arbitrary so the grid is said to be unstructured. From the connection information, an adjacency matrix can be constructed that is stored in a compressed storage format (CSR).

In the CSR format, the adjacency matrix of a global domain with n grid blocks and m connections is represented by two arrays, *xadj* and *adj*. The *xadj* array has a size of $n+1$, whereas the *adj* array has a size of $2m$. For grid block numbering starting from 1, the adjacency list of grid block i is stored in array *adj*, starting at index *xadj(i)* and ending at index *xadj(i+1)-1*. Array *adj* stores adjacency lists in consecutive locations and array *xadj* points to the start of a grid block adjacency list. Figure 3.4 shows a 15 grid block domain including

connections (as well as a partition among four processors) and Table 3.3 illustrates its corresponding CSR format arrays.

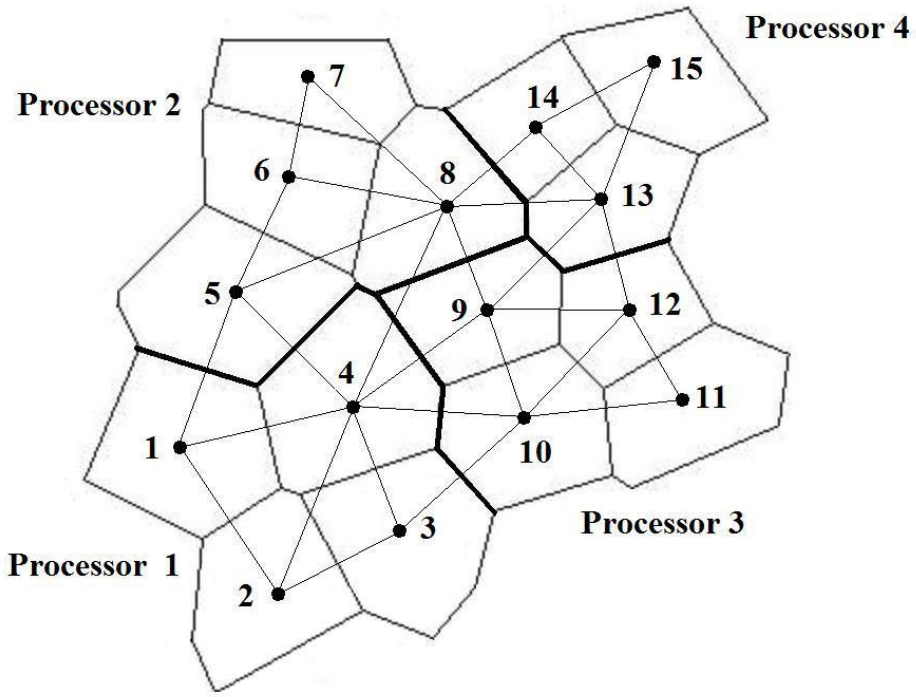

Figure 3.4. An unstructured grid containing fifteen grid blocks with four partitions on four processors

Algorithms from the METIS software package (Karypsis and Kumar, 1998) are used to partition the grid. The package contains three algorithms: *K-way*, *VK-way*, and *Recursive*. *K-way* is used for partitioning a grid into a large number of partitions (more than 8). This algorithm seeks to minimize the number of edges that are common to different partitions. If a small number of partitions is desired, the *Recursive* partitioning method, a recursive bisection algorithm, should be used. *VK-way* is a modification to *K-way* and seeks to minimize the total number of edges that are common to different partitions. Both *K-way* and *VK-way* belong to multilevel partitioning algorithms. Figure 3.4 shows a partitioning of the grid into four parts. Grid blocks are assigned to different processors through partitioning methods discussed above.

Table 3.3. Global xadj and adj arrays for grid in Figure 3.4

Grid block	xadj array	adj array	Grid block	xadj array	adj array
1	1	2	9	33	4
		4			8
		5			10
2	4	1			12
		3			13
		4	10	38	3
3	7	2			4
		4			9
		10			11
4	10	1			12
		2	11	43	10
		3			12
		5	12	45	9
		8			10
		9			11
		10			13
5	17	1	13	49	9
		4			8
		6			12
		8			14
6	21	5	14	54	15
		8			8
		7			13
7	24	6	15	57	15
		8			13
8	26	4			14
		5	N/A	59	N/A
		6			
		7			
		9			
		13			
		14			

As shown on Figure 3.4, grid blocks assigned to a processor are referred to as the *update* set. The *update* set is further divided into two subsets: *internal* and *border*. The *internal* set consists of grid blocks with no connections to grid blocks that are assigned to another processor. The *border* set consists of grid blocks with at least one connection to a grid block that is assigned to another processor. Those grid blocks connected to the border set that are not assigned to the processor is called the *external* set. The *border* set requires information from the other processors during a simulation but the *internal* set does not. Table 3.4 summarizes the partitioning in Figure 3.4 by update and external sets.

Table 3.4. Partitioning and grid block sets for Figure 3.4

Processor	Update		External
	Internal	Border	
1	2	1,3,4	5,8,9,10
2	6,7	5,8	1,4,9,13,14
3	11	9,10,12	3,4,8,13
4	15	13,14	8,9,12

A processor's *update* and *external* sets have a local numbering. The connection information for these sets is stored in similar CSR format arrays to the global arrays discussed above. Each processor stores only the rows of the Jacobian matrix that correspond to its *update* set. These rows form a sub matrix whose columns correspond to both the *update* set and the *external* set for the processor.

3.5 Organization of input and output data

TOUGH2-EGS-MP input data includes hydrogeologic parameters and constitutive relations of porous media and fluids, such as absolute and relative permeability, porosity, capillary pressure, thermophysical properties of fluids and rock, and initial and boundary conditions of the system. Other processing requirements include the specification of space-discretized geometric information (grid) and various program options (computational parameters and time-stepping information). For a large-scale, three-dimensional model, a computer memory on the order of gigabytes is generally required and the distribution of the memory to all processors is necessary for practical application of TOUGH2-EGS-MP.

To efficiently use the memory of each processor (considering that each processor has a limited memory available), the input data files for the TOUGH2-EGS-MP simulation are organized in sequential format. There are two large groups of data blocks within a TOUGH2-EGS-MP mesh file: one with dimensions equal to the number of grid blocks; the other with dimensions equal to the number of connections (interfaces). Large data blocks are read one by one through a temporary full-sized array and then distributed to different processors. This method avoids storing all input data in a single processor (whose memory space may be too small) and greatly enhances the I/O efficiency. Other small-volume data, such as simulation control parameters, are duplicated onto all processors.

All data input and output are carried out through the master processor. Time series outputs, however, are written out by the processors at which the specified grid blocks or connections for output are located.

3.6 Assembly and solution of linearized equation systems

In the TOUGH2-EGS-MP formulation, the discretization in space using the integral finite difference method leads to a set of strongly coupled nonlinear algebraic equations, which are linearized by the Newton/Raphson method. Within each Newton iteration step, the Jacobian matrix is first constructed by numerical differentiation. The resulting system of linear equations is then solved using an iterative linear solver with different preconditioning procedures. The following gives a brief discussion of assembling and solving the linearized equation systems with parallel simulation.

The discrete mass, momentum and energy balance equations are written with Equation 3.1 and 3.4 in a residual form. Applying Newton/Raphson method results in Equation 3.5, where the Jacobian matrix J(x) is defined as:

$$\left[J\left(x\right) \right]_{ij} = \frac{\partial R_i\left(x\right)}{\partial x_j} \tag{3.10}$$

The Jacobian matrix and the right-hand side of Equation 3.5 need to be recalculated for each iteration, and that computational effort may be extensive for a large simulation. In the parallel

code, the assembly of this linear equation system is shared by all processors, and each processor is responsible for computing the rows of the Jacobian matrix that correspond to grid blocks in the processor's *update* set. Computation of the elements in the Jacobian matrix is performed in two parts. The first part consists of the computations related to the individual grid blocks (accumulation and source/sink terms). Such calculations are carried out using the information stored on the current processor, without need of communication with other processors. The second part includes all the computations related to the connections or flow terms. Grid blocks in the *border* set need information from those in the *external* set, which requires communication with neighboring processors. Before performing these computations, an exchange of relevant information is required. For grid blocks in the *border* set, each processor sends their information to the relevant processors, which contain these grid blocks in their *external* set.

The Jacobian matrix for each processor's grid blocks is stored in the distributed variable block row (DVBR) format, a generalization of the VBR format. All matrix blocks are stored row wise, with the diagonal blocks stored first in each block row. Scalar elements of each matrix block are stored in column major order. The data structure consists of a real-type vector and five integer type vectors, forming the Jacobian matrix. Detailed explanation of the DVBR data format can be found in Tuminaro et al. (1999).

The linearized equation system arising at each Newton step is solved using an iterative linear solver from the AZTEC package. There are several different solvers and preconditioners from the package for users to select and the options include conjugate gradient, restarted generalized minimal residual, conjugate gradient squared, transposed-free quasi-minimal residual, and biconjugate gradient with stabilization methods. The work for solving the global linearized equation is shared by all processors, with each processor responsible for computing

its own portion of the partitioned domain equations. To accomplish the parallel solution, communication between a pair of processors is required to exchange data between the neighboring grid partitions. Moreover, global communication is also required to compute the norms of vectors for checking the convergence.

During a parallel simulation, the time-step size is automatically adjusted (increased or reduced), depending on the convergence rate of the Newton/Raphson method. In the TOUGH2-EGS-MP code, time step size is calculated at the master processor after collecting necessary data from all processors. The convergence rates may be different in different processors. Only when all processors reach stopping criteria will the time march to the next time step.

3.7 Communication between processors

Communication between processors working on grid block connections that cross partition boundaries is an essential component of the parallel algorithm. Moreover, global communication is also required to compute norms of vectors, contributed by all processors, for checking the convergence. In addition to the communication taking place inside the linear solver routine to solve the linear equation system, communication between neighboring processors is necessary to calculate the Jacobian matrix. A subroutine is used to manage data exchange between processors. When the subroutine is called by a processor, an exchange of vector elements corresponding to the processor's *external* set is performed. More discussion on the prototype scheme used for data exchange is given in Elmroth et al. (2001). In addition, non-blocking communication was introduced to the Aztec package and Newton/Raphson iterations (Zhang and Wu, 2006) to further improve them.

3.8 Updating thermophysical properties

The thermophysical properties of fluid mixtures (secondary variables) needed for assembling the governing conservation equations are calculated at the end of each Newton iteration step based on the updated set of primary variables. At the same time, the phase conditions are identified for all grid blocks, the appearance or disappearance of phases is recognized, and primary variables are switched and properly re-initialized in response to a change of phase. All these tasks must be done grid block by grid block for the entire simulation domain. The

computational work for these tasks is readily parallelized by each processor handling its corresponding sub domain. A tiny overlapping of computation is needed for the grid blocks at the neighboring sub domain border to avoid communication for secondary variables.

3.9 Data structure and simulation procedures

In TOUGH2-EGS-MP, *NEL* is the total number of grid blocks; *NK* is two, the number of components. Each element has *NKx* primary variables as shown in Table 3.4, stored sequentially in a one-dimensional array *X*; first the *NKx* variables for grid block *#1*, then the *NKx* variables for grid block *#2*, and so on, as shown in Figure 3.5. The starting location for primary variables for grid block *N* is *NLOC+1*, where *NLOC=(N-1)*NKx*. The thermophysical and stress-dependent properties needed to assemble the mass- and energy-balance equations for all volume elements are considered as secondary variables and stored sequentially in the large array *PAR*.

As shown in Figure 3.5, the first group of *NB (=8)* secondary parameters includes the parameters needed for the accumulation and flow terms. Starting in the location *NB+1*, there are *NK* component mass fractions, so the total number of secondary parameters per fluid phase is *NBK = NB+NK*. By TOUGH2 convention, the *NBK* gas phase parameters come first, followed by *NBK* parameters for the aqueous phase. The *NPH*NB*K phase-specific parameters are followed by 9 other parameters including geomechanical variables, temperature, and others. There are a total of *NPH*NBK+9* secondary variables. There are another *NEQ* (number of equations) set of secondary variables, which are used for evaluating numerical derivatives. The TOUGH2 user guide (Pruess, 1991) gives a description of it.

In TOUGH2-EGS-MP, dynamic memory allocation, modules, array operations, matrix manipulation, and other Fortran 90 features are implemented in the parallel code. In particular, the message-passing interface (MPI) library of Message Passing Forum (1994) is used for message passing. In summary, all data input and output are carried out through the master processor. The most time-consuming computations (assembling the Jacobian matrix, updating thermophysical parameters, solving linear equation systems) are distributed to all processors involved. The memory requirements are also distributed to all processors as well. Distributing

both computing and memory requirements is essential for solving large-scale problems and obtaining better parallel performance. Figure 3.6 shows an abbreviated program flow chart.

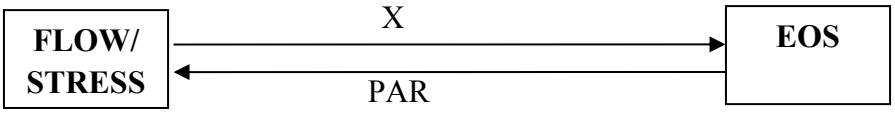

Volume Element	**Primary Variables**
#1	X(1)
	...
	X(NKx)
#2	**X(NKx+1)**
	...
	*X(2*NKx)*
	...
#N	X(NLOC+1)
	...
	X(NLOC+NKx)
	…
#NEL	...
	X(NEL*NKx)

Volume Element	**SECONDARY PARAMETERS** gas phase / aqueous phase
#1	phase saturation S PAR(1) PAR(NBK+1)
	relative permeability Kr PAR(2) …
	viscosity μ PAR(3) …
	density ρ PAR(4) …
	specific enthalpy h PAR(5) …
	capillary pressure P_c PAR(6) …
	diffusion factor 1 a PAR(7) …
	diffusion factor 2 b PAR(8) …
	mass fractions
	component 1 X^1 PAR(NB+1) …
	…
	component NK X^{NK} PAR(NB+NK) PAR(2*NBK)
	mean stress PAR(NSEC-8)
	mean stress PAR(NSEC-7)
	stain $(1-\varepsilon_v)$ PAR(NSEC-6)
	Permeability (kz) PAR(NSEC-5)
	Permeability (ky) PAR(NSEC-4)
	Permeability (kx) PAR(NSEC-3)
	Porosity (ϕ) PAR(NSEC-2)
	temperature T PAR(NSEC-1)
	(miscellaneous) PAR(NSEC)
	(second set of secondary parameters: X(1) incremented)
	PAR(NSEC+1)
	…
	PAR(2*NSEC)
	…
	PAR((NEQ+1)*NSEC)
#2	…
…	…
#NEL	…

Figure 3.5 Structure of thermophysical and stress property arrays in TOUGH2-EGS-MP

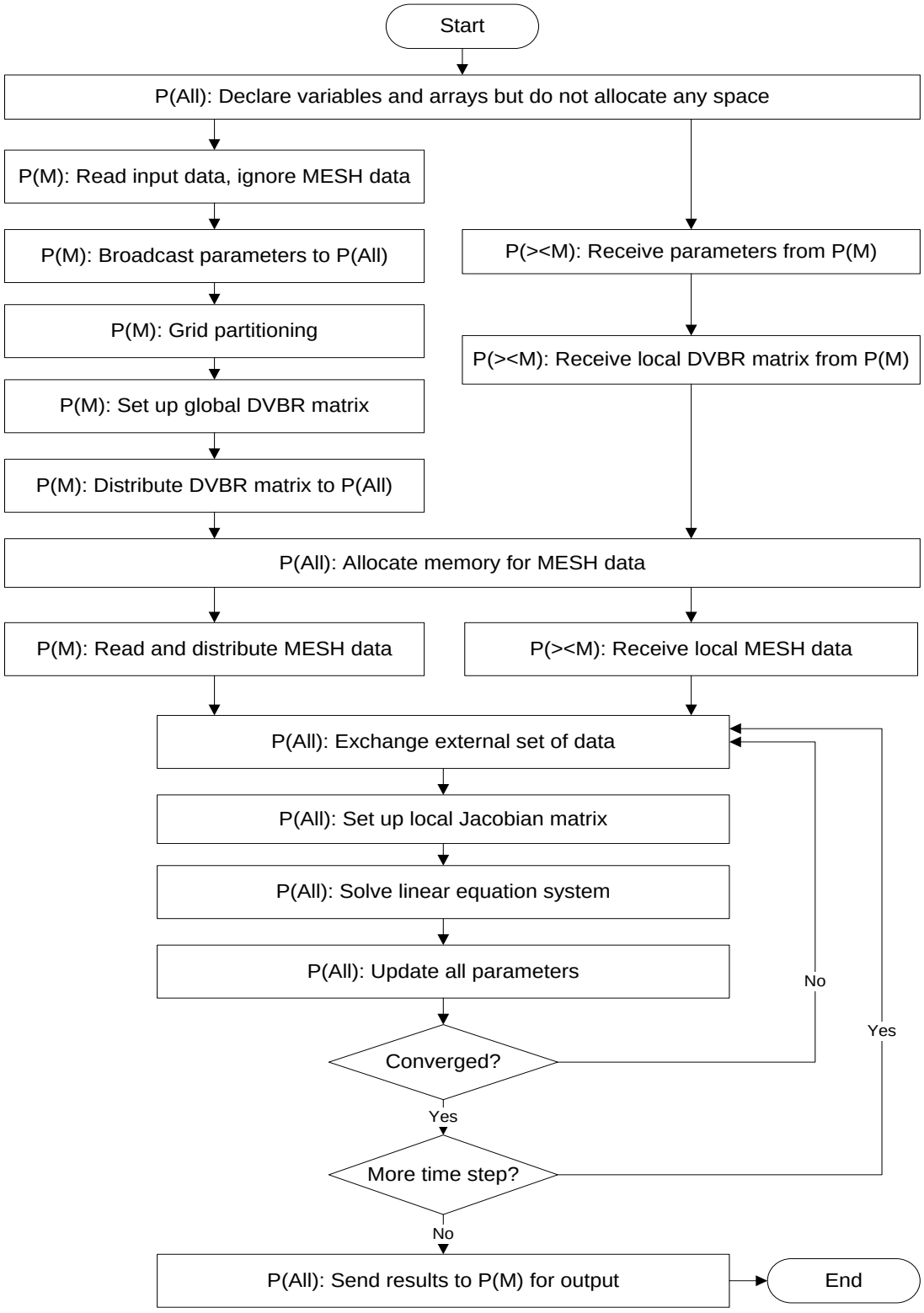

Figure 3.6. TOUGH2-EGS-MP flow chart (P(M) stand for master processor, P(><M) stands for the others, and P(All) stands for all processors

4 USING TOUGH2-EGS-MP

4.1 Compilation

TOUGH2-EGS-MP was written in standard Fortran 90, which can be compiled in any platform with compiler supporting Fortran 90. The Table 4.1 shows all the source files and its descriptions for TOUGH2-EGS-MP.

Table 4.1. Lists of source files of TOUGH2-EGS-MP

File name	Functions	Notes
Main_Comp.f	Main program for time stepping and parallel running control	Source codes
Data_DD.f	Data declaration and distribution	Source codes
Compu_Eos.f	EOS Modules and satellite functions	Source codes
Input_Output.f	Input and output	Source codes
Mem_Alloc.f	Memery allocation	Source codes
Mesh_Maker.f	Generate mesh	Source codes
MULTI.f	Jacobian assembly	Source codes
Para_Subs.f	Parallelization related subroutines	Source codes
TOUGH2.f	Program entrance	Source codes
Utility_F.f	Utility subroutines	Source codes
Mechanics.f	Geomechanics calculation	Source codes
mpi.h	Header file for MPI	Header file of MPI
az_aztecf.h	Header file for Aztec package	Header file of Aztec
libmetis.a	Compiled METIS functions Library file	Library file
libaztec.a	Compile AZTEC functions Library file	Library file

Although the deliverable package of TOUGH2-EGS-MP includes the complied library files of METIS and Aztec, the user can download the updated version from their official sites and build updated libraries. The provided libraries in the package were built on the Linux cluster version; thus the libraries must be rebuilt if users would like to build and run TOUGH2-EGS-

MP on different platforms. Figure 4.1 shows one sample makefile which is used to specify the build instructions for a typical Linux cluster. The user may modify it according to specific compiler and compiling environments.

```
# for clusters
FC = mpiifort
FFLAGS =  -limf -align all -r8 -nowarn

LIBPATH=-L/opt/intel/impi/4.1.0.024/lib64
INCLUDE=-I/opt/intel/impi/4.1.0.024/bin64

# The following specifies the files used for the "standard version"
OBJS = Data_DD.o Mem_Alloc.o MULTI.o Main_Comp.o TOUGH2.o \
       Compu_Eos.o Input_Output.o Mesh_Maker.o Paral_Subs.o \
       Utility_F.o Mechanics.o\

LIBS =  libmetis.a libaztec.a
tough2: $(OBJS)
        $(FC) -o T2EGSMP $(FFLAGS) $(OBJS) $(LIBS) $(LIBPATH) $(INCLUDE)
clean:
        rm -f *.o *.mod
```

Figure 4.1. Sample makefile for building TOUGH2-EGS-MP on Linux cluster

4.2 Execution

TOUGH2-EGS-MP is one MPI parallel program and has to be started with an MPI job launcher program, such as *mpiexec* or *mpirun*. There are usually two ways to run an MPI program, direct launching through a launcher command, or submitting batch job to the job scheduler of host machine. One good practice is that if the problem size is small and involves very few processors, the direct launch method works fine. On the other hand, if the problem size is large and involves many processors with complex computing configuration, the good practice dictates submission of batch job through a script file. Two different ways of running a TOUGH2-EGS-MP executable are illustrated below.

In the typical Linux cluster, the following sample command is usually used to run TOUGH2-EGS-MP:

mpirun -n 4 -f thehostfile ./T2EGSMP

The above command means *4* MPI processes of *T2EGSMP* are run on the hosts specified in the file *thehostfile*, where *T2EGSMP* is the name of executable compiled through the makefile

of Figure 4.1, and thehostfile is the name of file specifying the hosts or nodes of the cluster T2EGSMP is run on.

In the cases involving lots of processors, preparing a script file and submitting batch job to the scheduler is a better way. The script file for a parallel job depends on the scheduler used on the host machine. Figure 4.2 shows a sample script file for submitting a batch job through the PBS job scheduler. It specifies that TOUGH2-EGS-MP is to be run on 10 nodes with 16 processes per nodes, total 160 parallel processes running.

```
#!/bin/bash
#PBS -l nodes=10:ppn=16
#PBS -l walltime=05:30:00
#PBS -N T2EGSMP_JOB
#PBS -o out.$PBS_JOBID
#PBS -e err.$PBS_JOBID

#----------------------
# Go to the directoy from which our job was launched
cd $PBS_O_WORKDIR

# Create a "base name" for a directory in which our job will run
# For production runs this should be in $SCRATCH
MYBASE=$PBS_O_WORKDIR
#MYBASE=$SCRATCH/runit

# Create a directoy for our run based on the $JOBID and go there
mkdir -p $MYBASE/$JOBID
cd $MYBASE/$JOBID
cp  $MYBASE/worker_input $MYBASE/$JOBID/worker_input

# Run the job.
echo "running job"
mpirun  -np 160 $PBS_O_WORKDIR/T2EGSMP
echo "job has finished"
```

Figure 4.2. Sample script file for submitting batch job for PBS job scheduler

5 DESCRIPTION OF INPUT FILES

In this chapter, we describe the detailed format for the input files mentioned above. The start for each record for the input data block is in bold and underlined like **BOLD**, and the keywords and variables in each data block are in **BOLD**.

Table 5.1. Keywords of data blocks of main input file

KEYWORD	FUNCTION
TITLE (first record)	One data record (single line) with a title for the simulation problem
MESHM	Optional; parameters for internal grid generation through MESHMaker
ROCKS	Hydrogeologic parameters for various reservoir domains or rock types
MULTI	Optional; specifies number of fluid components and balance equations per grid block; applicable only for certain fluid property (EOS) modules
SELEC	Used with EOS-modules to supply thermophysical property data
START	Optional; one data record for more flexible initialization
PARAM	Computational parameters; time stepping and convergence parameters;
RPCAP	Optional; parameters for relative permeability and capillary pressure functions
TIMES	Optional; specification of times for generating printout
*ELEME	List of grid blocks (volume elements)
*CONNE	List of flow connections between grid blocks
*GENER	Optional; list of mass or heat sinks and sources
INDOM	Optional; list of initial conditions for specific reservoir domains
*INCON	Optional; list of initial conditions for specific grid blocks
NOVER (optional)	Optional; if present, suppresses printout of version numbers and dates of the program units executed in a TOUGH2-EGS-MP run
SOLVR	Introducing solver parameters;
REACT	Parameters for chemical reactions
GRMOD	Optional; setting individual properties for specific grid blocks
FOFT	Optional; list of grid blocks for time-dependent output
COFT	Optional; list of connections for time-dependent output
GOFT	Optional; list of sink/source grid blocks for time-dependent output
ENDCY (last record)	One record to close the TOUGH2-EGS-MP main input file and initiate the simulation
ENDFI	Alternative to “ENDCY” for closing a TOUGH2-EGS-MP main input file; will cause flow simulation to be skipped; useful if only mesh generation is desired

§Blocks labeled with a star * can be provided as separate disk files, in which case they would be omitted from the main input file.

5.1 Main Input files format

The main input file uses the TOUGH2 convention for the keywords of input data blocks. The Table 5.1 list the key words of the input data blocks for the main input file. The main input file has the fixed file name “INFILE”. This section presents the data input format of the main input file for TOUGH2-EGS-MP.

TITLE is the first record of the input file, containing a header of up to 80 characters, to be printed on output. This can be used to identify a problem. If no title is desired, leave this record blank.

MESHM introduces parameters for internal mesh generation and processing. The MESHMaker input has a modular structure which is organized by keywords. Detailed instructions for preparing MESHMaker input are given in Section 5.2.

Record MESHM.1

Variable: WORD

Format: A5

WORD enter one of several keywords, such as RZ2D, RZ2DL, XYZ, and MINC, to generate different kinds of computational meshes.

Record MESHM.2

A blank record closes the MESHM data block.

ENDFI is a keyword that can be used to close a TOUGH2 input file when no flow simulation is desired. This will often be used for a mesh generation run when some hand-editing of the mesh will be needed before the actual flow simulation.

ROCKS introduces material parameters for up to 27 different reservoir domains.

Record ROCKS.1

Variable: MAT, NAD, DROK, POR, (PER (I), I = 1, 3), CWET, SPHT

Format: A5, I5, 7E10.4

MAT material name (rock type).

NAD if zero or negative, defaults will take effect for a number of parameters (see below);

≥1: will read another data record to override defaults.

≥2: will read two more records with domain-specific parameters for relative permeability and capillary pressure functions.

≥3: will read three more records with domain-specific parameters for rock mechanics and stress-porosity, stress-permeability relations.

DROK rock grain density (kg/m^3)

POR default porosity (void fraction) for all elements belonging to domain "MAT" for which no other porosity has been specified in block INCON. Option "START" is necessary for using default porosity.

PER (I) absolute permeability along the three principal axes, as specified by ISOT in block CONNE.

CWET formation heat conductivity under fully liquid-saturated conditions (W/m ˚C).

SPHT rock grain specific heat (J/kg ˚C). Domains with SPHT > 104 J/kg ˚ C will not be included in global material balances. This provision is useful for boundary nodes, which are given very large volumes so that their thermo-dynamic state

remains constant. Because of the large volume, inclusion of such nodes in global material balances would make the balances useless.

Note: if SPHT < 0, then a table for temperature-dependent rock grain specific heat needs to be input following Record ROCKS.1.1.

Record ROCKS.1.1 (optional, NAD ≥ 1 only)

Variable: COM, EXPAN, CDRY, TORTX, GK

Format: 5E10.4

COM pore compressibility (Pa^{-1})

EXPAN linear temperature expansivity (1/ ˚C)

CDRY formation heat conductivity under desaturated conditions (W/m ˚C), default is CWET

TORTX tortuosity factor for binary diffusion.

GK Klinkenberg parameter *b* (Pa^{-1}) for enhancing gas phase

Record ROCKS.1.2 (optional, NAD ≥ 2 only)

Variable: IRP, (RP(I), I= 1,7)

Format: I5, 5X,7E10.4

IRP integer parameter to choose type of relative permeability function (see Appendix B).

RP(I) I = 1, ..., 7, parameters for relative permeability function (Appendix C).

Record ROCKS.1.3 (optional, NAD ≥ 2 only)

Variable: ICP, (CP(I), I = 1,7)

Format: I5, 5X,7E10.4)

ICP integer parameter to choose type of capillary pressure function (see Appendix C).

CP(I) I = 1, ..., 7, parameters for capillary pressure function (Appendix C).

Repeat records 1, 1.1, 1.2, and 1.3 for any number of reservoir domains.

Record ROCKS.1.4 (optional, NAD≥3 only)

Variable: IRPOPT, IRKOPT, IPORPERM, POIRAT, YOUNGM, CBIOT, TREF

Format: 2I5, I10, 7E10.4

IRPOPT Stress-porosity correlation options

IRKOPT Stress-permeability correlation options

IPORPERM Porosity-permeability correlation options. This option will be used in the THMC coupling scenario:

In the coupled geomechanical and geochemical simulations, the total permeability change for each time step is calculated from porosity change due to mechanical and chemical effects for given IPORPERM options. In this version, three correlation options are included, simplified Carman-Kozeny relation (Equation 2.55, IPORPERM = 1), cubic law relation for fracture (Equation 2.63, IPORPERM = 3), and Verma and Pruess relation (Equation 2.57, IPORPERM = 5).

POIRAT Poisson ratio

YOUNGM Young's modulus, (Pa)

CBIOT Biot's coefficient.

TREF Reference temperature, (℃)

Record ROCKS.1.5 (optional, NAD≥3 only)

Variable: RCKPAR(I),I=1,8

Format: 8E10.4

RCKPAR The parameters for porosity and permeability correlations with stress

Repeat records 1, 1.1, 1.2, and 1.5 for up to 27 reservoir domains.

Record ROCKS.2 A blank record closes the ROCKS data block.

ICOUP the keyword to specify the coupling process for the simulation

Record ICOUP. 1

Variable: ISTCAL, ICHCAL

Format: 2I10

ISTCAL the flag to specify the geomechanical coupling process.

= 1 coupling geomechanical process

= 0 no geomechanical coupling

ICHCAL this flag is not used in TOUGH2-EGS-MP, default is 0

START (optional) a record with START typed in columns 1-5 allows a more flexible initialization. More specifically, when START is present, INCON data can be in arbitrary order, and need not be present for all grid blocks (in which case

defaults will be used). Without START, there must be a one-to-one correspondence between the data in blocks ELEME and INCON.

PARAM introduces computation parameters, time stepping information, and default initial conditions.

Record PARAM.1

Variables: NOITE, KDATA, MCYC, MSEC, MCYPR, (MOP(I), I = 1, 24), TEXP, BE

Format: 2I2,3I4,24I1,E9.4,4E10.4

NOITE specifies the maximum number of Newtonian iterations per time step (default is 8)

KDATA specifies amount of printout (default is 1)

= 0 or 1: print a selection of the most important variables.

= 2: in addition, print mass and heat fluxes and flow velocities.

= 3: in addition, print primary variables and their changes.

If the above values for KDATA are increased by 10, printout will occur after each Newton-Raphson iteration (not just after convergence).

MCYC maximum number of time steps to be calculated

MSEC maximum duration, in CPU seconds, of the simulation (default is infinite).

MCYPR printout will occur for every multiple of MCYPR steps (default is 1).

MOP(I) I = 1,24 allows choice of various options, which are documented in printed output from a TOUGH2-EGS-MP run.

MOP(1) if unequal 0, a short printout for non-convergent iterations will be generated.

MOP(2) through MOP(6) generate additional printout in various subroutines, if set unequal 0. This feature should not be needed in normal applications, but it will be convenient when a user suspects a bug and wishes to examine the inner workings of the code. The amount of printout increases with MOP(I) (consult source code listings for details).

MOP(2) CYCIT (main subroutine).

MOP(3) MULTI (flow- and accumulation-terms).

MOP(4) QU (sinks/sources).

MOP(5) EOS (equation of state).

MOP(6) LINEQ (linear equations).

= 1: Jacobian matrix and right hand side.

= 2: Jacobian matrix and right hand side, and primary variables and primary variable increments.

MOP(7) if unequal 0, a printout of input data will be provided.

Calculation choices are as follows:

MOP(9) determines the composition of produced fluid with the MASS option (see GENER, below). The relative amounts of phases are determined as follows:

= 0: according to relative mobility in the source element.

= 1: produced source fluid has the same phase composition as the producing element.

MOP(10) chooses the interpolation formula for heat conductivity of rock as a function of liquid saturation (S_l)

= 0: $C(S_l) = CDRY + SQRT(S_l * [CWET - CDRY])$

= 1: $C(S_l) = CDRY + S_l * (CWET - CDRY)$

MOP(11) determines evaluation of mobility and permeability at interfaces.

= 0: mobilities are upstream weighted with WUP (see PARAM.3), permeability is upstream weighted.

= 1: mobilities are averaged between adjacent elements, permeability is upstream weighted.

= 2: mobilities are upstream weighted, permeability is harmonic weighted.

= 3: mobilities are averaged between adjacent elements, permeability is harmonic weighted.

= 4: mobility and permeability are both harmonic weighted.

MOP(12) determines interpolation procedure for time dependent sink/source data (flow rates and enthalpies).

= 0: triple linear interpolation; tabular data are used to obtain interpolated rates and enthalpies for the beginning and end of the time step; the average of these values is then used.

= 1: step function option; rates and enthalpies are taken as averages of the table values corresponding to the beginning and end of the time step.

= 2: rigorous step rate capability for time dependent generation data.

A set of time ti and generation rates qi provided in data block GENER is interpreted to mean that sink/source rates are piecewise constant and change in discontinuous fashion at table points. Specifically, generation is assumed to occur at constant rate qi during the time interval [ti,ti+1), and changes to qi+1 at ti+1. Actual rate used during a time step that ends at time t, with ti≤t≤ti+1, is automatically adjusted in such a way that total cumulative exchanged mass at time t

$$Q(t) = \int_0^t q dt' = \sum_{j=1}^{i-1} q_j (t_{j+1} - t_j) + q_i (t - t_i)$$

is rigorously conserved. If also tabular data for enthalpies are given, an analogous adjustment is made for fluid enthalpy, so preserve $\int qhdt$.

MOP(14) not used in this version

MOP(15) determines conductive heat exchange with impermeable confining layers

= 0: heat exchange is off.

= 1: heat exchange is on (for grid blocks that have a non-zero heat transfer area; see data block ELEME).

MOP(16) provides automatic time step control. Time step size will be doubled if convergence occurs within ITER ≤ MOP(16) Newton-Raphson iterations.

It is recommended to set MOP(16) in the range of 2 - 4.

MOP(17) not used in this version

MOP(18) selects handling of interface density.

= 0: perform upstream weighting for interface density.

> 0: average interface density between the two grid blocks. However, when one of the two phase saturations is zero, upstream weighting will be performed.

MOP(19) not used in this version

MOP(20) not used in this version

MOP(21) allows one more iteration if solution converges with 1 Newton iteration

= 0: one more iteration not needed

= 1: perform one more iteration

MOP(22) not used in this version

MOP(23) not used in this version

MOP(24) determines handling of multiphase diffusive fluxes at interfaces.

= 0: harmonic weighting of fully-coupled effective multiphase diffusivity.

= 1: separate harmonic weighting of gas and liquid phase diffusivities.

TEXP parameter for temperature dependence of gas phase diffusion coefficient.

BE (optional) parameter for effective strength of enhanced vapor diffusion; if set to a non-zero value, will replace the parameter group 0 for vapor diffusion.

Record PARAM.2

Variables: TSTART, TIMAX, DELTEN, DELTMX, ELST, GF, REDLT, SCALE

Format: 4E10.4, A5, 5X,3E10.4

TSTART starting time of simulation in seconds (default is 0).

TIMAX time in seconds at which simulation should stop (default is infinite).

DELTEN length of time steps in seconds. If DELTEN is a negative integer, DELTEN = - NDLT, the program will proceed to read NDLT records with time step information. Note that - NDLT must be provided as a floating point number, with decimal point.

DELTMX upper limit for time step size in seconds (default is infinite).

ELST writes a file for time versus primary variables for selected elements at all the times, when ELST = RICKA.

GF magnitude (m/sec^2) of the gravitational acceleration vector. Blank or zero gives "no gravity" calculation.

REDLT factor by which time step is reduced in case of convergence failure or other problems (default is 4).

SCALE scale factor to change the size of the mesh (default = 1.0).

Record PARAM.2.1, 2.2, etc.

Variables: DLT(I), I = 1, 100

Format: 8E10.4

DLT(I) Length (in seconds) of time step I. This set of records is optional for DELTEN = - NDLT, a negative integer. Up to 13 records can be read, each containing 8 time step data. If the number of simulated time steps exceeds the number of DLT(I), the simulation will continue with time steps equal to the last non-zero DLT(I) encountered. When automatic time step control is chosen (MOP (16) >

0), time steps following the last DLT (I) input by the user will increase according to the convergence rate of the Newton-Raphson iteration. Automatic time step reduction will occur if the maximum number of Newton-Raphson iterations is exceeded (parameter NOITE, record PARAM.1)

Record PARAM.3

Variables: RE1, RE2, U, WUP, WNR, DFAC

Format: 6E10.4

RE1 convergence criterion for relative error (default= 10^{-5}).

RE2 convergence criterion for absolute error (default= 1).

U not used in this version

WUP upstream weighting factor for motilities and enthalpies at interfaces (default = 1.0 is recommended). $0 \leq WUP \leq 1$.

WNR weighting factor for increments in Newton/Raphson - iteration (default = 1.0 is recommended). $0 < WNR \leq 1$.

DFAC increment factor for numerically computing derivatives (default value DFAC $=10^{-k/2}$, where k, evaluated internally, is the number of significant digits of the floating point processor used; for 64-bit arithmetic, DFAC $\approx 10^{-8}$).

Record PARAM.4

Introduces fluid and heat flow primary variables (first three primary variables in Table 3.4), which are used as default initial conditions for all grid blocks that are not assigned by means of data blocks INDOM or INCON. Option START is necessary to use default INCON.

Note: The fourth primary variable, stress, will be initialized in the keyword GENER and variable GX.

Variables: DEP (I), I = 1, 3

Format: 3E20.14

DEP The number of primary variables, 3, is normally assigned internally in the EOS module, and is usually equal to the number NEQ of equations solved per grid block. See data block MULTI for special assignments of 3. Different sets of primary variables are in use for different EOS modules.

INDOM introduces domain-specific initial conditions. These will supersede default initial conditions specified in PARAM.4, and can be overwritten by element-specific initial conditions in data block INCON. Option START is needed to use INDOM conditions.

Record INDOM. l

Variables: MAT

Format: A5

MAT name of a reservoir domain, as specified in data block ROCKS.

Record INDOM.2

A set of primary flow variables assigned to all grid blocks in the domain specified in record INDOM. l. Different sets of primary variables are used for different EOS modules.

Variables: Xl, X2, X3

Format: 3E20.13

Record INDOM.3

A blank record closes the INDOM data block. Repeat records INDOM. l and INDOM.2 for as many domains as desired. The ordering is arbitrary and need not be the same as in block ROCKS.

INCON introduces element-specific initial conditions.

Record INCON.1

Variables: ELNE, NSEQ, NADD

Format: A5, 2I5

ELNE code name of element.

NSEQ number of additional elements with the same initial conditions (used only for 5-character element name).

NADD increment between the code numbers of two successive elements with identical initial conditions (used only for 5-character element name).

Record INCON.2 specifies fluid and heat equation primary variables.

Variables: Xl, X2, X3

Format: 3E20.14

A set of fluid and heat primary variables for the element specified in record INCON.l. INCON specifications will supersede default conditions specified in PARAM.4, and domain-specific conditions that may have been specified in data block INDOM.

Record INCON.3

A blank record closes the INCON data block. Alternatively, initial condition information may terminate on a record with '+++' typed in the first three columns, followed by time stepping information. This feature is used for a continuation run from a previous TOUGH2 simulation.

SOLVR: (optional) introduces a data block with parameters for linear equation solvers.

Record SOLVR.1

Variables: MATSLV, ZPROCS, OPROCS, RITMAX, CLOSUR

Format: I1, 2X, A2, 3X, A2, 2E10.4

MATSLV: selects the linear equation solver.

= 1: Default (DSLUCS)

= 2: DSLUBC.

= 3: DSLUCS.

= 4: DSLUGM.

= 5: DLUSTB.

= 6: LUBAND.

ZPROCS selects the Z-preconditioning (Moridis and Pruess, 1998). Regardless of user specifications, Z-preprocessing will only be performed when iterative solvers are used ($2 \leq$MATSLV≤ 5), and if there are zeros on the main diagonal of the Jacobian matrix.

= Z0: no Z-preprocessing (default for NEQ=1)

= Z1: replace zeros on the main diagonal by a small constant (1.e-25; default for NEQ$\neq$1)

= Z2: make linear combinations of equations for each grid block to achieve non-zeros on the main diagonal

= Z3: normalize equations, followed by Z2

= Z4: affine transformation to unit main-diagonal submatrices, without center pivoting

OPROCS: selects the O-preconditioning (Moridis and Pruess, 1998).

= O0: no O-preprocessing (default, also invoked for NEQ=1)

= O1: eliminate lower half of the main-diagonal submatrix with center pivoting

= O2: O1, plus eliminate upper half of the main-diagonal submatrix with center pivoting

= O3: O2, plus normalize, resulting in unit main-diagonal submatrices.

= O4: affine transformation to unit main-diagonal submatrices, without center pivoting

RITMAX selects the maximum number of CG iterations as a fraction of the total number of equations ($0.0<RITMAX\leq 1.0$; default is RITMAX=0.1)

CLOSUR convergence criterion for the CG iterations ($1.e\text{-}12\leq CLOSUR\leq 1.e\text{-}6$; default is CLOSUR=1.e-6)

FOFT: (optional) introduces a list of elements (grid blocks) for which time-dependent data are to be written out for plotting to a file called FOFT during the simulation.

Record FOFT.1

FOFT is an element name. Repeat for up to 100 elements, one per record.

Variables: EOFT (I)

Format: A5

Record FOFT.2 A blank record closes the FOFT data block.

COFT: (optional) introduces a list of connections for which time-dependent data are to be written out for plotting to a file called COFT during the simulation.

Record COFT.1

ECOFT is a connection name, i.e., an ordered pair of two element names.

Variable: ECOFT (I)

Format: A10

Repeat for up to 100 connections, one per record.

Record COFT.2

A blank record closes the COFT data block.

GOFT: (optional) introduces a list of sinks/sources for which time-dependent data are to be written out for plotting to a file called GOFT during the simulation.

Record GOFT.1

Variables: EGOFT (I)

Format: A5

EGOFT is the name of an element in which a sink/source is defined. Repeat for up to 100 sinks/sources, one per record. When no sinks or sources are specified here, by default tabulation will be made for all.

Record GOFT.2 A blank record closes the GOFT data block.

NOVER: (optional) one record with NOVER typed in columns 1-5 will suppress printing of a summary of versions and dates of the program units used in a TOUGH2 run.

DIFFUSION (optional; needed only for NB≥8) introduces diffusion coefficients.

Record DIFFU.1

Diffusion coefficients for mass component #1 in all phases (I=1: gas; I=2: aqueous; etc.)

Variables: FDDIAG(I,1),I=1,NPH

Format: 8E10.4

Record DIFFU.2

Variables: FDDIAG(I,2),I=1,NPH

Format:8E10.4

FDDIAG diffusion coefficients for mass component #2 in all phases (I=1: gas; I=2: aqueous; etc.) provide a total of NK records with diffusion coefficients for all NK mass components.

SELEC: (optional) introduces a number of integer and floating point parameters that are used for different purposes in different TOUGH2 modules.

Record SELEC.1

Variables: IE (I), I=1, 16

Format: 16I5

IE (I) number of records with floating point numbers that will be read (default is IE(1) = 1; maximum values is 64).

Record SELEC.2, SELEC.3, ..., SELEC.IE(1)*8

provide as many records with floating point numbers as specified in IE(1), up to a maximum of 64 records

Variables: FE(I), I=1,IE(1)*8

Format: 8E10.4

RPCAP introduces information on relative permeability and capillary pressure functions, which will be applied for all flow domains for which no data were specified in records ROCKS.1.2 and ROCKS.1.3. A catalog of relative permeability and capillary pressure functions is presented in Appendix B and Appendix C, respectively.

Record RPCAP.1

Variables: IRP, (RP (I), I = 1, 7)

Format: I5, 5X, 7E10.4

IRP: integer parameter to choose type of relative permeability function (see Appendix B).

RP (I) I = 1, ..., 7 parameters for relative permeability function (Appendix B).

Record RPCAP.2

Variable: ICP, (CP (I), I = 1, 7)

Format: I5, 5X, 7E10.4

ICP integer parameter to choose type of capillary pressure function (see Appendix C).

CP(I) I = 1, ..., 7 parameters for capillary pressure function (Appendix C).

TIMES permits the user to obtain printout at specified times (optional). This printout will occur in addition to printout specified in record PARAM.1.

Record TIMES.1

Variables: ITI, ITE, DELAF, TINTER

Format: 2I5, 2E10.4

ITI number of times provided on records TIMES.2, TIMES.3, etc., (see below; restriction: ITI $\leq$ 100).

ITE total number of times desired (ITI $\leq$ ITE $\leq$ 100; default is ITE = ITI).

DELAF maximum time step size after any of the prescribed times have been reached (default is infinite).

TINTER time increment for times with index ITI, ITI+1, ..., ITE.

Record TIMES.2, TIMES.3, etc.

Variables: TIS (I), I = l, ITI

Format: 8E10.4

TIS (I) list of times (in ascending order) at which printout is desired.

ELEME introduces element (grid block) information.

Record ELEME.1

Variables: ELEM, NSEQ, NADD, MA1, MA2, VOLX, AHTX, PMX, X, Y, Z

Format: A5,2I5,A3,A2,6E10.4

ELEM five-character code name of an element.

NSEQ number of additional elements having the same volume and belonging to the same reservoir domain (used only for 5-character element name).

NADD increment between the code numbers of two successive elements. (Note: the maximum permissible code number NE + NSEQ *NADD is ≤ 99 and used only for 5-character element name)

MA1, MA2 a five-character material identifier corresponding to one of the reservoir domains as specified in block ROCKS. If the first three characters are blanks and the last two characters are numbers then they indicate the sequence number of the domain as entered in ROCKS. If both MA1 and MA2 are left blank the element is by default assigned to the first domain in block ROCKS.

VOLX element volume (m^3).

AHTX interface area (m^2) for heat exchange with semi-infinite confining beds.

PMX permeability modifier (optional, active only when a domain ‘SEED’ has been specified in the ROCKS block), will be used as multiplicative factor for the permeability parameters from block ROCKS. Simultaneously, strength of capillary pressure will be scaled as 1/SQRT (PMX). PMX=0 will results in an impermeable block. Radom permeability modifiers can be generated internally. The PMX may be used to specify spatially correlated heterogeneous fields, but users need their own preprocessing programs for this, as TOUGH2 provides no internal capabilities for generating such fields.

X, Y, Z Cartesian coordinates of grid block centers. These may be included in the ELEME data to make subsequent plotting of results more convenient. Repeat record ELEME.1 for the number of elements desired.

Record ELEME.2

A blank record closes the ELEME data block.

CONNE introduces information for the connections (interfaces) between elements.

Record CONNE.1

Variables: ELEM1, ELEM2, NSEQ, NAD1, NAD2, ISOT, D1, D2, AREAX, BETAX, SIGX

Format: A5,A5,4I5,5E10.4)

ELEM1 code name of the first element.

ELEM2 code name of the second element.

NSEQ number of additional connections in the sequence (used only for 5-character element).

NAD1 increment of the code number of the first element between two successive connections (used only for 5-character element).

NAD2 increment of the code number of the second element between two successive connections (used only for 5-character element).

ISOT set equal to 1, 2, or 3; specifies absolute permeability to be PER (ISOT) for the materials in elements (EL1, NE1) and (EL2, NE2), where PER is read in block ROCKS. This allows assignment of different permeability, e.g., in the horizontal and vertical direction.

D1, D2 distance (m) from first and second element, respectively, to their common interface.

AREAX interface area (m^2).

BETAX cosine of the angle between the gravitational acceleration vector and the line between the two elements. GF * BETAX > 0 (<0) corresponds to first element being above (below) the second element.

SIGX "radiant emittance" factor for radiative heat transfer, which for a perfectly "black" body is equal to 1. The rate of radiative heat transfer between the two grid blocks is

$$G_{rad} = SIGX * \sigma_0 * AREAX * \left(T_2^4 - T_1^4\right) \tag{5.1}$$

where σ_0 = 5.6687e-8 J/m^2 K^4 s is the Stefan-Boltzmann constant, and T_1 and T_2 are the absolute temperatures of the two grid blocks. SIGX may be entered as a negative number, in which case the absolute value will be used, and heat conduction at the connection will be suppressed. SIGX = 0 will result in no radiative heat transfer.

Repeat record CONNE.1 for the number of connections desired.

Record CONNE.2

A blank record closes the CONNE data block. Alternatively, connection information may terminate on a record with '+++' typed in the first three columns, followed by element cross-referencing information. This is the termination used when generating a MESH file with TOUGH2-EGS-MP.

GRMOD set properties for a grid block range. Properties are set for a grid block index range KJI given by

$$KJI = (I-1) * NUMI + (J-1) * NUMJ + (K-1) * NUMK + KJI0 \tag{5.2}$$

where index *I* varies from *I1* to *I2*, index *J* varies from *J1* to *J2*, and index *K* varies from *K1* to *K2*. For MINC (Multiple Interacting Continua) simulations, *KJI* refers to the primary grid (before subdivision into multiple interacting continua) and the parameter *JMINC* refers to one of the continua. Continua in a

MINC grid block are assumed to be numbered consecutively from 1 to *NMINC* (number of multiple interacting continua), for example, in a double-porosity fracture-matrix system, fracture is 1 and matrix is 2.

Record GRMOD.1

Variables: TYPE, NUMI, NUMJ, NUMK, KJI0, JMINC

Format: A5, 5X, 5I10

TYPE must be "COEFS."

NUMI gridblock index multiple for I.

NUMJ gridblock index multiple for J.

NUMK gridblock index multiple for K.

KJI0: gridblock index offset.

JMINC MINC index, 1≤JMINC≤NMINC.

Record GRMOD.2.1

Variables: PROP, ISOT, I1, I2, J1, J2, K1, K2, VALUE

Format: A5, I5,6(I10),E10.4

PROP Property identifier must be PERM, permeability, m^2.

IDIR Permeability direction, ISOT = 1, 2, or 3.

I1 Start index for gridblock index multiple I.

I2 End index for gridblock index multiple I.

J1 Start index for gridblock index multiple J.

J2 End index for gridblock index multiple J.

K1 Start index for gridblock index multiple K.

K2 End index for gridblock index multiple K.

VALUE Property value.

Record GRMOD.2.2

Variables: PROP, I1, I2, J1, J2, K1, K2, VALUE

Format: A5, 5X,6(I10),E10.4

PROP Property identifier, options are:

POROS - porosity;

PRESS - pressure, Pa;

PVAR2 - primary variable position 2;

PVAR3 - primary variable position 3;

TEMPR - temperature, ℃;

STRES - mean stress, Pa.

The variables *I1*, *I2*, *J1*, *J2*, *K1*, *K2* and *VALUE* have the same meaning as previous record.

Record GRMOD.2.3

Variables: PROP, I1, I2, J1, J2, K1, K2, IVALUE

Format: A5, 5X,6(I10),I10

PROP Property identifier, options are:

BNDST - boundary status for mean stress equation, values are

0: gridblock does not border surroundings;

1: gridblock borders surroundings;

MATRG - material region.

The variables *I1*, *I2*, *J1*, *J2*, *K1*, *K2* have the same meaning as previous record

IVALUE Property value (integer).

Record GRMOD.3

A blank record closes the GRMOD data block.

Data specified from a GRMOD.1 record are in effect until they are overwritten by that from a subsequent record. Any number of GRMOD records may appear. Entered grid block properties overwrite previous ones.

GENER introduces sinks or sources, or specify initial stress for specified grid blocks.

Record GENER.1

Variables: EL1, SL1, NSEQ, NADD, NADS, LTAB, TYPE, ITAB, GX, EX,HX

Format: A5, A5, 4I5, 5X, A4, A1, 3E10.4)

EL1 code name of the element containing the sink/source, or reference initial stress.

SL1 code name of the sink/source or reference initial stress. The first three characters are arbitrary; the last two characters must be numbers.

NSEQ number of additional sinks/sources with the same injection/production rate, or same reference initial stress (not applicable for TYPE = DELV).

NADD increment between the code numbers of two successive elements with identical sink/source, or reference initial stress.

NADS increment between the code numbers of two successive sinks/sources only for 5-character element).

LTAB number of points in table of generation rate versus time. Set 0 or 1 for constant generation rate. For wells on deliverability, LTAB denotes the number of open layers, to be specified only for the bottommost layer.

TYPE specifies different options for fluid or heat production and injection. For example, different fluid components may be injected, the nature of which depends on the EOS module being used. Different options for considering wellbore flow effects may also be specified.

HEAT	introduces a heat sink/source
WATE	component 1(water), injection only
COM1	component 1 (water), injection only
COM2	component 2, injection only
MASS	mass production rate specified.
DELV	well on deliverability, i.e., production occurs against specified bottomhole pressure. If well is completed in more than one layer, bottommost layer must be specified first, with number of layers given in LTAB. Subsequent layers must be given sequentially for a total number of LTAB layers.
RSTR	reference inital stress at a specified elevation and temperature used only for stress initialization
DELT	heat loss occurs against a specified temperature

ITAB unless left blank, table of specific enthalpies will be read (LTAB > 1 only)

GX constant generation rate; positive for injection, negative for production; GX is mass rate (kg/sec) for generation types COMl, COM2, and MASS; it is energy rate (J/s) for a HEAT sink/source.

For wells on deliverability, GX is productivity index PI (m^3);

For reference stress calculation, GX is reference initial stress (Pa). The stress of other grid blocks will be calculated from this reference stress under stress equilibrium condition.

For heat loss against a specified temperature, GX is heat transfer coefficient ($J/s\text{-}m^2$)

EX fixed specific enthalpy (J/kg) of the fluid for mass injection (GX>0). For wells on deliverability against fixed bottomhole pressure, EX is bottomhole pressure P_{wb} (Pa), at the center of the topmost producing layer in which the well is open.

HG thickness of layer (m; wells on deliverability with specified bottomhole pressure only).

Record GENER.l.l (optional, LTAB > l only)

Variables: Fl(L), L=l, LTAB

Format: 4E14.7

F1 generation times

Record GENER.1.2 (optional, LTAB > 1 only)

Variable: F2 (L), L=1, LTAB

Format (4E14.7)

F2: generation rates.

Record GENER.1.3 (optional, LTAB > 1 and ITAB non-blank only)

Variables: F3 (L), L=1, LTAB

Format: 4E14.7

F3 specific enthalpy of produced or injected fluid.

Repeat records GENER.1, 1.1, 1.2, and 1.3 for the number of sinks/sources desired.

Record GENER.2

A blank record closes the GENER data block.

Alternatively, generation information may terminate on a record with '+++' typed in the first three columns, followed by element cross-referencing information.

ENDCY closes the input file and initiates the simulation.

Note on closure of blocks CONNE, GENER, and INCON

The ordinary way to indicate the end of any of the above data blocks is by means of a blank record. There is an alternative available if the user makes up an input file from files MESH, GENER, or SAVE, which have been generated by a previous run. These files are written exactly according to the specifications of data blocks ELEME and CONNE (file MESH), GENER (file GENER), and INCON (file SAVE), except that the CONNE, GENER, and INCON data terminate on a record with "+++" in columns 1-3, followed by some cross-referencing and restart information. TOUGH2-EGS-MP will accept this type of input, and in this case there is no blank record at the end of indicated data block.

5.2 Input Formats for MESHMAKER

The MESHMaker module performs internal mesh generation and processing. The input for MESHMaker has a modular structure and a variable number of records; it begins with keyword MESHM and ends with a blank record.

At the present time there are three sub-modules available in MESHMaker: keywords RZ2D or RZ2DL invoke generation of a one or two-dimensional radially symmetric R-Z mesh; XYZ

initiates generation of a one, two, or three dimensional Cartesian X-Y-Z mesh; and MINC calls a modified version of the GMINC program (Pruess, 1983) to sub-partition a primary porous medium mesh into a secondary mesh for fractured media, using the method of "multiple interacting continua" (Pruess and Narasimhan, 1985). The meshes generated under keyword RZ2D or XYZ are internally written to file MESH. The MINC processing operates on the data in file MESH, so that invoking the RZ2D or XYZ options, or assignment of ELEME and CONNE blocks in the INPUT file must precede the MESHMaker/MINC data. We shall now separately describe the preparation of input data for the three MESHMaker sub-modules.

5.2.1 Generation of radially symmetric grids

Keyword RZ2D (or RZ2DL) invokes generation of a radially symmetric mesh. Values for the radii to which the grid blocks extend can be provided by the user or can be generated internally (see below). Nodal points will be placed half-way between neighboring radial interfaces. When RZ2D is specified, the mesh will be generated by columns; i.e., in the ELEME block we will first have the grid blocks at smallest radius for all layers, then the next largest radius for all layers, and so on. With keyword RZ2DL the mesh will be generated by layers; i.e., in the ELEME block we will first have all grid blocks for the first (top) layer from smallest to largest radius, then all grid blocks for the second layer, and so on. Apart from the different ordering of elements, the two meshes for RZ2D and RZ2DL are identical. Assignment of inactive elements would be made by using a text editor on the RZ2D-generated MESH file, and moving groups of elements towards the end of the ELEME block, past a dummy element with zero volume. RZ2D makes it easy to declare a vertical column inactive, facilitating assignment of boundary conditions in the vertical, such as a gravitationally equilibrated pressure gradient. RZ2DL on the other hand facilitates implementation of areal (top and bottom layer) boundary conditions.

RADII is the first keyword following RZ2D; it introduces data for defining a set of interfaces (grid block boundaries) in the radial direction.

Record RADII.l

Variables: NRAD

Format: I5

NRAD number of radius data that will be read. At least one radius must be provided, indicating the inner boundary of the mesh.

Record RADII.2, RADII.3, etc.

Variables: RC(I), I = 1, NRAD

Format: 8E10.4

RC(I) a set of radii in ascending order.

Record EQUID. L

Equidistant introduces data on a set of equal radial increments.

Variables: NEQU, DR

Format: I5, 5X, E10.4

NEQU number of desired radial increments.

DR magnitude of radial increment.

Note: At least one radius must have been defined via block RADII before EQUID can be invoked.

Record LOGAR. l

Logarithmic introduces data on radial increments that increase from one to the next by the same factor ($R_{n+l} = f \bullet R_n$).

Variables: NLOG, RLOG, DR

Format: A5, 5X, 2E10.4

NLOG number of additional interface radii desired.

RLOG desired radius of the last (largest) of these radii.

DR reference radial increment: the first R generated will be equal to f • DR, with f internal determined such that the last increment will bring total radius to RLOG.f < 1 for decreasing radial increments is permissible. If DR is set equal to zero, or left blank, the last increment DR generated before keyword LOGAR will be used as default.

Additional blocks RADII, EQUID, and LOGAR can be specified in arbitrary order.

Note: At least one radius must have been defined before LOGAR can be invoked. If DR = 0, at least two radii must have been defined.

LAYER introduces information on horizontal layers, and signals closure of RZ2D input data.

Record LAYER. L

Variables: NLAY

Format: I5

NLAY number of horizontal grid layers.

Record LAYER.2

Variables: H(I), I = 1, NLAY

Format: 8E10.4

H(I) a set of layer thicknesses, from top layer downward. By default, zero or blank entries for layer thickness will result in assignment of the last preceding non-zero entry. Assignment of a zero layer thickness, as needed for inactive layers, can be accomplished by specifying a negative value.

The LAYER data close the RZ2D data block. Note that one blank record must follow to indicate termination of the MESHM data block. Alternatively, keyword MINC can appear to invoke MINC-processing for fractured media (see below).

5.2.2 Generation of rectilinear grids

XYZ invokes generation of a Cartesian (rectilinear) mesh.

Record XYZ.l

Variables: DEG

Format: E10.4

DEG angle (in degrees) between the Y-axis and the horizontal. If gravitational acceleration (parameter GF in record PARAM.2) is specified positive, -90 ° < DEG < 90 ° corresponds to grid layers going from top down. Grids can be specified from bottom layer up by setting GF or BETA negative. Default (DEG = 0) corresponds to horizontal Y- and vertical Z-axis. X-axis is always horizontal.

Record XYZ.2

Variables: NTYPE, NO, DEL

Format: A2, 3X, I5, E10.4

NTYPE set equal to NX, NY or NZ for specifying grid increments in X, Y, or Z direction.

NO number of grid increments desired.

DEL constant grid increment for NO grid blocks, if set to a non-zero value.

Record XYZ.3 (optional, DEL = 0. or blank only)

Variables: DEL (I), I = 1, NO

Format: 8E10.4

DEL(I) a set of grid increments in the direction specified by NTYPE in record XYZ.2. Additional records with formats as XYZ.2 and XYZ.3 can be provided, with X, Y, and Z-data in arbitrary order.

Record XYZ.4 a blank record closes the XYZ data block.

Note that the end of block MESHMaker is also marked by a blank record. Thus, when MESHMaker/XYZ is used, there will be two blank records at the end of the corresponding input data block.

5.2.3 MINC processing for fractured media

MINC invokes post processing of a primary porous medium mesh from file MESH. The input formats in data block MINC are identical to those of the GMINC program (Pruess, 1983), with two enhancements: there is an additional facility for specifying global matrix-matrix connections ("dual permeability"); further, only active elements will be subjected to MINC-processing, the remainder of the MESH remaining unaltered as porous medium grid blocks.

PART is the first keyword following MINC; it will be followed on the same line by parameters TYPE and DUAL with information on the nature of fracture distributions and matrix-matrix connections.

Variables: PART, TYPE, DUAL

Format: 2A5, 5X, A5

PART identifier of data block with partitioning parameters for secondary mesh.

TYPE a five-character word for selecting one of the six different proximity functions provided in MINC (Pruess, 1983).

ONE-D: a set of plane parallel infinite fractures with matrix block thickness between neighboring fractures equal to PAR(l).

TWO-D: two sets of plane parallel infinite fractures, with arbitrary angle between them. Matrix block thickness is PAR(l) for the first set, and PAR(2) for the second set. If PAR(2) is not specified explicitly, it will be set equal to PAR(l).

THRED: three sets of plane parallel infinite fractures at right angles, with matrix block dimensions of PAR(l), PAR(2), and PAR(3), respectively. If PAR(2) and/or PAR(3) are not explicitly specified, they will be set equal to PAR(l) and/or PAR(2), respectively.

STANA: average proximity function for rock loading of Stanford large reservoir model (Lam et al., 1988).

STANB: proximity function for the five bottom layers of Stanford large reservoir model.

STANC: proximity function for top layer of Stanford large reservoir model.

Note: a user wishing to employ a different proximity function than provided in MINC needs to replace the function subprogram PROX(x) in file meshm.f with a routine of the form:

```
FUNCTION PROX(x)

PROX = (arithmetic expression in x)

RETURN

END
```

It is necessary that PROX(x) is defined even when x exceeds the maximum possible distance from the fractures, and that PROX = 1 in this case. Also, when the user supplies his/her own proximity function subprogram, the parameter TYPE has to be chosen equal to ONE-D, TWO-D, or THRED, depending on the dimensionality of the proximity function. This will assure proper definition of innermost nodal distance (Pruess, 1983).

DUAL is a five-character word for selecting the treatment of global matrix flow.

blank: (default) global flow occurs only through the fracture continuum, while rock matrix and fractures interact locally by means of interporosity flow (“double-porosity” model).

MMVER: global matrix-matrix flow is permitted only in the vertical; otherwise like the double-porosity model; for internal consistency this choice should only be made for flow systems with one or two predominantly vertical fracture sets.

MMALL: global matrix-matrix flow in all directions; for internal consistency only two continua, representing matrix and fractures, should be specified ("dual-permeability").

Record PART.l

Variables: J, NVOL, WHERE, (PAR(I), I = 1, 7)

Format: 2I3, A4, 7E10.4

J total number of multiple interacting continua (J < 36).

NVOL total number of explicitly provided volume fractions (NVOL < J). If NVOL < J, the volume fractions with indices NVOL+l, ..., J will be internally generated; all being equal and chosen such as to yield proper normalization to 1.

WHERE specifies whether the sequentially specified volume fractions begin with the fractures (WHERE = 'OUT ') or in the interior of the matrix blocks (WHERE = 'IN ').

PAR(I) I = 1, 7holds parameters for fracture spacing (see above).

Record PART.2.1, 2.2, etc.

Variables: VOL(I), I = 1, NVOL

Format: 8E10.4

VOL (I) volume fraction (between 0 and 1) of continuum with index I (for WHERE = 'OUT') or index J+ l - I (for WHERE = 'IN'). NVOL volume fractions will be read. For WHERE = 'OUT', I = 1 is the fracture continuum, I = 2 is the matrix

continuum closest to the fractures, I = 3 is the matrix continuum adjacent to I = 2, etc. The sum of all volume fractions must not exceed 1.

5.3 Special input requirements

5.3.1 Mesh files

In TOUGH2-EGS-MP, MESHA and MESHB files are used or generated to replace original MESH files. The purpose of replacing file MESH (or blocks ELEME and CONNE in an input file) with MESHA and MESHB is to reduce the memory requirement for the master processor and to enhance I/O efficiency. Both MESHA and MESHB are binary files. These two files contain all information provided by file MESH. There are two groups of large data blocks within a TOUGH2-EGS-MP mesh file: one with dimensions equal to the number of grid blocks, the other with dimensions equal to the number of connections (interfaces). To read and use computer memory efficiently, the input data are organized in sequential and binary format. Large data blocks are read one by one through a temporary full-size array and then distributed to processors one by one. This method avoids storing all input data in one single processor and enhances the I/O efficiency and total storage capacity.

The file MESHA is written (to file unit 20 that was opened as an unformatted file) in the following sequence:

```
write(20) NEL,NCON

write(20) (EVOL(iI),iI=1,NEL)

write(20) (AHT(iI),iI=1,NEL)

write(20) (PMX(iI),iI=1,NEL)

write(20) (GCOORD(iI,1),iI=1,NEL)

write(20) (GCOORD (iI,2),iI=1,NEL)

write(20) (GCOORD (iI,3),iI=1,NEL)

write(20) (IMINC(iI),iI=1,NEL)
```

write(20) (DEL1(iI), iI=1,NCON)

write(20) (DEL2(iI), iI=1,NCON)

write(20) (AREA(iI), iI=1,NCON)

write(20) (BETA(iI), iI=1,NCON)

write(20) (SIG(iI), iI=1,NCON)

write(20) (ISOX(iI),iI=1,NCON)

write(20)(ELEM1(iI), iI=1,NCON)

write(20)(ELEM2(iI), iI=1,NCON)

where

NEL	total gridblock number, in 8-byte integer.
NCON	total connection number, in 8-byte integer.
EVOL	element volume (m3), in 8-byte real
AHT	interface area (m2) for heat exchange with semi-infinite confining beds, in 8-byte real.
PMX	permeability modifier, in 8-byte real.
GCOORD	Cartesian coordinates (X=1,Y=2,Z=3) of gridblock center, in 8-byte real.
IMINC	MINC continuum number, in 8-byte integer.
DEL1, DEL2	distance (m) from first and second element, respectively, to their common interface, in 8-byte real.
AREA	interface area (m2), in 8-byte real.
BETA	cosine of the angle between the gravitational acceleration vector and the line between two elements, in 8-byte real.
SIG	"radiant emittance" factor for radiative heat transfer, in 8-byte real.
ISOX	specify absolute permeability for the connection, in 4-byte integer.
ELEM1	code name for the first element of a connection, in 5 characters.
ELEM2	code name for the second element of a conection, in 5 characters.

The file MESHB is written (to file unit 30, unformatted) in the following sequence:

```
write(30) NCON,NEL
write(30) (ELEM(iI),iI=1,NEL)
write(30) (MA12(iI),iI=1,NEL)
write(30) (NEX1(iI),iI=1,NCON)
write(30) (NEX2(iI),iI=1,NCON)
```

where

ELEM code name of the element, in 5 characters.

MA12 material identifier of the element, in 5 characters.

NEX1, NEX2 first and second element number of the connection, in 4-byte integer.

MESHA and MESHB can also be created directly from MESH file through a preprocessing program. For extremely large problems, generation of MESHA and MESHB is the bottleneck of memory requirement for a simulation using TOUGH2-EGS-MP. By using a preprocessing program, the bottleneck for memory requirement can be avoided.

5.3.2 PARAL.prm and part.dat

PARAL.prm is an optional file providing TOUGH2-EGS-MP some parameters. If this file does not exist in the working folder, the code will take default parameters. These parameters are needed if a user wants to try different options with the parallel linear solver, partitioning algorithms, and main program. The following is an example of the file.

```
1008680, 4000000, 0
AZ_solver AZ_bicgstab
AZ_scaling AZ_BJacobi
AZ_precond AZ_dom_decomp
AZ_tol 1.0e-6
AZ_overlap 0
AZ_max_iter 250
AZ_conv AZ_rhs
AZ_subdomain_solve AZ_ilut
```

AZ_output AZ_none

EE_partitioner METIS_Kway

EE_output 100

END OF INPUTS

The three numbers at first line are:

MNEL Estimated total gridblocks, must be larger than model gridblock number.

MCON Estimated total connections must be larger than model connection number.

PartReady A parameter to inform the program that domain partitioning was done by a preprocessing program or will be done inside TOUGH2-EGS-MP. If PartReady=0, the parallel code will perform domain partitioning during running the code. If PartReady>0, the code will not perform domain partitioning and partition data will be read directly from file "part.dat" at the working directory. Default PartReady=0.

The default values of MNEL and NCON are 500,000 and 2,300,000. The two parameters are required only in generating MESHA and MESHB and when a model has more than 500,000 gridblocks or 2,300,000 connections.

From the second line and below, each line provides a parameter. These parameters give options or parameters for running the Aztec and METIS packages, and SAVE and SAVEST file output frequency control. The parameters can be in any order. If one parameter is not present, its default value will be used. Each line in the file consists of two terms. The first term is parameter's name and the second term is its value. Detailed content of the parameters is discussed below.

AZ_solver specifies solution algorithm, available solvers:

AZ_cg conjugate gradient (only applicable to symmetric positive definite matrices).

AZ_gmres restarted generalized minimal residual.

AZ_cgs conjugate gradient squared.

AZ_tfqmr transpose-free quasi-minimal residual.

AZ_bicgstab bi-conjugate gradient with stabilization.

AZ_lu sparse direct solver (single processor only).

AZ_scaling specifies scaling algorithm, user can select from:

AZ_none no scaling.

AZ_Jacobi point Jacobi scaling.

AZ_B Jacobi block Jacobi scaling where the block size corresponds to the VBR blocks.

Az_row_sum scale each row so the magnitude of its elements sum to 1.

AZ_sym_diag symmetric scaling so diagonal elements are 1.

AZ_sym_row_sum symmetric scaling using the matrix row sums.

AZ_precond specifies preconditioner. Available selections include:

AZ_none no preconditioning.

AZ_Jacobi k step Jacobi (or block Jacobi for DVBR matrices).

AZ_Neumann Neumann series polynomial.

AZ_ls least-squares polynomial.

AZ_sym_GS non-overlapping domain decomposition (additive Schwarz) k step symmetric Gauss-Seidel.

AZ_dom_decomp domain decomposition preconditioner (additive Schwarz).

AZ_tolspecifies tolerance value used in conjunction with convergence tests.

AZ_type_overlap determines how overlapping subdomain results are combined when different processors have computed different values for the same unknown. Available selections include:

- AZ_standard — the resulting value of an unknown is determined by the processor owning that unknown.
- AZ_symmetric — average the results obtained from different processors corresponding to the same unknown.

AZ_overlap determines the submatrices factored with the domain decomposition algorithms.

AZ_max_iter maximum number of iterations.

AZ_conv determines the residual expression used in convergence check and printing. Available selections include: AZ_r0, AZ_rhs, AZ_Anorm, AZ_noscaled, AZ_sol, AZ_weighted.

AZ_subdomain_solve specifies the solver to use on each subdomain when AZ_precond is set to AZ_dom_decomp, available selections include: AZ_lu, AZ_ilut, AZ_ilu, AZ_rilu, AZ_bilu, and AZ_icc.

AZ_reorder determines whether RCM reordering will be done in conjunction with domain decomposition incomplete factorizations, 1 yes; 0 no.

AZ_pre_calc indicates whether to use factorization information from previous calls to AZ_solve, three selections: AZ_calc, AZ_recalc, and AZ_reuse.

AZ_output specifies information to be printed, available selections: AZ_all, AZ_none, AZ_warnings, AZ_last, and >0.

EE_partitioner specifies the partitioner to be used, user can select partitioners from:

METIS_Kway uses the multilevel k-way partitioning algorithm. The objective of this partitioning method is to minimize the edge cut. It should be used to partition a graph into a large number of partitions (greater than 8).

METIS_Vkway uses the multilevel k-way partitioning algorithm. The objective of this partitioning method is to minimize the total communication volume.

METIS_Recursive uses multilevel recursive bisection. The objective of this partitioning method is to minimize the edgecut, this function should be used to partition a graph into a small number of partitions (less than 8).

EE_output Output control for solution results. The SAVE file will be written every EE_output time steps. If EE_output=0, no SAVE file will be written out until last time step. A special value of 666888 for this parameter will evoke debugging run, which will produce more informative output.

More options or parameters for the Aztec parallel linear equation solver can be specified. For further discussion, readers may refer to Tuminaro et al. (1999). Table 5.2 presents the default value used in TOUGH2-EGS-MP.

Table 5.2. Default values of the options and parameters

Parameters	Values
AZ_solver	AZ_bicgstab
AZ_scaling	AZ_Bjacobi
AZ_pecond	AZ_dom_decomp
AZ_tol	1x10-6
AZ_type_overlap	AZ_standard

AZ_max_iter	500
AZ_conv	AZ_r0
AZ_subdomain_solve	AZ_ilut
AZ_reorder	1
AZ_pre_calc	AZ_calc
AZ_output	AZ_none
EE_partitioner	METIS_Kway
EE_output	200

part.dat

If parameter "PartReady" in "PARAL.prm" has a value larger than 0, the parallel code will read file "part.dat" from working directory during run-time. The file contains domain-partitioning results. It is read by the following code:

```
open (unit=50,file='part.dat',form='formatted',status='old')

read(50,133) nparts, edgecut, NEL

read(50,144) (part(iI),iI=1,NEL) 133 format(3I10)

133 format(3I10)

144 format(10I8)
```

where

nparts number of portions, equal to the number of processors used, that the domain has been partitioned into.

edgecut number of cut edges.

nel total number of gridblocks in the simulation domain.

part partition for each gridblock, an integer value indicating the processor associated with each gridblock.

The file “part.dat” can be generated by the user through a preprocessing program.

5.4 Output from TOUGH2-EGS-MP

TOUGH2-EGS-MP produces a variety of output, most of which can be controlled by the user. Information written in the initialization phase on to the standard output file includes parameter settings in the main program for dimensioning of problem-size dependent arrays, and disk files in use. This is followed by documentation on settings of the MOP-parameters for choosing program options, and on the EOS-module. During execution, the parallel program can optionally generate a brief message for Newtonian iterations and time steps. At the end, a summary of subroutines used and parallel computation information are provided. In TOUGH2-EGS-MP, standard output at user-specified simulation times or time steps is generated by a subroutine called FINALOUT, contained in the EOS module. The output files in TOUGH2-EGS-MP are named OUTPUT and OUTPUT_DATA. The first file provides problem initialization, time-stepping, and parallel computing information, and the second file gives a complete report of grid block thermodynamic state variables and other important parameters. Grid block output from each processor is assembled into one for the global grid.

Figure 5.1 shows the parallel computing information, which is written out near the end of OUTPUT file. The output provides detailed information of the number of processors used, timing for tasks, code performance for each time step, Newton iteration, and linear iteration, algorithm used for domain partitioning, and domain decomposition results. At the end of the list of Figure 5.1, linear solver, preconditioner, and options and parameters selected for solving the linear equations are presented. This information is very important for evaluating the parallel code performance.

```
EEE Number of processors = 8
EEE Time perform model computaion = 36.9248681068420
EEE of which spent in lin. solv. = 25.6461408138275
EEE and spent on other = 11.2787272930145
EEE
EEE Total number of time steps = 49
EEE Average time in Aztec per time step = 0.523390628853623
EEE Average time spent on other per time step = 0.230178108020705
EEE
EEE Total number Newton steps = 110
```

```
EEE Average number of Newton steps per time step 2.24489795918367
EEE Average time per Newton step = 0.233146734671159
EEE Average time spent on other per Newton st = 0.102533884481950
EEE
EEE Total number of iter in Aztec = 6686
EEE Average number of iter per call to Aztec 60.7818181818182
EEE Average time per iter in Aztec = 3.835797309875488E-003
EEE
EEE Partitioning algorithm used: METIS_Kway
EEE Number of edges cut = 2411
EEE
EEE Average number elements per proc = 2050.00000000000
EEE Maximum number elements at any proc = 2085
EEE Minimum number elements at any proc = 1990
EEE Allocated LNEL = 2727
EEE Average number connections per proc = 6196.37500000000
EEE Minimum number connections at any proc = 6048
EEE Maximum number connections at any proc = 6404
EEE Allocated LMNCON = 6404
EEE
EEE Average number of neighbors per proc = 4.25000000000000
EEE Maximum number of neighbors at any proc = 6
EEE Minimum number of neighbors at any proc = 3
EEE
EEE Average number of external elem. per proc = 521.500000000000
EEE Maximum number of external elem. per proc = 651
EEE Minimum number of external elem. per proc = 404
EEE
EEE Maximum size for local matrix (in Kbyte) = 1193.00000000000
EEE Maximum size data in matvec (in Kbyte) = 1305.00000000000
EEE
EEE ====
EEE
EEE Linear Solver Used: BICGSTAB
EEE Scaling method: No Scaling
EEE Preconditioner: Domain Decomposition
EEE with overlap type: Standard
EEE and size of overlap: 0
EEE and subdomain solver: ILUT
EEE without RCM reordering
EEE Residual norm: ||r||2 / ||b||2
EEE Max. number of iterations: 250
EEE Tolerance: 1.000000000000000E-006
EEE ==========================================
```

Figure 5.1. Example for output of parallel computing information (OUTPUT file)

The second main output file OUTPUT_DATA gives a complete report of grid block thermodynamic state variables and other important parameters. The important variables in both output files are list as table 5.3.

Table 5.3 List of output variables

DELTEX	time step size, seconds
DG	gas phase density, kg/m^3
DL	liquid (aqueous phase) density, kg/m^3
DT	time step size, seconds
DW	water (aqueous phase) density, kg/m^3
DX1, DX2, etc.	changes in first, second, etc. thermodynamic variable
DX1M, DX2M, DX3M	maximum change in first, second, and third primary variable in current time step
ELEM	code name of element
ELEM1, ELEM2	code name of first and second element, respectively, in a flow connection
ENTHALPY	flowing specific enthalpy for mass sinks/sources, J/kg
FF(GAS), FF(LIQ)	mass fraction of flow in gas and liquid phases, respectively (mass production wells only)
FLO(BRINE)	total rate of brine flow, kg/s (positive if from ELEM2 into ELEM1)

FLOF	total rate of fluid flow, kg/s (positive if from ELEM2 into ELEM1)
FLO(GAS)	total rate of gas flow, kg/s (positive if from ELEM2 into ELEM1)
FLOH	total rate of heat flow, W (positive if from ELEM2 into ELEM1)
FLO(LIQ)	total rate of liquid (aqueous phase) flow, kg/s (positive if from ELEM2 into ELEM1)
GENERATION RATE	sink (> 0) or source (< 0) rate, kg/s (mass), W (heat)
INDEX	internal indexing number of elements, connections, sinks/sources
ITER	number of Newtonian iterations in current time step
ITERC	total cumulative number of Newtonian iterations in simulation run
KCYC	time step counter
KER	index number of equation with largest residual
K(GAS)	gas phase relative permeability
K(LIQ)	liquid (aqueous) phase relative permeability

KON	convergence flag; KON = 2: converged; KON = 1: not converged
MAX. RES.	maximum (relative) residual in any of the mass and energy balance equations
NER	index number of element (grid block) with largest residual
P	pressure, Pa
PER.MOD.	permeability modification coefficient
PCAP	capillary pressure, Pa
PSAT	saturated vapor pressure, Pa
P(WB)	flowing bottomhole pressure (production wells on deliverability only), Pa
RH	Relative humidity
SG	gas saturation
SL	liquid saturation
SOURCE	code name of sink/source
ST	simulation time, in seconds
STRAIN	volumetric strain.
STRESS	mean normal stress.
SW	water (aqueous phase) saturation
T	temperature, ˚C
TOTAL TIME	simulation time, in seconds

VEL(GAS)	gas phase pore velocity, m/s (positive if from ELEM2 into ELEM1)
VEL(LIQ)	liquid (aqueous) phase pore velocity, m/s (positive if from ELEM2 into ELEM1)
VIS(LIQ)	liquid (aqueous) phase viscosity, Pa-s
X1, X2, etc.	first, second, etc. thermodynamic variable
XAIRG	mass fraction of air in gas phase
XAIRL	mass fraction of air in liquid phase

For a certain time-step plot, the OUTPUT_DATA file is shown as figure 5.2.

```
        OUTPUT DATA AFTER (   69,   3)-2-TIME STEPS                                          THE TIME IS  0.91250E+02 DAYS

@@@@@@@@@@@@@@@@@@@@@@@@@@@@@@@@@@@@@@@@@@@@@@@@@@@@@@@@@@@@@@@@@@@@@@@@@@@@@@@@@@@@@@@@@@@@@@@@@@@@@@@@@@@@@@@@@@@@@@@@@@@@@@@@@@

 TOTAL TIME      KCYC    ITER  ITERC    KON         DX1M         DX2M         DX3M          MAX. RES.      NER     KER         DELTEX
 0.78840E+07      69       3    317      2       0.25131E+04  0.13195E-03  0.13785E-02     0.26976E-08      9       1       0.93333E+06

@@@@@@@@@@@@@@@@@@@@@@@@@@@@@@@@@@@@@@@@@@@@@@@@@@@@@@@@@@@@@@@@@@@@@@@@@@@@@@@@@@@@@@@@@@@@@@@@@@@@@@@@@@@@@@@@@@@@@@@@@@@@@@@@@@@@

    ELEM.  INDEX      P            T           SG          SL           XAIRG        XAIRL        PER.MOD.    PCAP          DG           DL
    STRESS       STRAIN
                    (PA)       (DEG-C)                                                                       (PA)       (KG/M**3)    (KG/M**3)

0000J          19 0.39409E+07 0.23221E+03 0.77305E+00 0.22695E+00 0.32714E+00 0.16524E-03 0.10000E+01 -.10000E+06 0.21658E+02 0.82537E+03
0.28253E+08 0.98226E-06
0000K          20 0.39611E+07 0.23584E+03 0.76679E+00 0.23321E+00 0.27238E+00 0.13683E-03 0.10000E+01 -.10000E+06 0.21387E+02 0.82027E+03
0.30197E+08 0.12151E-05
0000L          21 0.39817E+07 0.23949E+03 0.76056E+00 0.23944E+00 0.21346E+00 0.10667E-03 0.10000E+01 -.10000E+06 0.21121E+02 0.81503E+03
0.32141E+08 0.12735E-05
0000M          22 0.40023E+07 0.24316E+03 0.75385E+00 0.24615E+00 0.15021E+00 0.74667E-04 0.10000E+01 -.10000E+06 0.20862E+02 0.80965E+03
0.34084E+08 0.12917E-05
0000N          23 0.40229E+07 0.24681E+03 0.74368E+00 0.25632E+00 0.82926E-01 0.41019E-04 0.10000E+01 -.10000E+06 0.20614E+02 0.80416E+03
0.36024E+08 0.12337E-05
0000O          24 0.40438E+07 0.25022E+03 0.72141E+00 0.27859E+00 0.16788E-01 0.82737E-05 0.10000E+01 -.10000E+06 0.20404E+02 0.79891E+03
0.37932E+08 0.13069E-05
0000P          25 0.40654E+07 0.25130E+03 0.71848E+00 0.28152E+00 0.11956E-04 0.59149E-08 0.10000E+01 -.10000E+06 0.20439E+02 0.79725E+03
0.39558E+08 0.15663E-05
0000Q          26 0.40862E+07 0.25160E+03 0.71822E+00 0.28178E+00 0.93404E-08 0.46478E-11 0.10000E+01 -.10000E+06 0.20547E+02 0.79679E+03
0.41089E+08 0.14367E-05
0000R          27 0.41068E+07 0.25190E+03 0.71817E+00 0.28183E+00 0.35188E-10 0.17611E-13 0.10000E+01 -.10000E+06 0.20654E+02 0.79634E+03
0.42616E+08 0.14414E-05
0000S          28 0.41275E+07 0.25220E+03 0.71814E+00 0.28186E+00 0.75731E-11 0.38121E-14 0.10000E+01 -.10000E+06 0.20762E+02 0.79589E+03
0.44141E+08 0.14614E-05
0000T          29 0.41483E+07 0.25250E+03 0.71811E+00 0.28189E+00 0.72645E-09 0.36779E-12 0.10000E+01 -.10000E+06 0.20870E+02 0.79544E+03
0.45663E+08 0.14824E-05
0001E          76 0.39409E+07 0.23221E+03 0.77305E+00 0.22695E+00 0.32715E+00 0.16524E-03 0.10000E+01 -.10000E+06 0.21658E+02 0.82537E+03
0.28253E+08 0.98179E-06
0001F          77 0.39612E+07 0.23584E+03 0.76678E+00 0.23322E+00 0.27240E+00 0.13684E-03 0.10000E+01 -.10000E+06 0.21387E+02 0.82027E+03
0.30197E+08 0.11969E-05
0001G          78 0.39818E+07 0.23949E+03 0.76056E+00 0.23944E+00 0.21349E+00 0.10668E-03 0.10000E+01 -.10000E+06 0.21122E+02 0.81503E+03
0.32141E+08 0.12579E-05
0001H          79 0.40024E+07 0.24316E+03 0.75385E+00 0.24615E+00 0.15024E+00 0.74687E-04 0.10000E+01 -.10000E+06 0.20863E+02 0.80965E+03
0.34084E+08 0.12761E-05
0001I          80 0.40230E+07 0.24681E+03 0.74369E+00 0.25631E+00 0.82974E-01 0.41044E-04 0.10000E+01 -.10000E+06 0.20614E+02 0.80416E+03
0.36024E+08 0.12181E-05
0001J          81 0.40439E+07 0.25022E+03 0.72150E+00 0.27850E+00 0.16860E-01 0.83094E-05 0.10000E+01 -.10000E+06 0.20405E+02 0.79891E+03
0.37932E+08 0.12943E-05
```

Figure 5.2 Snapshot of the OUTPUT_DATA file

6 EXAMPLE PROBLEMS

Seven sample problems are included in this section. They may be used as benchmarks for testing the code's capabilities and for verifying any changes to the recent codes. The input data files for each problem also can be used as templates to facilitate preparation of new simulations. The first three examples illustrate the accuracy of the geomechanical model against analytical solutions. The fourth example verifies results from other commercial simulator. The fifth example is a simulation with the MINC model in a dual porosity system. The sixth example simulates the Geyser geothermal field and is verified against published data. The last example shows the parallel computing capability and the computing performance of TOUGH2-EGS-MP.

6.1 1-D consolidation

6.1.1 Problem description

The 1-D consolidation problem is a porous and permeable column that undergoes uniaxial strain in the vertical direction. The column is subjected to a constant load on the top, the fluid boundary pressure is set to zero gauge right after the load is imposed, and only vertical displacement takes place as shown in Figure 6.1.

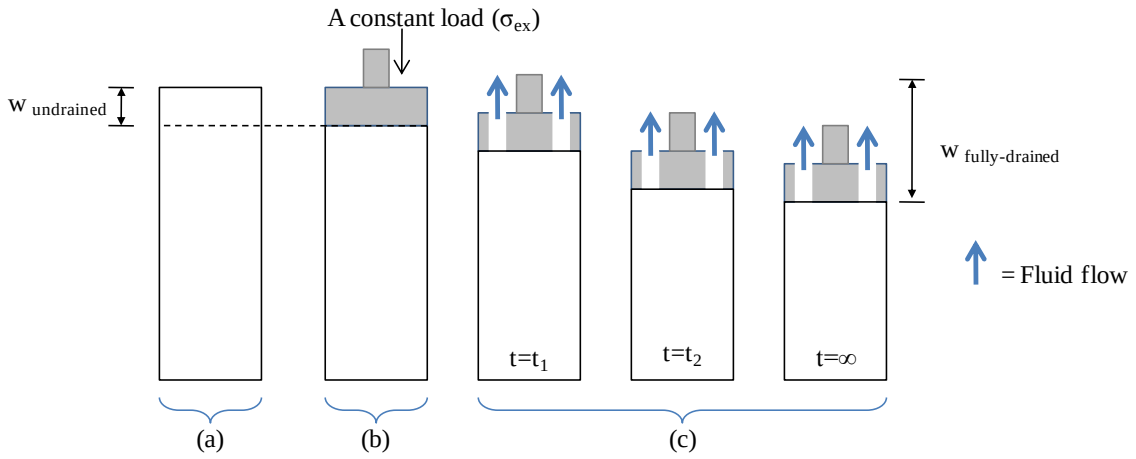

Figure 6.1 Evolution of column displacement for an 1-D consolidation problem; (a) The initial condition (no compaction); (b) the column is subjected to a constant load, pressure is being increased and no fluid is drained (undrained condition); (c) Fluid is drained from the column and pressure is being decreased (drained condition): Charoenwongsa et al. (2010).

6.1.2 Numerical simulation setup

We simulated this problem in two steps. The first step was the load application to produce the pore pressure increase, shown in Figures 6.1a to 6.1b. We started from a relaxed state where pore pressures and mean stress were initialized at 3.0 MPa and 5.0 MPa, respectively. Then, the additional vertical stress of 3.0 MPa was imposed at the column top that induced a pore pressure increase in the column after the system equilibrated; see the input data in Figure 6.2. 'OPTIO' 5 in 'GRMOD' entry was used to allow the in-equilibrium stress initialization. The model was run without sink or source term until reaching the equilibrium where the pore pressure was increased due to the additional load. Then, the 'SAVE' file, which contains the equilibrated results from the initialization, was renamed to 'INCON' and used as the initial condition for the next runs.

For uniaxial deformation in an isothermal medium, the additional mean stress can be calculated from the additional vertical stress, and pore pressures as follows:

$$\Delta\sigma_m = \frac{1}{3}\frac{(1+\nu)}{(1-\nu)}\left(\Delta\sigma_{zz} - \alpha\Delta p\right) + \alpha\Delta p \tag{6.1}$$

where ν is the Poisson's ratio, α is Biot constant, σ_{zz} is the z direction stress and σ_m is the mean effective stress.

The second step was simulation of fluid drainage, shown in Figure 6.1c. The column was initially at the above equilibrated state. We set the pore pressures at the column top to the initial pore pressures (3.0MPa). We also set the mean stress at the column top to that calculated from Equation 6.1 using the constant additional vertical-direction stress (3.0MPa). Fluid then drained out of the column top as the pore pressures in the column returned to the initial values from the input data in Figure 6.3. The detailed input parameters are shown in Table 6.1.

Table 6.1 Input parameters used in simulation of the 1-D consolidation problem

Parameters	**Value**	**Unit**
Rock properties (Berea sandstone)		
Elastic modulus (E)	8.0	GPa
Poisson ratio (ν)	0.20	
Porosity (ϕ)	0.20	
Permeability (k)	1.00×10^{-13}	m^2
Biot coefficient (α)	0.20	
Fluid properties		
Water viscosity (μ)	0.89	Pa.s
Water compressibility (c_w)	4.55×10^{-10}	Pa^{-1}
Initial and Boundary Conditions		
Pressure at relaxed condition	3.0	MPa
Mean stress at relaxed conditions	5.0	MPa
Imposed additional vertical stress	3.0	MPa

```
* ONE-DIMENSION CONSOLIDATION
ROCKS----1----*----2----*----3----*----4----*----5----*----6----*----7----*----8
ROCK1    5     2.e90      0.20    1.E-13    1.E-13    1.E-13       2.0     8.E99
4.4E-10
    7        0.45000    9.6E-4        1.
    7        0.45000    1.0E-3   8.0E-05      5.E8        1.
   00    0       0     0.2000    8.00E09     0.200     25.0
  0.00     0.0E6

ICOUP----1----*----2----*----3----*----4----*----5----*----6----*----7----*----8
       1         0
START----1----*----2----*----3----*----4----*----5----*----6----*----7----*----8
----*----1 MOP: 123456789*123456789*1234 ---*----5----*----6----*----7----*----8
PARAM----1----*----2----*----3----*----4----*----5----*----6----*----7----*----8
   29999     25000003010000002 47   1                   1.80
           1.00000E4  0.5e+01  100.0
     1.E-8     1.E00                                  1.E-7
             3.00e6               0.0E1                25.0

SOLVR----1----*----2----*----3----*----4----*----5----*----6----*----7----*----8
4  Z1   O0    8.0e-1    1.0e-7

TIMES----1----*----2----*----3----*----4----*----5----*----6----*----7----*----8
   3
 1.0e+03   4.0000E+3 1.0000E+4


GRMOD----1----*----2----*----3----*----4----*----5----*----6----*----7----*----8
COEFS              1         1         1         1         1
BNDST              1         1         1         1         1         1         1
STRES              1         1         1         1         1         1 6.5700E06   % for ini
STRES              1         1         1         1         2       400 5.0000E06   % for ini
OPTIO              5                                                             1


GENER----1----*----2----*----3----*----4----*----5----*----6----*----7----*----8

ELEME
00001              10.2500E+000.1000E+01          0.5000E+000.5000E+00-.1250E+00         0
00002              10.2500E+000.0000E+00          0.5000E+000.5000E+00-.3750E+00         0
00003              10.2500E+000.0000E+00          0.5000E+000.5000E+00-.6250E+00         0
00004              10.2500E+000.0000E+00          0.5000E+000.5000E+00-.8750E+00         0
00005              10.2500E+000.0000E+00          0.5000E+000.5000E+00-.1125E+01         0
00006              10.2500E+000.0000E+00          0.5000E+000.5000E+00-.1375E+01         0
00007              10.2500E+000.0000E+00          0.5000E+000.5000E+00-.1625E+01         0
00008              10.2500E+000.0000E+00          0.5000E+000.5000E+00-.1875E+01         0
00009              10.2500E+000.0000E+00          0.5000E+000.5000E+00-.2125E+01         0
0000A              10.2500E+000.0000E+00          0.5000E+000.5000E+00-.2375E+01         0
```

Figure 6.2 Input data for the initialization of 1-D consolidation

```
* ONE-DIMENSION CONSOLIDATION
ROCKS----1----*----2----*----3----*----4----*----5----*----6----*----7----*----8
ROCK1    5     2.e90      0.20    1.E-13    1.E-13    1.E-13       2.0     8.E99
4.4E-10
    7        0.45000    9.6E-4        1.
    7        0.45000    1.0E-3   8.0E-05      5.E8        1.
   00    0       0     0.2000    8.00E09     0.200     25.0
  0.00     0.0E6

ICOUP----1----*----2----*----3----*----4----*----5----*----6----*----7----*----8
       1         0
START----1----*----2----*----3----*----4----*----5----*----6----*----7----*----8
----*----1 MOP: 123456789*123456789*1234 ---*----5----*----6----*----7----*----8
PARAM----1----*----2----*----3----*----4----*----5----*----6----*----7----*----8
   29999     25000003010000002 47   1                   1.80
         1.00000E8  0.5e+01  000.0
     1.E-8     1.E00                                  1.E-7
             3.00e6               0.0E1                25.0

SOLVR----1----*----2----*----3----*----4----*----5----*----6----*----7----*----8
4  Z1   O0    8.0e-1    1.0e-7

TIMES----1----*----2----*----3----*----4----*----5----*----6----*----7----*----8
   3
 1.0e+03   4.0000E+3 1.0000E+4

GRMOD----1----*----2----*----3----*----4----*----5----*----6----*----7----*----8
COEFS              1         1         1         1         1
BNDST              1         1         1         1         1         1         1
STRES              1         1         1         1         1         1 6.5000E06
STRES              1         1         1         1         2       400 6.5700E06

ELEME
00001              10.2500E+000.1000E+01          0.5000E+000.5000E+00-.1250E+00
...

CONNE
0000100002                  30.1250E+000.1250E+000.1000E+010.1000E+01
...

INCON -- INITIAL CONDITIONS FOR  400 ELEMENTS AT TIME  0.100000E+09
00001           0.20000000E+00 0.10000000E-12 0.10000000E-12 0.10000000E-12
 0.3718557007113E+07 0.0000000000000E+00 0.2500000000000E+02
...

ENDCY
```

Figure 6.3 Input data for the drained condition of 1-D consolidation

6.1.3 Comparison of analytical solution and numerical results

The pressure comparison in Figure 6.4 indicates that our simulator produces essentially the same answers as the analytical solution. This agreement supports the credibility of our computational approach.

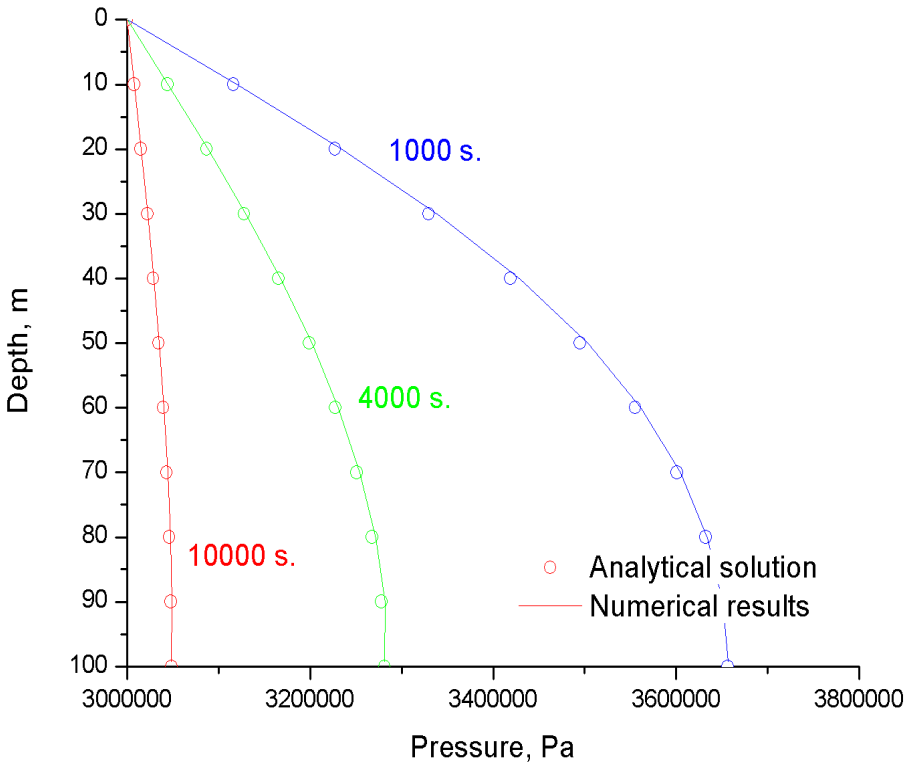

Figure 6.4 The comparison between numerical results and analytical solutions for pressure profiles

6.2 1-D heat conduction

6.2.1 Problem description

The 1-D heat conduction problem is an impermeable column that undergoes uniaxial strain in the vertical direction only. The column is subjected to a constant temperature on the top, and

only heat conduction occurs through the column. Here, 'OPTIO' 4 in 'GRMOD' entry was used to generate vertical displacement from the top column.

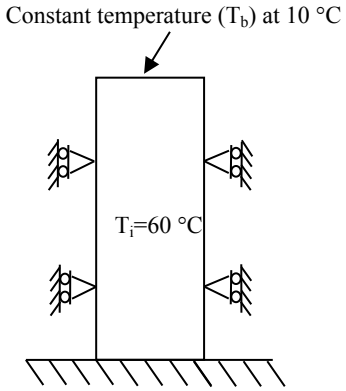

Figure 6.5 Problem description for 1-D heat conduction

6.2.2 Numerical simulation setup

An impermeable solid column with very small porosity was initialized with the temperature at 60 °C. A low temperature of 10 °C was imposed at the column top. Detailed input parameters are shown in Table 6.2, and the input data is shown in Figure 6.6.

Table 6.2 Input parameters for the 1D heat conduction problem

Parameters	**Value**	**Unit**
Rock properties (Berea sandstone)		
Elastic modulus (E)	14.40	GPa
Poisson ratio (ν)	0.20	
Porosity (ϕ)	0.01	
Heat conduction (k_T)	2.34	W/m°K
Heat capacity (c_v)	690	J/kg°K
Linear thermal expansion(β)	$1.5x10^{-6}$	$°K^{-1}$
Initial and Boundary Conditions		
Initial temperature condition	60	°C
Initial mean stress	2.0	MPa
A temperature at the top boundary	10	°C

```
* ONE-DIMENSION HEAT CONDUCTION
ROCKS----1----*----2----*----3----*----4----*----5----*----6----*----7----*----8
ROCK1    5     2550.    0.1e-1     0.E-13    0.E-13    0.E-13      2.34     690.2
4.4E-10   1.5E-6
    7        0.45000    9.6E-4        1.
    7        0.45000    1.0E-3   8.0E-05      5.E8        1.
    0    0         0      0.20   1.44E10    0.00      6.0E01
    0

ICOUP----1----*----2----*----3----*----4----*----5----*----6----*----7----*----8
       1         0
START----1----*----2----*----3----*----4----*----5----*----6----*----7----*----8
----*----1 MOP: 123456789*123456789*1234 ---*----5----*----6----*----7----*----8
PARAM----1----*----2----*----3----*----4----*----5----*----6----*----7----*----8
   29999     25000003000000002 47 0 1                    1.80
           1.10000E80.1000e03 0.1000e06
     1.E-6     1.E00                                  1.E-7
               5.0E6                 0.0              6.0E1
SOLVR----1----*----2----*----3----*----4----*----5----*----6----*----7----*----8
2  Z1   OO    8.0e-1    1.0e-7

TIMES----1----*----2----*----3----*----4----*----5----*----6----*----7----*----8
    3
 1.0000E+6 1.0000E+7 1.0000E+8

INCON----1----*----2----*----3----*----4----*----5----*----6----*----7----*----8
0001d
               5.0E6                 0.0              1.0E1

FOFT
00001

GRMOD----1----*----2----*----3----*----4----*----5----*----6----*----7----*----8
COEFS              1         1         1         1         1
BNDST              1         1         1         1       101       101         1
STRES              1         1         1         1         1       101 2.0000E06
OPTIO              4                                                         1

ELEME
00001              10.5000E+020.1000E+03          0.5000E+010.5000E+01-.2500E+00
00002              10.5000E+020.0000E+00          0.5000E+010.5000E+01-.7500E+00
00003              10.5000E+020.0000E+00          0.5000E+010.5000E+01-.1250E+01
00004              10.5000E+020.0000E+00          0.5000E+010.5000E+01-.1750E+01
00005              10.5000E+020.0000E+00          0.5000E+010.5000E+01-.2250E+01
00006              10.5000E+020.0000E+00          0.5000E+010.5000E+01-.2750E+01
00007              10.5000E+020.0000E+00          0.5000E+010.5000E+01-.3250E+01
```

Figure 6.6 TOUGH2-EGS input file for 1-D heat conduction problem

6.2.3 Comparison of analytical solution with numerical results

The temperature and displacement comparisons in Figure 6.7 indicate that our numerical results produce essentially the same answers as the analytical solutions for simulation of heat flow.

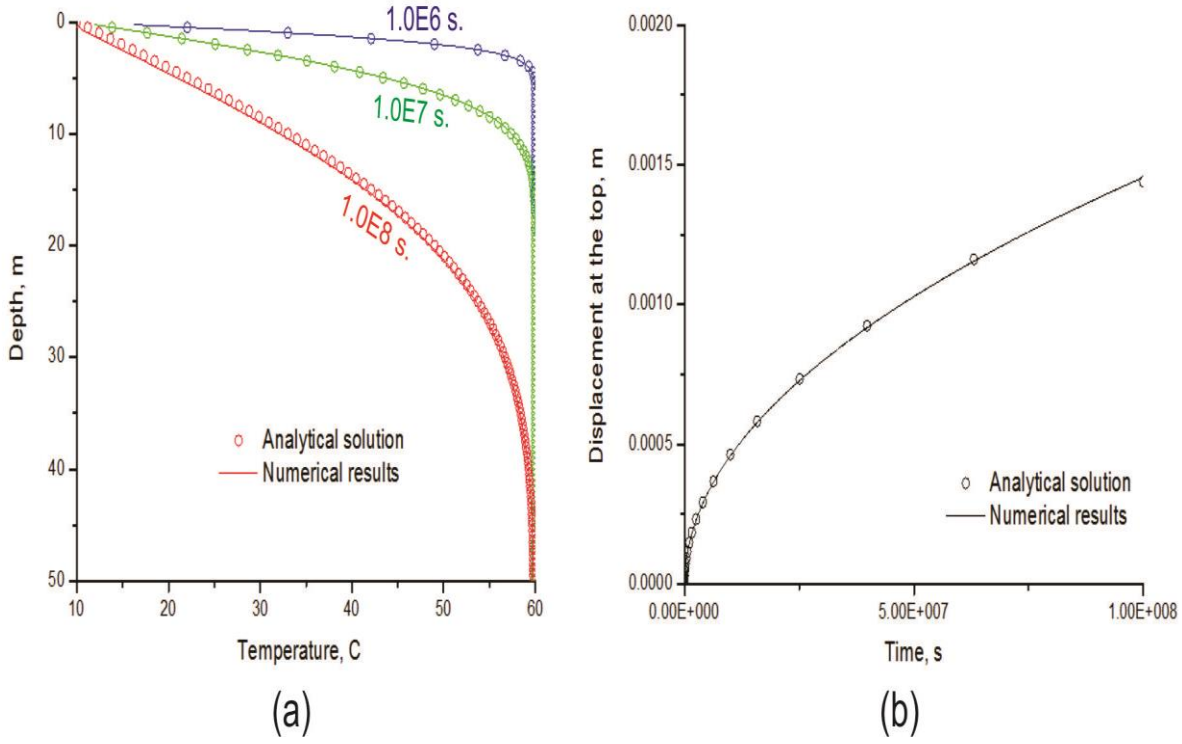

Figure 6.7. The comparison between numerical results and analytical solutions: (a) pressure profiles and (b) the displacement of the top column.

6.3 2-D compaction

6.3.1 Problem description

A constant compressive force is applied to the top of a fluid-filled poroelastic material, inducing an instantaneous uniform pore pressure increase and compression (Figure 6.8). Afterwards, the material is allowed to drain laterally. Because the pore pressure near the edges must decrease due to drainage, the material there becomes less stiff and there is a load transfer to the center, resulting in a further increase in center pore pressure that reaches a maximum

and then declines. This pore pressure behavior is called the Mandel-Cryer effect (Mandel, 1953) and Abousleiman and et al., (1996) present an analytical solution to the above problem

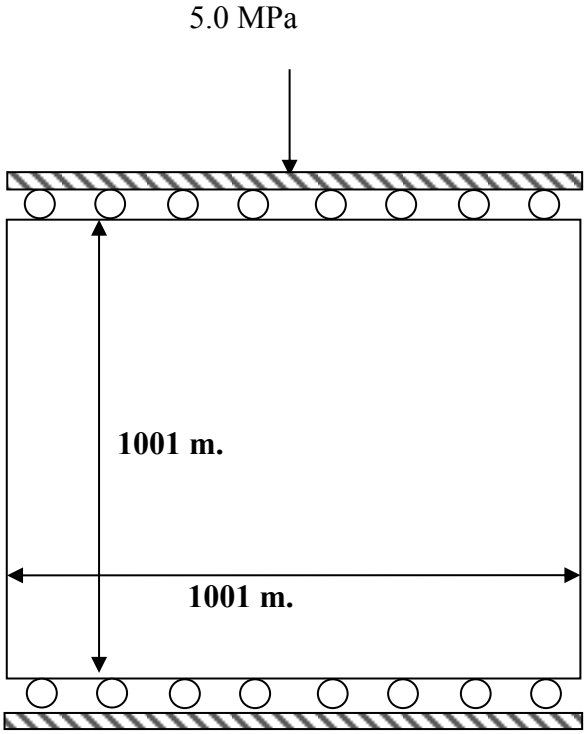

that we compare our simulated results to.

Figure 6.8 Problem description for 2-D compaction

6.3.2 Numerical simulation setup

We simulated this problem in two steps, as we did for the 1-D consolidation problem. The first step was to simulate the application of force that induced the pore pressure increase. We started from the initial state where pore pressure and mean stress were initialized at 0.1 MPa and 0.1 MPa, respectively. Then, the addition stress was imposed of 5.0 MPa was imposed and produced the pore pressure increase. We then allowed the system to reach equilibrium. Next, we simulated fluid drainage. The system was allowed to drain from both sides that were set at a constant pressure of 0.1 MPa. Table 6.3 contains simulation parameters and Figure 6.8 shows the sample input files.

Table 6.3 input parameters used in simulation of the 2-D compaction problem

Parameters	**Value**	**Unit**
Rock properties		
Elastic modulus (E)	5.0	GPa
Poisson ratio (ν)	0.25	
Porosity (ϕ)	0.10	
Permeability (k)	1.00×10^{-14}	m^2
Biot coefficient (α)	1.0	
Fluid properties		
Water viscosity (μ_w)	0.89	Pa.s
Water compressibility (c_w)	4.5×10^{-10}	Pa^{-1}
Initial and Boundary Conditions		
Pressure at relaxed condition	0.1	MPa
Mean stress at related condition	0.1	MPa
Additional stress on the top	5.1	MPa
Pressure at the lateral sides	0.1	MPa

```
2-D compaction or Mandel-Cryer
ROCKS----1----*----2----*----3----*----4----*----5----*----6----*----7----*----8
ROCK1    3  2260.e20     0.100   1.0e-13   1.0e-13   1.0e-13      2.51     900.
   0.0e-10       0.0
    1           0.00      0.00       1.0       1.0
    7          0.457      0.20      0.05      19.6       1.0
    0    0         0      0.25     5.0e9       1.0      60.0
         0      0.00   0.0e-00       0.0       0.0       0.0       0.0       0.0

ICOUP----1----*----2----*----3----*----4----*----5----*----6----*----7----*----8
         1         0
START----1----*----2----*----3----*----4----*----5----*----6----*----7----*----8
PARAM----1----*----2----*----3----*----4----*----5----*----6----*----7----*----8
   29999     25000003010000002 47 1 1                   1.80
         0 5.0000e04 0.500e01 5.0000e01
     1.E-8     1.E00
           1.000e5              0.0e-2                 60.0
SOLVR----1----*----2----*----3----*----4----*----5----*----6----*----7----*----8
2  Z1   O1    1.0e-1   1.0e-07

FOFT ----1----*----2----*----3----*----4----*----5----*----6----*----7----*----8
0000z

GRMOD----1----*----2----*----3----*----4----*----5----*----6----*----7----*----8
COEFS             11         1         1         1         1
BNDST              1        11         1         1         1         1         1
STRES              1        11         1         1         1        11   5.00E06

GENER----1----*----2----*----3----*----4----*----5----*----6----*----7----*----8
00001PRO 1                         DELV  5.0E-13   0.10E6
...

ELEME
00001              10.1000E+050.1000E+03          0.5000E+020.5000E+00-.5000E+02
...

CONNE
000010000C                  10.5000E+020.5000E+020.1000E+03
...

INCON -- INITIAL CONDITIONS FOR  121 ELEMENTS AT TIME  0.500000E+10
00001           0.10000000E+00 0.10000000E-12 0.10000000E-12 0.10000000E-12
 0.2203713200626E+07 0.0000000000000E+00 0.6000000000000E+02
...

ENDCY----1----*----2----*----3----*----4----*----5----*----6----*----7----*----8
```

Figure 6.9 input file for 2-D compaction

6.3.3 Comparison of analytical solution and numerical results

The pressure comparison shown in Figure 6.10 indicates that our simulator produces essentially the same answers as the analytical solution for this two dimensional stress simulation.

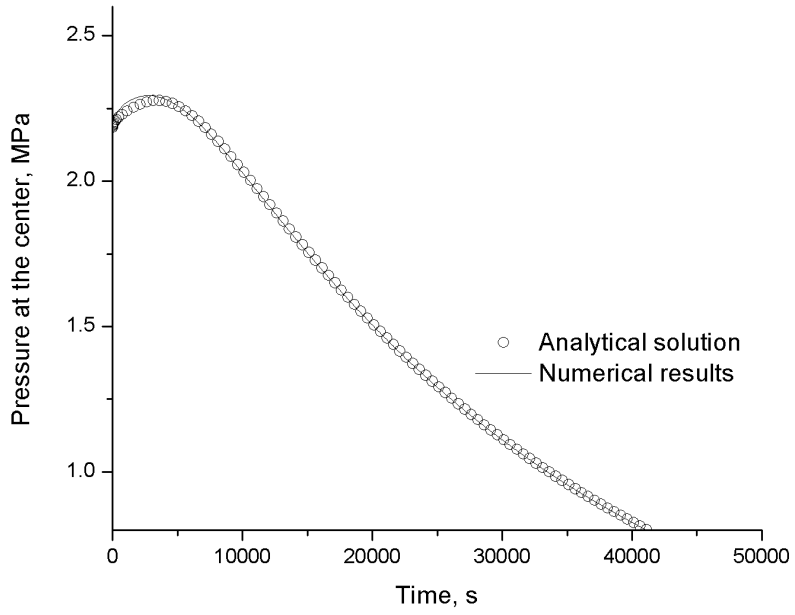

Figure 6.10 The comparison between numerical results and analytical solutions for the pressure profile at the center of the model

6.4 Heat sweep in a vertical fracture

In this example, we compared TOUGH2-EGS-MP with a non-isothermal commercial reservoir simulator, STARS (CMG, 2009).

6.4.1 Description

In many geothermal fields, there is evidence of rapid migration of injected fluids along preferential flow paths, presumably along fractures. The present problem is designed to study thermal interference along such paths, by modeling non-isothermal injection into and production from a single vertical fracture, as illustrated in Figure 6.11 (Pruess and Bodvarsson, 1984). The fracture is bounded by semi-infinite half-spaces of impermeable rock,

which provide a conductive heat supply. Initial temperature is 300 ℃ throughout. Water at 100 ℃ temperature is injected at one side of the fracture at a constant rate of 3.75 kg/s, while production occurs at the other side against a specified wellbore pressure. Problem parameters are given in Table 6.4 for injecting at point I and producing at point P.

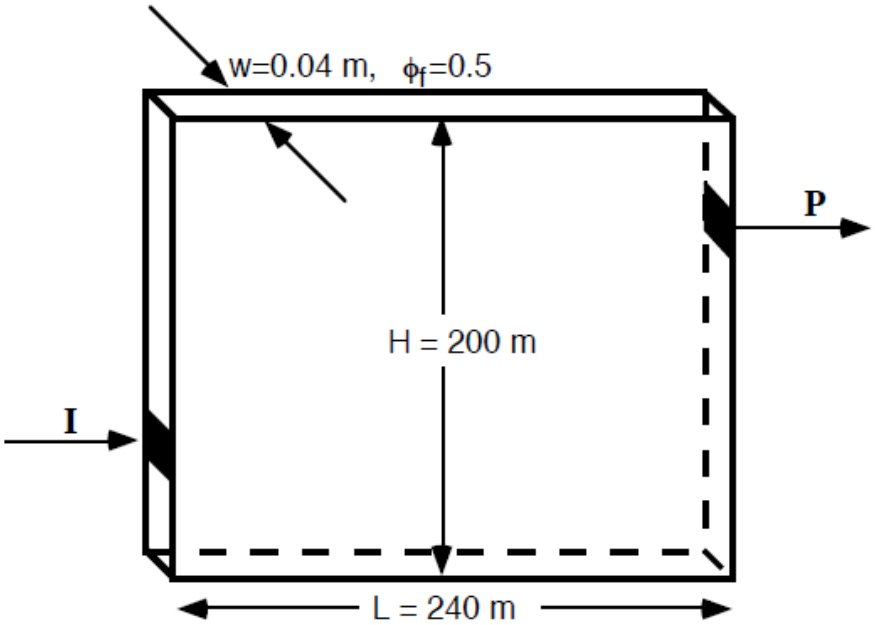

Figure 6.11. Schematic diagram of injection-production system in vertical fracture injection occurs at I, production at P. (Pruess et al.,1999)

Table 6.4 Input parameters used in simulation of the heat sweep in a vertical fracture

Parameters	**Value**	**Unit**
Rock properties		
Rock grain density	2650	kg/m^3
Specific heat	1000	J/kg ℃
Heat conductivity	2.1	W/m ℃
Fracture		
Height	200	m
Length	240	m
Aperture	0.04	m
Permeability	200	Darcy
Porosity	50	%
Initial Conditions		
Pressure	10.0	MPa
Temperature	300	℃

6.4.2 Numerical simulation setup

We simulated this problem in three steps. The first step was to generate the mesh data. In this problem, heat conduction from the semi-infinite half spaces occurs laterally. However, MESHM models heat conduction vertically. Thus, the model was constructed by rotating the horizontal plane by 90 °, as seen in Figure 6.12.

```
*rvfgrid* - Heat sweep in a vertical fracture
MESHMAKER1----*----2----*----3----*----4----*----5----*----6----*----7----*----8
XYZ
     90.
NX      12       20.
NY      10       20.
NZ       1       .04

ENDFI----1----*----2----*----3----*----4----*----5----*----6----*----7----*----8
** FOR GRID GENERATION
```

Figure 6.12 Mesh generation for the heat sweep in vertical fracture problem

We initialized pressure in the model by running it without sink and source term until the pressure reached gravity equilibrium. Then, the 'SAVE' file, which contains the equilibrated pressures, was renamed to 'INCON' and used as the initial conditions for the next runs. Rock heat capacity was set as infinity so the run would be isothermal. This is shown in Figure 6.13.

```
ROCKS----1----*----2----*----3----*----4----*----5----*----6----*----7----*----8
ROCK1          2650.       .50  200.E-12  200.E-12  200.E-12       2.1   1.0E+93
```

Figure 6.13 ROCKS data for model initialization

Finally, the source term was included at element '00008' which represents point I and the sink term was added at element '0001p' which represents point P in Figure 6.21. Two cases were run to demonstrate the effect of heat conduction from infinite impermeable layers. The two cases were achieved by switching MOP (15) option.

6.4.3 *Results and comparison*

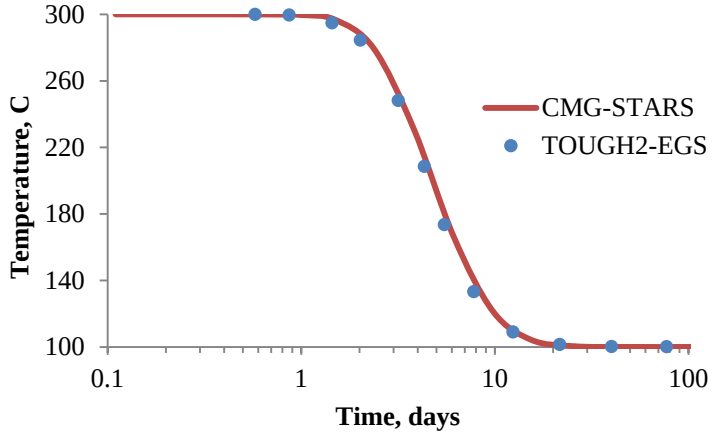

Figure 6.14 Comparison between CMG-STARS and TOUGH2-EGS: production fluid temperature of the vertical sweep in a vertical fracture problem: no heat gain from surrounding rock

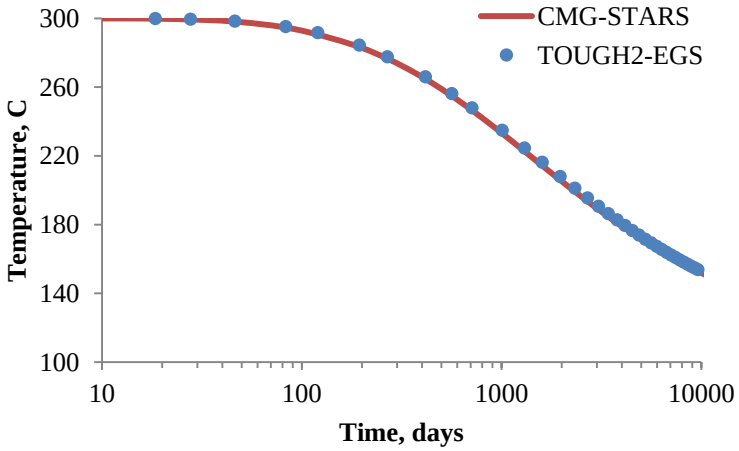

Figure 6.15 Comparison between CMG-STARS and TOUGH2-EGS: production fluid temperature of the vertical sweep in a vertical fracture problem: with heat gain from surrounding rock

6.5 *Effects of cold water injection in fractured reservoirs*

For some geothermal reservoirs, water injection is required to replace steam or water produced from them. Several reports have indicated that cold water injection could achieve increasing water injectivity due to stress changes around the injector. In this example, we demonstrate how to incorporate stress induced-permeability enhancement during cold water injection.

6.5.1 Description

A 2-D radial grid model represents the geothermal reservoir. The reservoir formation, shown in Figure 6.16, is fractured rock with low matrix permeability. Multiple interacting continuum (MINC) was used to represent the formation. The reservoir is overlain by a caprock layer, modeled by single porosity media. Constant pressure and temperature was imposed at the top of the model.

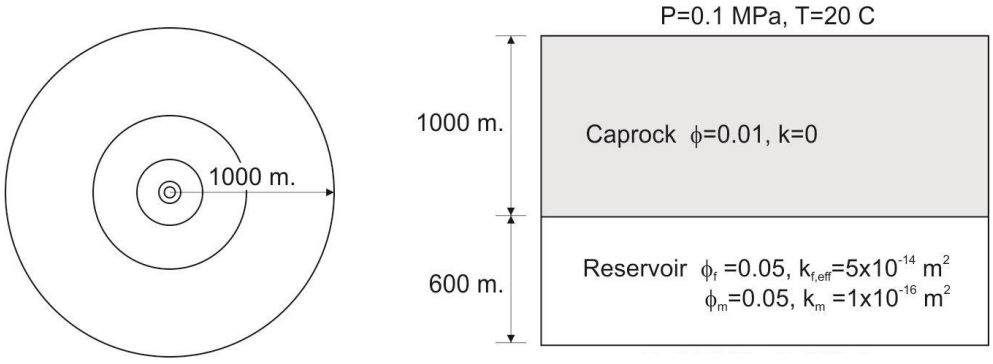

Figure 6.16 Model configuration

Table 6.5 Input parameters

Properties	Values
Young's Modulus *(GPa)*	14.4
Poisson's ratio *(dimensionless)*	0.20
Pore compressibility*(Pa^{-1})*	1×10^{-10}
Thermal expansion coefficient *($^oC^{-1}$)*	3.0×10^{-5}
Rock grain specific heat *(J/kg ^oC)*	1000
Rock grain density *(kg/m^3)*	2750
Formation thermal conductivity *(W/m ^oC)*	2.5

6.5.2 Numerical simulation setup

We first generated the mesh data. In this problem, the primary mesh was constructed as a 2-D radial grid system where the radii were logarithmically distributed. The input file for this is shown in Figure 6.17. This process generated mesh data in the "MESH" file. Then, the reservoir layers were subdivided into fracture and matrix ones, where fracture volume is 10% of the primary mesh volume. The input file for this is shown in Figure 6.18. It should be noted that the caprock layer was not refined and its volume was the same as the primary mesh. This combined model of single- and multiple-porosity was generated by specifying the refinement flag at the end of mesh data; only the elements with the flag of "0" are refined to fracture and matrix elements. This is shown in Figure 6.19. This process generated mesh data in the "MINC" file.

```
* WELL grid ... 1-D radial flow for geomechanical simulation
MESHMAKER1----*----2----*----3----*----4----*----5----*----6----*----7----*----8
RZ2D
RADII
    2
    0.15      0.3000
LOGAR
   19         1000.0         0
LAYER----1----*----2----*----3----*----4----*----5----*----6----*----7----*----8
    6
       1.0     1000.      200.      200.     200.0       1.0

ENDFI
```

Figure 6.17 Primary mesh generation input

```
MESHM
MINC
PART THRED
  2  1OUT      20.0     20.0      20.0
  0.1

ENDFI----1----*----2----*----3----*----4----*----5----*----6----*----7----*----8
```

Figure 6.18 Input for mesh division from primary mesh to double porosity mesh

```
---------1----*----2----*----3----*----4----*----5----*----6----*----7----*----8----*----9
ELEME
00001              10.5498E-010.5498E-010.0000E+000.1750E+000.0000E+00-.5000E+00         1
00002              10.5498E+020.0000E+000.0000E+000.1750E+000.0000E+00-.5010E+03         1
00003              10.1100E+020.0000E+000.0000E+000.1750E+000.0000E+00-.1101E+04         0
00004              10.1100E+020.0000E+000.0000E+000.1750E+000.0000E+00-.1301E+04         0
```

Figure 6.19 Primary mesh data as input for double porosity mesh

```
ICOUP----1----*----2----*----3----*----4----*----5----*----6----*----7----*----8
         0         0

GRMOD----1----*----2----*----3----*----4----*----5----*----6----*----7----*----8
COEFS              6         1         1         1         1
VOLMU              1        20         1         1         1         1   1.0E+98
MATRG              1        20         1         1         2         2         2
MATRG              1        20         1         1         3         5         3
MATRG              1        20         1         1         6         6         5
TEMPR              1        20         1         1         1         1     20.00
PRESS              1        20         1         1         1         1   1.0E+05
TEMPR              1        20         1         1         6         6    250.00
COEFS              6         1         1         1         2
MATRG              1        20         1         1         3         5         4
```

Figure 6.20 ICOUP and GRMOD data for reservoir initialization

The model was initialized by imposing constant temperature of 250 ℃ at the bottom layer and constant pressure of 0.1MPa and temperature of 20 ℃ at the top layer, which represents surface conditions. We used the "GRMOD" keyword to assign the specific conditions including pressure, temperature, rock material region, and boundary flag, shown in Figure 6.20. The model was run without stress, indicated under "ICOUP" keyword shown in Figure 6.20, until it reached thermodynamic equilibrium. Then, the 'SAVE' file, which contains the results from the initialization, was renamed to 'INCON' and used as the initial condition for the next runs.

```
FRACT    3  2750.e00      0.5  1.00e-14  1.00e-14  1.00e-14      2.51     1000.0
1.e-10     3.00e-5                 .25
    7        0.45000    9.6E-4        1.
    7        0.45000    1.0E-3   8.0E-05      5.E8        1.
    4    4         0      0.20   1.44E10    0.1      150.0
    0    0     80.    500.        80.      5.000E08  5.000E08 5.000E08       0.44
MATRX    3  2750.e00      0.05 1.00e-17  1.00e-17  1.00e-17      2.51     1000.0
1.e-10     3.00e-5                 .25
    7        0.45000    9.6E-4        1.
    7        0.45000    1.0E-3   8.0E-05      5.E8        1.
    4    0         0      0.20   1.44E10    0.45     150.0
    0    0
```

Figure 6.21 ROCKS data for fracture and matrix continuum

The permeability enhancement around the injector is arguably dominated by that of fractures. Thus, the fracture permeability was set as stress sensitive permeability using the Ostensen (1986) correlation (Equation 2.56) while the matrix permeability was constant. Detailed fracture and rock matrix parameters are shown in Figure 6.21. Cold water was injected into the reservoirs for 2 years.

6.5.3 Simulation Results

After two years of constant rate cold-water injection, the pressure propagated deep into the reservoir (Figure 6.22a) while the temperature changed occurred around the injector (Figure 6.22b). As a result, the effective stress was reduced and the permeability was increased (Figure 6.23). Two additional simulations were run to investigate the effect of pressure- and temperature-induced permeability enhancement. Pressure-induced permeability was minimal while the temperature-induced stress dominated the overall permeability enhancement. Figure 6.23 shows permeability profile after two years of injection; Figure 6.24 shows the bottom hole pressure profile where the pressure decreased in the cases of temperature and combined pressure-temperature induced permeability because the permeability increase caused reduction in pressure.

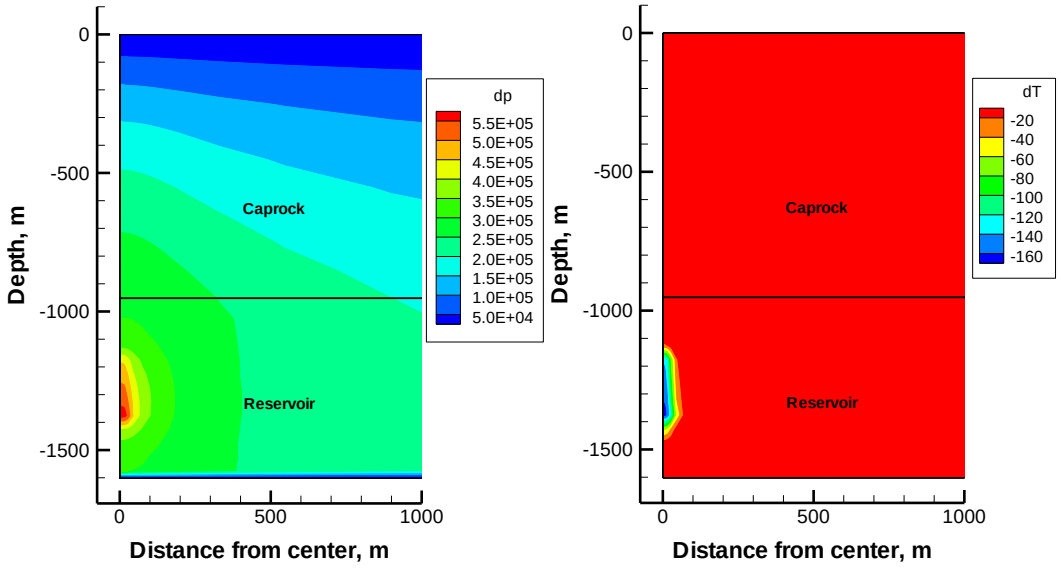

(a) (b)

Figure 6.22 Simulation results after 2 years of injection: (a) Pressure and (b) Temperature changes. The pressure change propagates away from the injector while the temperature change occurs around the injector.

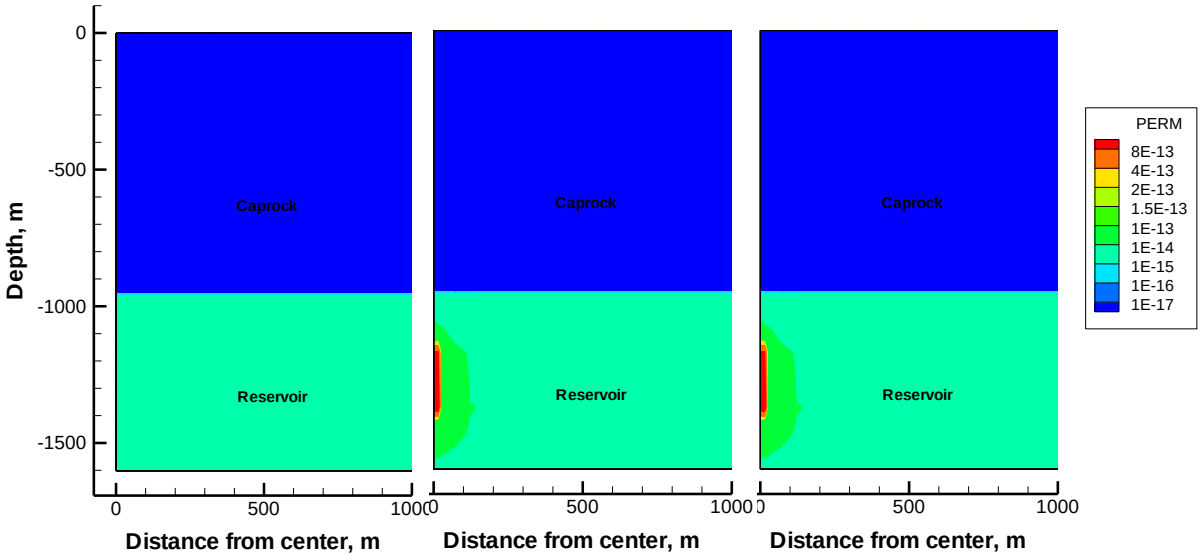

(a) (b) (c)

Figure 6.23 Permeability profiles after 2 years of injection, where the stress change was induced by: (a) Pressure, (b) Temperature, and (c) Pressure and temperature changes. The temperature-induced stress significantly affects the permeability enhancement while the pressure-induced stress has minimal effect on permeability around the injector.

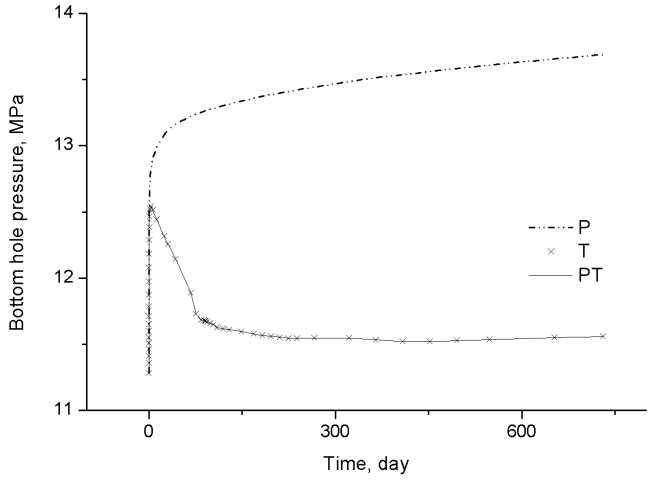

Figure 6.24 The injector bottomhole pressure profiles, where the stress change was induced by: Pressure (p), Temperature (T), and Pressure and temperature changes (PT). The bottomhole pressure is decreased in both (T) and (PT) cases because of the permeability enhancement around the injector.

6.6 The Geyser Geothermal Field cases

6.6.1 Problem description

The Geysers is the site of the largest geothermal electricity generating operation in the world and has been in commercial production since 1960 (Mossop and Segall, 1997 and 1999; Rutqvist and Tsang, 2002a; Rutqvist et al., 2006a; Rutqvist et al., 2006b; Rutqvist and Oldenburg 2008; Rutqvist et al., 2010; Khan and Truschel 2010; Rutqvist 2011). It is a vapor-dominated geothermal reservoir system that is hydraulically confined by low permeability rock. As a result of high steam withdrawal rates, the reservoir pressure declined until the mid-1990s, when increasing water injection rates resulted in a stabilization of the steam reservoir pressure. Archival INSAR images were acquired from approximately monthly satellite passes over the region for a seven-year period, from 1992 to 1999, and the data is compared with displacement calculated from our model.

The combined effects of steam production and water injection in 44 years and their influences on ground deformation will be analyzed. Based on the work by Rutqvist and Oldenburg (2008) and Rutqvist et al. (2010), a cross-axis (NE-SW) two-dimensional model grid of the Geysers

Geothermal Field was established. Permeability, temperature, and boundary conditions are shown in Figure 6.25. The initial thermal and hydrological conditions (vertical distributions of temperature, pressure and liquid saturation) are typically established through steady-state multi-phase flow simulations. According to previous studies, the adopted rock-mass bulk modulus is 3 GPa and the linear thermal expansion coefficient is 3×10^{-5} ℃$^{-1}$. Pore compressibility and the reservoir Poisson's ratio of the reservoir is 1.0×10^{-10} Pa^{-1} and 0.25, respectively. The injection well is about 217.5 m away from the production well. The steam-production and water-injection rate used in the model is estimated from the field-wide production and injection data (Mossop and Segall, 1997; Majer and Peterson, 2007; Khan and Truschel, 2010; Sanyal and Enedy, 2011).

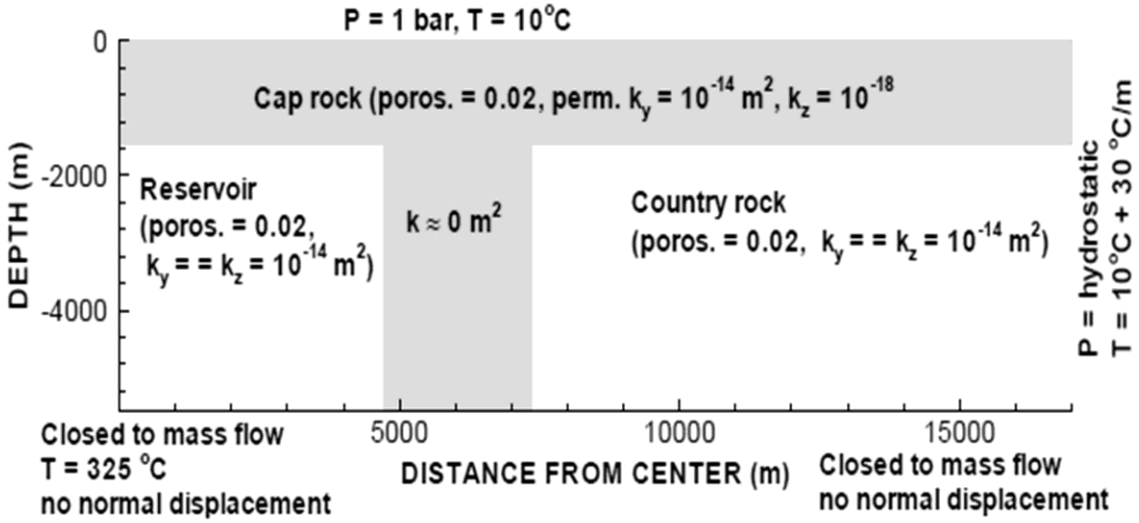

Figure 6.25. Half-symmetric model domain with hydraulic properties and boundary conditions (Rutqvist and Oldenburg, 2008).

6.6.2 Change of pressure and temperature after 44 years

Figure 6.26 shows simulated liquid saturation and changes in fluid pressure and temperature after 44 years of production and injection. Figure 6.26a shows the injection caused formation of a wet zone that extends towards 1,000m. Figure 6.26b demonstrates the pressure decrement is about 2×10^{6} Pa after steam production and water injection. Figure 6.26c indicates a local cooling effect and the maximum temperature decrement is about 50 ℃. All the results are almost the same as the results from Rutqvist and Oldenburg (2008).

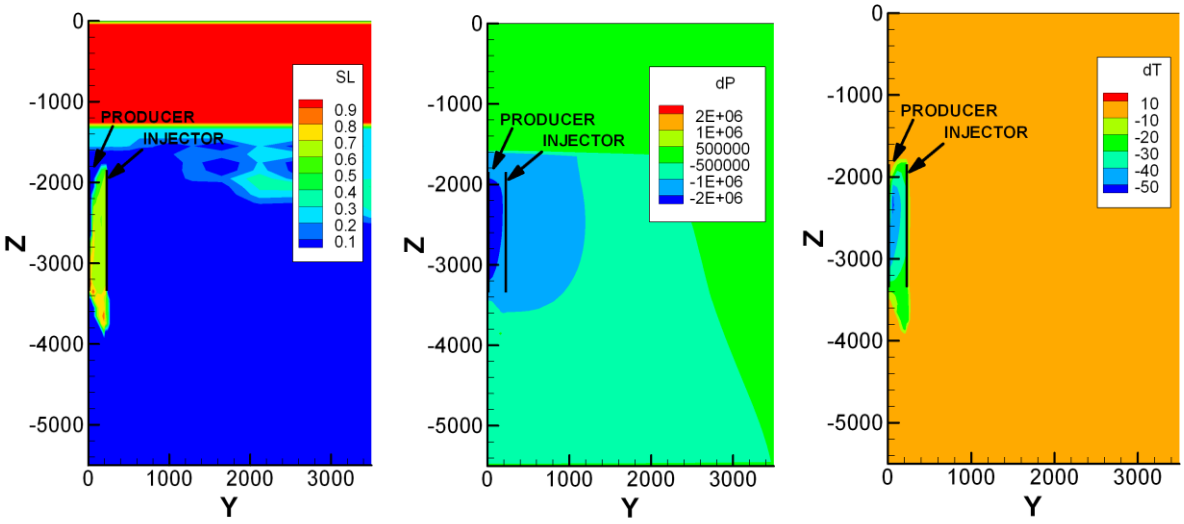

Figure 6.26. Simulated profile of liquid saturation (a), changes in fluid pressure (b), changes in temperature(c) after 44 years of production and injection.

6.6.3 Changes in stress and volumetric strain

Figure 6.27a and 6.27b display changes in mean total stress and volumetric strain, respectively. The mean total stress change in the rock mass depends on the production-induced depletion and injection-induced cooling. The change in mean total stress is about 0.5-1.5 MPa and the volumetric strain change is about 0.0001-0.0004. Figure 6.28 shows the change of simulated ground displacement with time and the comparison with INSAR data and results from TOUGH2-FLAC (Rutqvist, 2011). Figure 6.29 shows the change of displacement along the cross-section of the model and the comparison with observed and known simulated results. It can be seen from these two figures that there is good agreement between simulated ground displacement and INSAR data.

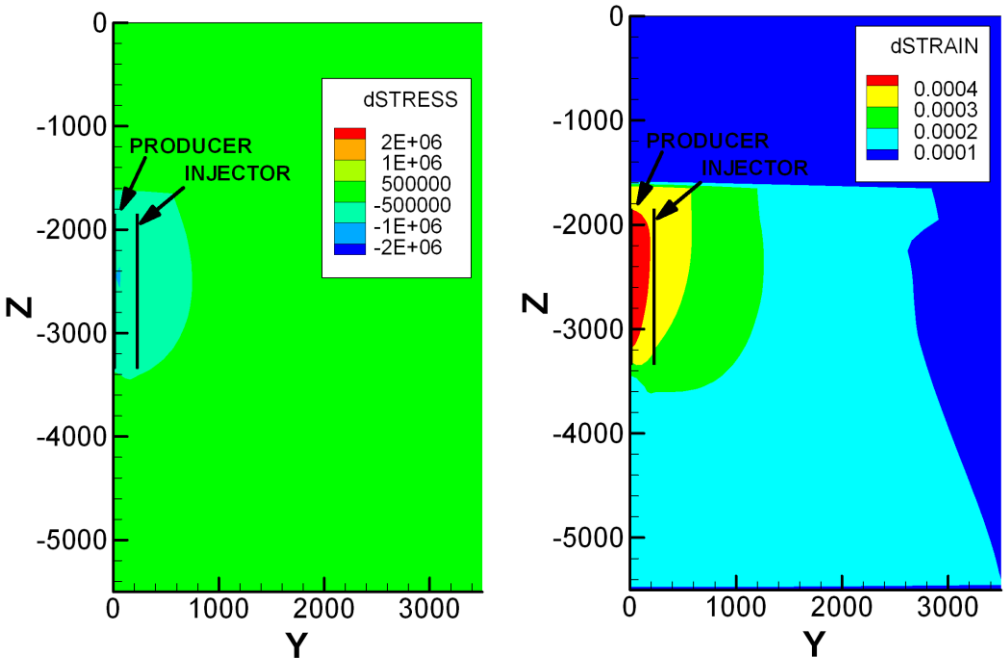

Figure 6.27 Simulated profile of stress (a) and strain (b) after 44 years of production and injection

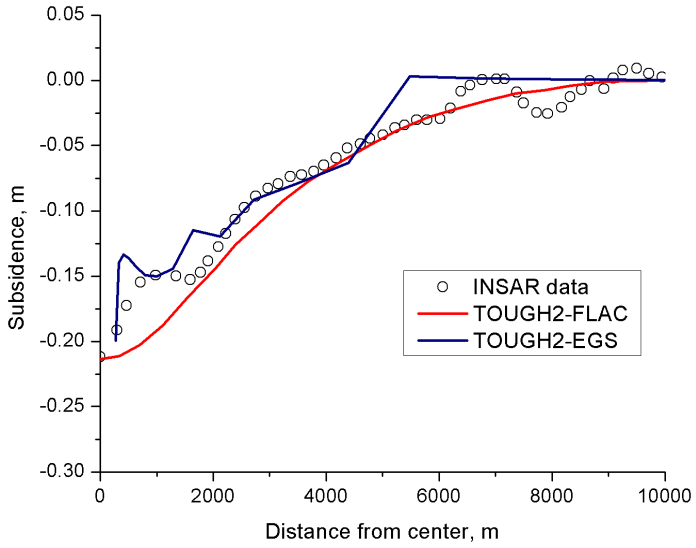

Figure 6.28 Subsidence profile comparison between INSAR data, TOUGH2-FLAC, and TOUGH2-EGS-MP simulation results after 44 years of production and injection.

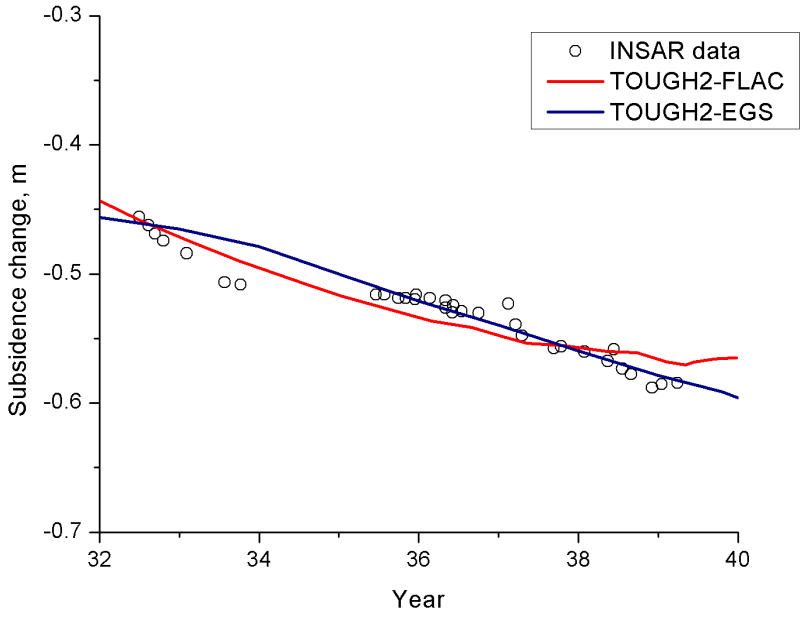

Figure 6.29 Subsidence profile comparison between INSAR data, TOUGH2-FLAC, and TOUGH2-EGS-MP simulation results from year 32 to 40 (1992 -2000).

6.7 High performance computing cases

In this section, we ran two simulation cases to analyze the computing performance of TOUGH2-EGS-MP. The first case is same as Example 6.6, the Geyser geothermal field case, and run under multiple processers. Another case is one large scale simulation problem with tens of millions of grid blocks. The two cases illustrate that TOUGH2-EGS-MP may not only be used for small and medium size problem for computing efficiency, but has sufficient scalability and speedup factor for large sized problems.

The Geyser geothermal field case has about 1700 grid blocks for a 44-year simulation. We ran it on 2, 4, 8, 16 and 32 processes, with 2, 4, 8, 16 on same compute node and 32 processes on two different compute nodes. Table 6.6 presents the results of the computation. Figure 6.30 shows the plots of computation time and iterations/second as function of number of processes.

Table 6.6 The computation performance results for Geyser case

No. of Process	Elements/Process	Computation Time (minutes)	linear solver Time (minutes)	Iterations/second
2	857-910	72	34	864
4	434-445	41	16	1279
8	214-227	8	4	2478
16	107-113	7	4	2404
32	53-57	43	19	2336

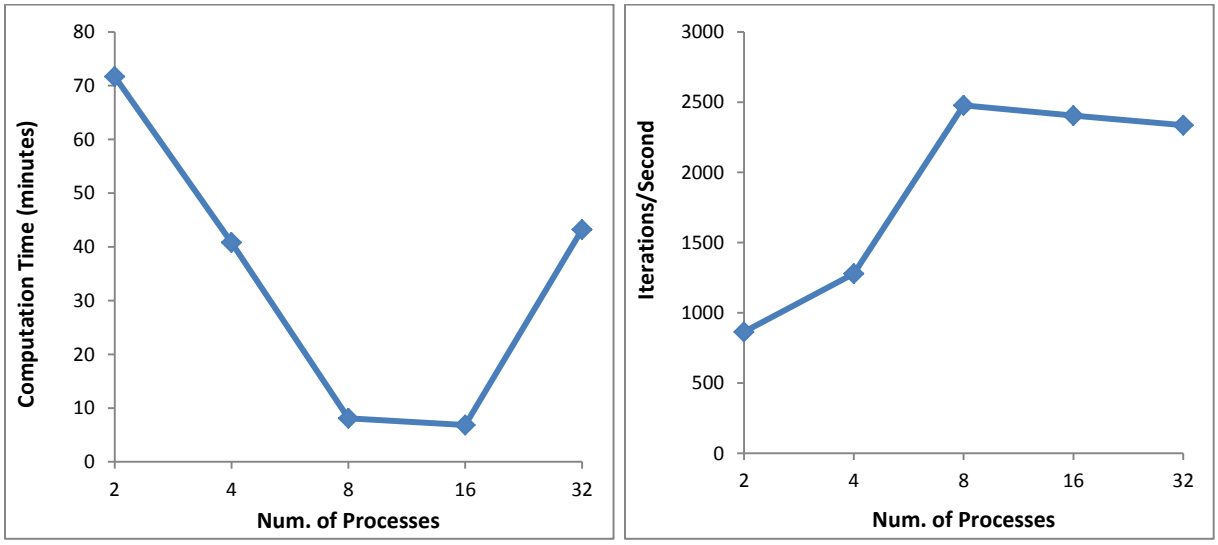

Figure 6.30. Computation performance as function of number of processes for Geyser field case

The data from Table 6.6 and the plot of figure 6.30 illustrate that the computation performance significantly improves as the number of processors increases. For example, the computation time of 16 processes is only 7 minutes while it is 72 minutes for 2 processes. The computation time decreases linearly from 2 to 8 processes, and becomes flatter from 8 to 16 processes. The program was run on 1 node with 16 processors. The computation time increase as the number of processes increases to 32. In this situation, the MPI communication cost is much higher than for smaller numbers of processes. Another observation is that our simulation program does good job for grid block partitioning. Table 6.6 shows that each compute node has very similar numbers of elements, which enables the workload to be evenly distributed.

Besides the Geyser geothermal field case with small/medium problem size, we tested large sized simulation with about 12.5 million grid blocks for various numbers of processors.

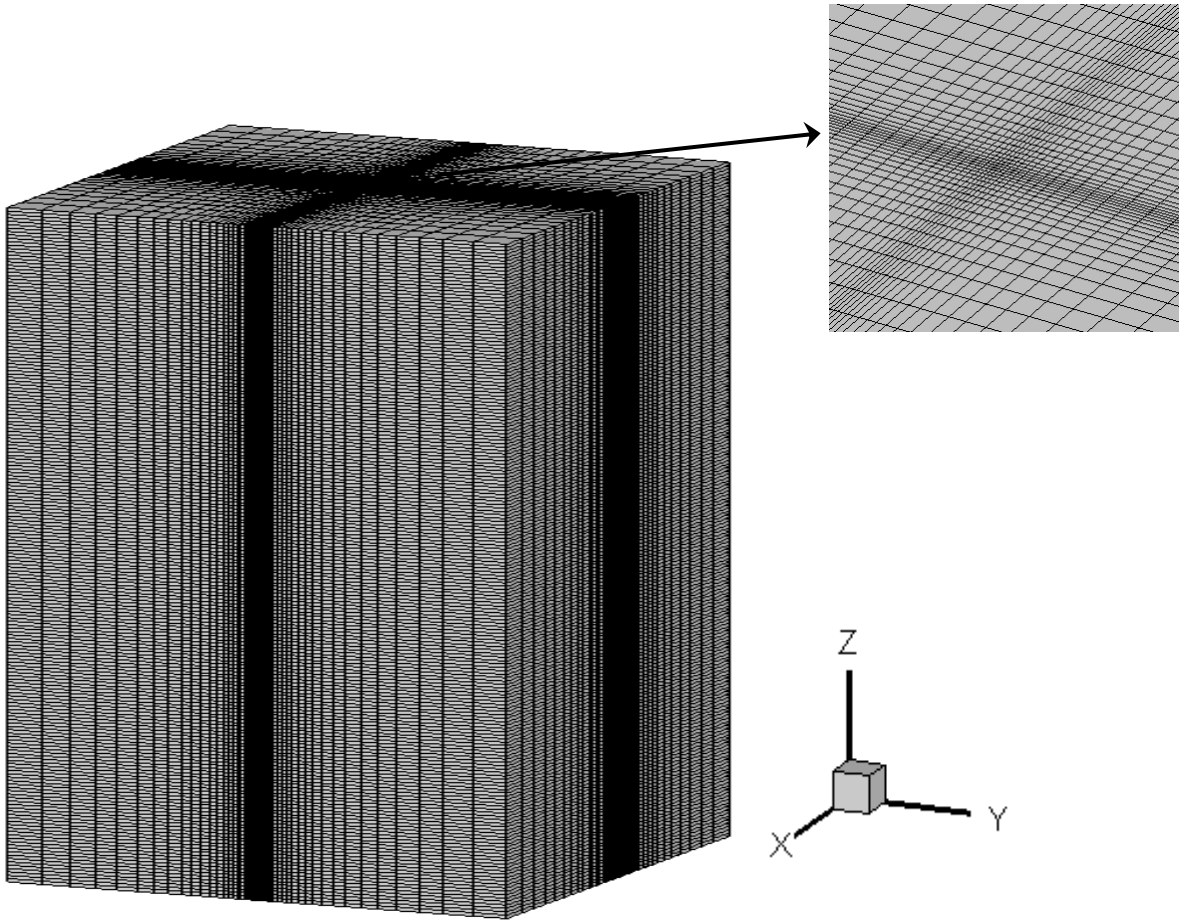

Figure 6.31. The mesh of 12.5 million grid blocks

Figure 6.31 shows the mesh for the simulation case. The mesh is distributed logarithmically in the X and Y directions starting from the center, which is the simulation area of interest. The center of the XY plane has so many small grid blocks that it looks dark. It actually contains grid blocks with logarithmically increasing size as shown on the top right. In order to simplify the physical process and only focus on computing performance, we set up boundary conditions for pressure and temperature, and simulate for one year to set the initial condition of each grid block. There are a total of 251*251*200 = 12,600,200 elements for this simulation; thus, we have to partition the mesh into sub-domains that are assigned to different cluster nodes due to the memory limitations of each node. Figure 6.32 presents a snapshot of memory use on the Linux cluster with 27 nodes and 512 processes involved in the computing. The last column shows the memory use for each node. It is observed that the memory use

ranges from 5.3 to 7.9 Giga Bytes (GB) due to the different number of processes running on it. There are 16 and 24 processes running on the nodes with 5.3 and 7.9 GB memory use. Thus for one single process, the memory use is almost the same, around 0.33 GB (5.3/16 or 7.9/24). The nodes with less memory use, like compute-0-13 to 15 and compute-0-31 to 32, are not involved in the computing.

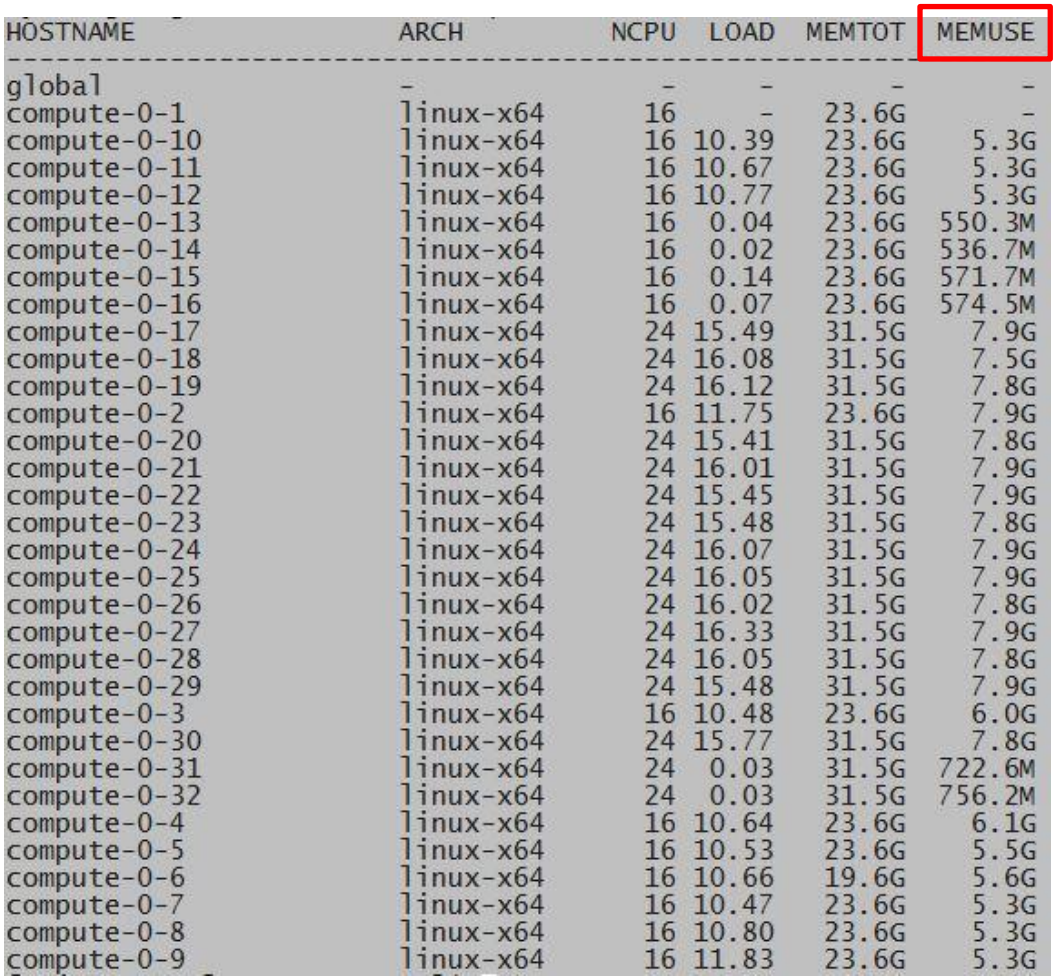

HOSTNAME	ARCH	NCPU	LOAD	MEMTOT	MEMUSE
global	-	-	-	-	-
compute-0-1	linux-x64	16	-	23.6G	-
compute-0-10	linux-x64	16	10.39	23.6G	5.3G
compute-0-11	linux-x64	16	10.67	23.6G	5.3G
compute-0-12	linux-x64	16	10.77	23.6G	5.3G
compute-0-13	linux-x64	16	0.04	23.6G	550.3M
compute-0-14	linux-x64	16	0.02	23.6G	536.7M
compute-0-15	linux-x64	16	0.14	23.6G	571.7M
compute-0-16	linux-x64	16	0.07	23.6G	574.5M
compute-0-17	linux-x64	24	15.49	31.5G	7.9G
compute-0-18	linux-x64	24	16.08	31.5G	7.5G
compute-0-19	linux-x64	24	16.12	31.5G	7.8G
compute-0-2	linux-x64	16	11.75	23.6G	7.9G
compute-0-20	linux-x64	24	15.41	31.5G	7.8G
compute-0-21	linux-x64	24	16.01	31.5G	7.9G
compute-0-22	linux-x64	24	15.45	31.5G	7.9G
compute-0-23	linux-x64	24	15.48	31.5G	7.8G
compute-0-24	linux-x64	24	16.07	31.5G	7.9G
compute-0-25	linux-x64	24	16.05	31.5G	7.9G
compute-0-26	linux-x64	24	16.02	31.5G	7.8G
compute-0-27	linux-x64	24	16.33	31.5G	7.9G
compute-0-28	linux-x64	24	16.05	31.5G	7.8G
compute-0-29	linux-x64	24	15.48	31.5G	7.9G
compute-0-3	linux-x64	16	10.48	23.6G	6.0G
compute-0-30	linux-x64	24	15.77	31.5G	7.8G
compute-0-31	linux-x64	24	0.03	31.5G	722.6M
compute-0-32	linux-x64	24	0.03	31.5G	756.2M
compute-0-4	linux-x64	16	10.64	23.6G	6.1G
compute-0-5	linux-x64	16	10.53	23.6G	5.5G
compute-0-6	linux-x64	16	10.66	19.6G	5.6G
compute-0-7	linux-x64	16	10.47	23.6G	5.3G
compute-0-8	linux-x64	16	10.80	23.6G	5.3G
compute-0-9	linux-x64	16	11.83	23.6G	5.3G

Figure 6.32. The snapshot of memory use of each computing node

We started this case on 2 nodes with 32 processes and incrementally to 25 nodes with 512 processes. Table 6.7 summarized the results of computation configuration and performance for each running case, and Figure 6.33 shows the comparison of the real computation time and the ideal time.

Table 6.7. Summary of computation configuration and performance

No. of Processes	Processes/Node	No. of Nodes	No. of Elements/Process	Computation Time (s)	Computation Time (hours)
32	16	2	382320-405526	26502	7.4
64	16	4	191167-202684	14873	4.1
128	16	8	95575-101391	8786	2.4
256	16/24	11	47788-50694	5097	1.4
512	16/24	25	23894-25348	1008	0.3

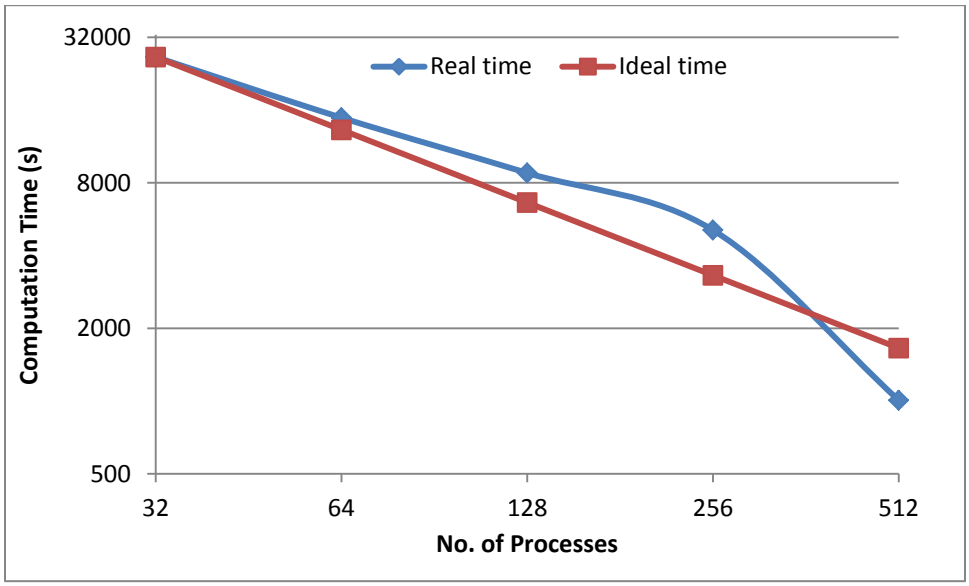

Figure 6.33. Computation time vs. number of processes

Table 6.7 summarizes the total number of processes, processes number per nodes, number of nodes involving computing, the range of number of elements partitioned for each process, and total computation time. Figure 6.33 shows the computation time from Table 6.7, compared with the ideal linear speedup case. The ideal case refers the computation time with 32 processes as the benchmark. The real computation time is close to the ideal time for 64, 128 and 256 processes, and even better for 512 processes. One possible reason is that the reference time is the computation time with 32 processes on 2 nodes; each node has 16 processors; therefore each computation node is fully loaded, or even over-fully loaded if those two nodes

are not exclusively for the computation tasks. The 512 processes case was run on 25 nodes; it has low possibility that every node among 25 nodes is fully or over-fully loaded.

Two cases with different problem size are tested for the computing performance analysis, the small/medium size with order of thousands of grid blocks, and large size with order of tens of millions of grid blocks. The former case shows satisfactory performance enhancement with one node of multi-processors, which implies the performance enhancement of TOUGH2-EGS-MP running on multi-core PCs; the latter case shows almost linear speedup for performance improvement for the large/super-large problem size.

7 CONCLUSIONS

We present a fully-coupled fluid and heat flow and geomechanics simulator (TOUGH2-EGS-MP) with parallel computing capability for simulating multiphase flow, heat transfer and rock deformation in porous and fractured media. The flow, heat and stress equations are solved simultaneously in this fully coupled simulator. Primary variables in TOUGH2-EGS-MP are pressure, air mass fraction (or gas saturation), temperature, and mean total stress. Secondary variables, such as phase saturation, capillary pressure, volumetric strain, etc., are evaluated from their relations with primary variables. Message Passing Interface (MPI) is used for implementing parallel computing of multi-processes. Each process solves the partitioned sub-domain and exchanges messages with other processes to achieve higher computing performance.

Our geomechanical model is verified against analytical solutions, other numerical simulators, and a field case in the examples discussed in Section 6. The one-dimensional consolidation in porous media (Example 1), one-dimensional heat conduction in deformation media (Example 2), and two-dimensional Mandel's problem (Example 3) are verified against analytical solutions. The heat sweep case (Example 4) is verified against another commercial simulator, CMG-STARS. The MINC model is demonstrated in Example 5 to simulate the rock deformation effects of cold water injection in the multi porosity systems of a fractured reservoir. The Geyser field case (Example 6) shows a field scale application and TOUGH2-EGS-MP, is verified against the published and observed data. Example 7 tests the parallel computing capabilities for small/medium and large problem sizes respectively, and the results show the satisfactory speedup of computing performance for TOUGH2-EGS-MP.

Compared with other numerical modeling codes for geotechnical analysis of soil, rock, and structural support, such as FLAC3D and ECLIPSE, our numerical geomechanical model only calculates mean normal stress instead of the total stress tensor. This simplification saves computation workload but may be unable to analyze the phenomena dependent on shear stress. Overall, TOUGH2-EGS-MP is rigorous in handling simulations of coupled flow and rock deformation. It can be applied to stress-sensible geothermal reservoirs for analyzing multiphase fluid, heat flow, rock deformation, and chemical reactions.

ACKNOWLEDGEMENT

This work was supported by the U.S. Department of Energy under Contract No. DE-EE0002762, "Development of Advanced Thermal-Hydrological-Mechanical-Chemical (THMC) Modeling Capabilities for Enhanced Geothermal Systems". This work was also supported by the Foundation CMG (Computer Modeling Group).

REFERENCES

Abousleiman, Y., AH-D. Cheng, L. Cui, E. Detournay and J.-C. Roegiers. Mandel's Problem Revisited. *Géotechnique* 46(2), 187-195, 1996.

Biot, M. A. and D. G. Willis. The Elastic Coefficients of the Theory of Consolidation. *J. Appl. Mech.* 24, 594–601, 1957.

Charoenwongsa, S., H. Kazemi, J. Miskimins, and P. Fakcharoenphol, A Fully-coupled Geomechanics and Flow Model for Hydraulic Fracturing and Reservoir Engineering Applications, SPE 137297, the Canadian Unconventional Resources & International Petroleum Conference held in Calgary, Alberta, Canada, 19–21 October, 2010.

Computer Modeling Group. User's Guide of STARS: Advanced Process and Thermal Reservoir Simulator Version 2009. By Computer Modeling Group Ltd., 2009

Corey, A. T. The Interrelation Between Gas and Oil Relative Permeabilities, *Producers Monthly 19*, 38-41, November 1954.

Davies J. P. and D. K. Davies. Stress-Dependent Permeability: Characterization and Modelling. *Society of Petroleum Engineers*, SPE 56813, 1999.

Edwards, A. L. TRUMP: A Computer Program for Transient and Steady State Temperature Distributions in Multidimensional Systems, National Technical Information Service, National Bureau of Standards, Springfield, VA, 1972.

Elmroth, E., C. Ding, and Y. S. Wu, High Performance Computations for Large-Scale Simulations of Subsurface Multiphase Fluid and Heat Flow, *The Journal of Supercomputing*, 18(3), pp. 233-256, 2001.

Fatt, I. and W.A. Klikoff. Effect of Fractional Wettability on Multiphase Flow Through Porous Media, *Journal of Petroleum Technology 11*, no. 10, 71-76, 1959.

Gutierrez, M. and R. W. Lewis. Petroleum Reservoir Simulation Coupling Fluid Flow and Geomechanics. *SPE Reservoir Evaluation & Engineering*, June, pp. 164-172, 2001.

Jaeger, J. C., N. G. W. Cook, and R. W. Zimmerman, *Fundamentals of Rock Mechanics.* Blackwell, Fourth edition, 2007.

Karypsis, G. and V. Kumar, METIS. A Software Package for Partitioning Unstructured Graphs,Partitioning Meshes, and Computing Fill-Reducing Orderings of Sparse Matrices, V4.0. Technical Report, Department of Computer Science, University of Minnesota, 1998.

Khan, M. A. and J. Truschel. The Geysers Geothermal Field, an Injection Success Story. *GRC Transactions, Volume 34: Celebrating 50 years of clean, renewable power*, 1239-1242, 2010.

Klinkenberg, L. J. The Permeability of Porous Media to Liquids and Gases. *API Drilling and Production Practice* 200-213, 1941.

Lam, S.T., A. Hunsbedt, P. Kruger, and K. Pruess. Analysis of the Stanford Geothermal Reservoir Model Experiments Using the LBL Reservoir Simulator, *Geothermics*, 17 (4), 595 - 605, LBL-25957, 1988.

Leverett, M. C. Capillary Behavior in Porous Media. *The AIME Transactions* 142, 341–358, 1941.

Longuemare, P., M. Mainguy, P. Lemonnier, A. Onaisi, C. Gerard, and N. Koutsabeloulis. Geomechanics in Reservoir Simulation: Overview of Coupling Methods and Field Case Study. *Oil & Gas Science and Technology-Rev*. IFP 57(5), 471-483, 2002.

Majer, E. L. J. E. Peterson. The Impact of Injection on Seismicity at The Geysers, California Geothermal Field. *International Journal of Rock Mechanics and Mining Sciences* 44, 1079-1090, 2007.

Mandel, J. Consolidation des sols (etude mathematique). *Geotechnique* pp. 3287–3299,1953.

McKee, C. R., A. C. Bumb, and R. A. Koenig. Stress-Dependent Permeability and Porosity of Coal and Other Geologic Formations. *SPE Formation Evaluation* 3(1), 81-91, 1988.

Mercer Jr, J. W., Faust, C., & Pinder, G. F. Geothermal reservoir simulation. In *Research for the Development of Geothermal Energy Resources* (Vol. 1, pp. 256-267), 1974

Message Passing Forum, A Message-Passing Interface Standard, *International Journal of Supercomputing Applications and High performance Computing*, 8(3-4), 1994.

Milly, P. C. D. Moisture and Heat Transport in Hysteretic, Inhomogeneous Porous Media: A Matric-Head Based Formulation and a Numerical Model, *Water Resour. Res.,* Vol. 18, No. 3, pp. 489 - 498, 1982.

Moridis, G. and K. Pruess. T2SOLV: An Enhanced Package of Solvers for the TOUGH2 Family of Reservoir Simulation Codes, *Geothermics*, Vol. 27, No. 4, pp. 415 - 444, 1998.

Mossop, A. and P. Segall. Subsidence at the Geysers Geothermal Field, N. California From a Comparison of GPS and Leveling Surveys. *Geophysical Research Letters* 24(14), 1839-1842, 1997.

Mossop, A. and P. Segall. Volume Strain Within the Geysers Geothermal Field. *Journal of Geophysical Research,* 104(b12), 29,113-29,131, 1999.

Mualem, Y. A New Model for Predicting the Hydraulic Conductivity of Unsaturated Porous Media, *Water Resour. Res.,* Vol. 12(3), pp. 513 - 522, 1976.

Narasimhan, T. N. and P. A. Witherspoon. An Integrated Finite Difference Method for Analyzing Fluid Flow in Porous Media, *Water Resour. Res.*, Vol. 12, No. 1, pp. 57 – 64, 1976.

Narasimhan, T. N., P. A. Witherspoon, and A. L. Edwards. Numerical Model for Saturated-Unsaturated Flow in Deformable Porous Media, Part 2: The Algorithm, *Water Resour. Res.*, 14 (2), 255-261, 1978.

Ostensen, R. W. The Effect of Stress-Dependent Permeability on Gas Production and Well Testing. SPE 11220. *SPE Formation Evaluation* 1(3), 227–235, 1986.

Pickens, J. F., R. W. Gillham, and D. R. Cameron. Finite Element Analysis of the Transport of Water and Solutes in Tile-Drained Soils, *J. of Hydrology*, 40, 243-264, 1979.

Pruess, K. and G. S. Bodvarsson. Thermal Effects of Reinjection in Geothermal Reservoirs With Major Vertical Fractures. *Journal of Petroleum Technology*, *36*(9), 1567-1578, 1984.

Pruess, K. TOUGH2-A General Purpose Numerical Simulator for Multiphase Fluid and Heat Flow. Lawrence Berkeley Laboratory Report LBL-29400, Berkeley, CA, 1991.

Pruess, K. and T. N. Narasimhan. On Fluid Reserves and the Production of Superheated Steam from Fractured, Vapor-Dominated Geothermal Reservoirs, *J. Geophys. Res.*, Vol. 87, No. B11, pp. 9329 - 9339, 1982.

Pruess, K. and T. N. Narasimhan. A Practical Method for Modeling Fluid and Heat Flow in Fractured Porous Media. *Society of Petroleum Engineers Journal* 25, (1), 14-26, 1985.

Pruess, K., C. M. Oldenburg, and G. M. Moridis. TOUGH2 User's Guide Version 2. E. O. Lawrence Berkeley National Laboratory Report LBNL-43134, 1999.

Pruess, K., and Y. Tsang, Thermal Modeling for a Potential High-Level Nuclear Waste Repository at Yucca Mountain, Nevada, Lawrence Berkeley Laboratory Report, LBL-35381, UC-600, Lawrence Berkeley National Laboratories, Berkeley, CA, 1994.

Pruess, K. GMINC–A Mesh Generator for Flow Simulations in Fractured Reservoirs. Lawrence Berkeley National Laboratory Report LBL-15227, 1983

Rutqvist, J. Status of the TOUGH-FLAC Simulator and Recent Applications Related to Coupled Fluid Flow and Crustal Deformations. *Computers & Geosciences* 37, 739-750, 2011.

Rutqvist, J., J. T. Birkholzer, F. Cappa, C. M. Oldenburg, and C. F. Tsang. Shear-slip Analysis in Multiphase Fluid-Flow Reservoir Engineering Applications Using TOUGH-FLAC. Proceedings of the TOUGH symposium 2006, Lawrence Berkeley National Laboratory, Berkeley, California, May 15–17, 2006a.

Rutqvist, J., E. Majer, C. M. Oldenburg, J. Peterson, J., and D. Vasco. Integrated Modeling and Field Study of Potential Mechanisms for Induced Seismicity at The Geysers Geothermal Field, California. Geothermal Research Council Annual Meeting, San Diego, California, September 10–13, GRC Transactions, Vol 30, 2006b.

Rutqvist, J., C. M. Oldenburg. Analysis of Injection-Induced Micro-Earthquakes in a Geothermal Steam Reservoir, Geysers Geothermal Field, California. Proceedings of the 42th U.S. Rock Mechanics Symposium, San Francisco, California, USA, June 29-July 2, 2008: American Rock Mechanics Association ARMA, Paper No. 151, 2008.

Rutqvist, J., C. M. Oldenburg, P. F. Dobson, J. Garcia, and M. Walters. Title Predicting the Spatial Extent of Injection-Induced Zones of Enhanced Permeability at the Northwest Geysers EGS Demonstration Project. Source 44th U.S. Rock Mechanics Symposium and 5th U.S.-Canada Rock Mechanics Symposium, June 27 - 30, 2010, Salt Lake City, Utah, 2010.

Rutqvist, J. and C. F. Tsang. A Study of Caprock Hydromechanical Changes Associated With CO2-Injection Into a Brine Formation. *Environmental Geology* 42, 296–305, 2002a.

Rutqvist, J., Y. S. Wu, C. F. Tsang, and G. Bodvarsson. A Modeling Approach for Analysis of Coupled Multiphase Fluid Flow, Heat Transfer, and Deformation in Fractured Porous Rock. *International Journal of Rock Mechanics and Mining Science & Geomechanics* 39, 429–42, 2002b.

Sanyal, S. K. and S. L. Enedy. Fifty Years of Power Generation at the Geysers Geothermal Field, California: the Lessons Learned. Proceedings of Thirty-sixth Workshop on Geothermal Reservior Engineering, Stanford University, Stanford, California, January 31-February 2. SGP-TR-191, 2011.

Settari, A. and D. A. Walters. Advances in Coupled Geomechanical and Reservoir Modeling With Applications to Reservoir Compaction. *SPE Journal* 6(3), 334-342, 2001.

Settari, A., D. A. Walters, and G. A. Beihie. Use of Coupled Reservoir and Geomechanical Modeling for Integrated Reservoir Analysis and Management, Paper CIM 2000-78, presented at Canadian International Petroleum Conference 2000, Calgary, Alberta, Canada, June 4-8, 2000.

Terzaghi, K. The Shearing Resistance of Saturated Soils and the Angle Between the Planes of Shear. Proceedings of International Conference on Soil Mechanics and Foundation Engineering, Harvard University Press, Cambridge, MA, USA, pp. 54-56, 1936.

Thomas, L., & Pierson, R. Three-dimensional geothermal reservoir simulation. *Old SPE Journal, 18(2)*, 151-161, 1978

Tuminaro, R. S., M. Heroux, S. A. Hutchinson, and J. N. Shadid, Official Aztec user's guide,Ver 2.1, Massively Parallel Computing Research Laboratory, Sandia National Laboratories, Albuquerque, NM, 1999.

Udell, K. S. and J.S. Fitch. Heat and Mass Transfer in Capillary Porous Media Considering Evaporation, Condensation, and Non-Condensible Gas Effects, paper presented at 23rd ASME/AIChE National Heat Transfer Conference, Denver, CO, 1985.

Van Genuchten, M. Th. A Closed-Form Equation for Predicting the Hydraulic Conductivity of Unsaturated Soils, *Soil Sci. Soc.* , Vol. 44, pp. 892 - 898, 1980.

Verma, A. and K. Pruess. Thermohydrological Conditions and Silica Redistribution Near High-Level Nuclear Wastes Emplaced in Saturated Geological Formations. *J. Geophys. Res.* 93, 1159-1173, 1988.

Verma, A. K., K. Pruess, C. F. Tsang, and P. A. Witherspoon. A Study of Two-Phase Concurrent Flow of Steam and Water in an Unconsolidated Porous Medium, Proc. 23rd National Heat Transfer Conference, Am. Society of Mechanical Engineers, Denver, CO, 135–143, 1985.

Warren, J. E. and P. J. Root. The Behavior of Naturally Fractured Reservoirs. *Soc. Pet. Eng. J. Transactions, AIME* 228, 245-255, September, 1963.

Wu, Y. S. USERS MANUAL (UM) for TOUGH2, Version 1.4, STN: 10007-1.4-01, Research Report, Earth Sciences Division, Lawrence Berkeley National Laboratory, Berkeley, CA, 2000.

Wu, Y. S., C. F. Ahlers, P. Fraser, A. Simmons, and K. Pruess, Software Qualification of Selected TOUGH2 Modules, Research Report, Earth Sciences Division, Lawrence Berkeley National Laboratory, LBL-39490, UC-800, October, 1996.

Wu, Y. S. and K. Pruess, A Multiple-Porosity Method for Simulation of Naturally Fractured Petroleum Reservoirs, *SPE Reservoir Engineering*, 3, 327-336, 1988.

Zhang K. and YS Wu, Enhancing Scalability and Efficiency of the TOUGH2_MP for Linux Clusters, *Proceedings of TOUGH symposium 2006*, Berkeley, CA, 2006

Zhang, K., Wu, Y. S., and Pruess, K. User's guide for TOUGH2-MP-a massively parallel version of the TOUGH2 code. *Report LBNL-315E, Lawrence Berkeley National Laboratory,* Berkeley, CA, 2008

NOMENCLATURE

A_j Cross area of grid *j*, m^2

A_{ij} Cross area between grid *i* and *j*, m^2

C_R Heat conductivity, $W K^{-1} m^{-1}$

C_ϕ Pore compressibility, Pa^{-1}

c_s *S*pecific heat capacity of rock, $Jkg^{-1}{}^\circ C^{-1}$

c_t Bulk total compressibility, Pa^{-1}

D_T Thermal diffusivity, $m^2 s^{-1}$

E Young modulus, Pa

F Body force per area, Pa

F^κ Mass or energy flux terms due to advective processes, $W m^{-1}$

F_l *l*-direction body force (gravity), $Pa m^{-1}$

g Gravitational acceleration constant, $m s^{-2}$

h Total column height, m

h_β Specific enthalpy in phase β, $J kg^{-1}$

k Absolute permeability, m^2

k_T Heat conductivity of rock $Wm^{-1}{}^\circ C^{-1}$

K Bulk modulus, Pa

$k_{r\beta}$ Relative permeability to phase

M Biot's modulus, Pa

M^{κ} Accumulation terms of the components and energy, kg m^{-3}

M_n^{κ} Accumulation terms of the components and energy of grid n, kg m^{-3}

$\boldsymbol{n}$ Normal vector on surface element, dimensionless

t Time, s

T Temperature, ˚C or K

T_{ref} Reference temperature, ˚C or K

u_{β} Darcy velocity in phase, m s^{-1}

U_{β} Internal energy of phase per unit mass, J kg^{-1}

V_n Volume of the n^{th} grid cell, m^3

P Pressure. Pa

P_0 Incremental pressure due to load, Pa

P_c Capillary pressure. Pa

P_{c0} Reference capillary pressure. Pa

P_{β} Fluid pressure of phase , Pa

q^{κ} Source/sink terms for mass or energy components, kg $m^{-3}s^{-1}$

q_n^{κ} Source/sink terms for mass or energy components of grid *n*, kg $m^{-3}s^{-1}$

R_n^{κ} Residual of component κ for grid block n, kg s^{-1}

R_n^4 Residual of stress for grid block n, Pa m^{-2}

S Storage coefficient, Pa^{-1}

S_l Saturation of liquid phase, dimensionless

S_β Saturation of phase, dimensionless

T_b Constant temperature boundary, °C

T_i Initial temperature, °C

w Vertical displacement of the upper surface, m

x^t Primary variables at time t, pressure, temperature, air fraction, or stress

X_β^κ Mass fraction of component in fluid phase, dimensionless

V_b Bulk volume, m^3

z Distance along-column coordinate, m

Greek Letters

α Biot's coefficient, dimensionless

α_P Biot's coefficient, dimensionless

α_T Biot's coefficient, dimensionless

β Linear thermal expansion coefficient, $℃^{-1}$

μ_β Viscosity, Pa.s

μ_f Fluid viscosity, Pa.s

ϕ Porosity, dimensionless

λ Thermal conductivity, $W K^{-1} m^{-1}$

λ_s Lame's constant, Pa

ε_{ll} Strain components, l=x, y, z, dimensionless

ε_{ls} Strain components, ls=xy, yz, zx, dimensionless

ε_{il} Strain components, j=x, y, z, l=x, y, z, dimensionless

ε_v Volumetric strain, dimensionless

$\overline{\overline{\varepsilon}}$ Strain tensor, dimensionless

$\overline{u}$ Displacement vector, m

u_l Displacement component, l=x, y, z, m

ν Poisson's ratio of rock, dimensionless

ν_u Undrained Poisson's ratio of rock, dimensionless

σ' Effective stress, Pa

σ_{ex} External load per area at the top column, Pa

ρ_{tot} Density of rock, kg m^{-3}

ρ_R Density of rock grain. kg m^{-3}

ρ_β Density of phase, kg m^{-3}

Γ Perimeter of the cross-section, m

Γ_n Area of closed surface, m^2

APPENDIX A. POROSITY-STRESS CORELATION OPTIONS

IRPOPT=0 Constant porosity

IRPOPT=1 Equation 2.49 from Rutqvist et al. (2002b), usually used with IRKOPT =1

RCKPAR(1) = ϕ_r

RCKPAR(2) = a

IRPOPT= 2 Equation 2.52 from Rutqvist et al. (2002), usually used with IRKOPT=2

RCKPAR(1) = $b_{1,0}$

RCKPAR(2) = $\Delta b_{1,0}$

RCKPAR(3) = $b_{2,0}$

RCKPAR(4) = $\Delta b_{2,0}$

RCKPAR(5) = $b_{3,0}$

RCKPAR(6) = Δb_3

RCKPAR(7) = d

IRPOPT = 3 Equation 2.54 from McKee et al. (1988).

IRPOPT = 4 Slightly compressible rock and thermal expansion.

$$\phi = \phi_0 \left(1 + c_p \left(P - P_{ref}\right) + 3\beta\left(T - T_{ref}\right)\right)$$

c_p is pore compressibility and β is linear thermal expansion coefficient

RCKPAR(1) = P_{ref}

RCKPAR(2) = T_{ref}

IRPOPT = 5 Equation 2.61

APPENDIX B. PERMEABILITY-STRESS CORELATION OPTIONS

IRKOPT = 0 Constant permeability

IRKOPT = 1 Equation 2.49 from Rutqvist et al. (2002), usually used with IRPOPT =1

RCKPAR(5) = c

IRKOPT = 2 Equation 2.52 from Rutqvist et al. (2002), usually used with IRPOPT=2

RCKPAR(1) = $b_{1,0}$

RCKPAR(2) = $\Delta b_{1,0}$

RCKPAR(3) = $b_{2,0}$

RCKPAR(4) = $\Delta b_{2,0}$

RCKPAR(5) = $b_{3,0}$

RCKPAR(6) = Δb_3

RCKPAR(7) = d

IRKOPT = 3 Equation 2.55, Carman-Kozeny equation

IRKOPT = 4 Equation 2.56 from Ostensen (1986)

RCKPAR(5) = x-direction σ'^{*}

RCKPAR(6) = y-direction σ'^{*}

RCKPAR(7) = z-direction σ'^{*}

RCKPAR(8) = n

IRKOPT = 5 Equation 2.57, Verma and Pruess (1988)

RCKPAR(6) = k_r/k_0

RCKPAR(7) = ϕ_r/ϕ_0

RCKPAR(8) = n

APPENDIX C. RELATIVE PERMEABILITY FUNCTIONS

IRP = 1 Linear functions

k_{rl} increases linearly from 0 to 1 in the range

$RP(1) \le S_l \le RP(3)$;

k_{rg} increases linearly from 0 to 1 in the range

$RP(2) \le S_g \le RP(4)$

Restrictions: RP(3) > RP(1); RP(4) > RP(2).

IRP = 2 $k_{rl} = S_l^{**}RP(1)$

$k_{rg} = 1.$

IRP = 3 Corey's curves (1954)

$$k_{rl} = \hat{S}^4$$

$$k_{rg} = \frac{\left(1-\hat{S}\right)^2}{\left(1-\hat{S}^2\right)}$$

where $$\hat{S} = \frac{\left(S_l - S_{lr}\right)}{\left(1 - S_{lr} - S_{gr}\right)}$$

with $S_{lr} = RP(1)$; $S_{gr} = RP(2)$

Restrictions: RP(1) + RP(2) < 1

IRP = 4 Grant's curves (Grant, 1977)

$$k_{rl} = \hat{S}^4$$

$$k_{rg} = 1 - k_{rl}$$

where $\hat{S} = \dfrac{(S_l - S_{lr})}{(1 - S_{lr} - S_{gr})}$

with S_{lr} = RP(1); S_{gr} = RP(2)

Restrictions: RP(1) + RP(2) < 1

IRP = 5 All phases perfectly mobile

$k_{rg} = k_{rl} = 1$ for all saturations; no parameters

IRP = 6 Functions of Fatt and Klikoff (1959)

$$k_{rl} = (S^*)^3$$

$$k_{rg} = (1 - S^*)^3$$

where $S^* = \dfrac{(S_l - S_{lr})}{(1 - S_{lr})}$

with S_{lr} = RP(1).

Restriction: RP(1) < 1.

IRP = 7 van Genuchten-Mualem model (Mualem, 1976; van Genuchten, 1980)

$$k_{rl} = \begin{cases} \sqrt{S^*}\left\{1 - \left(1 - [S^*]^{1/\lambda}\right)^{\lambda}\right\}^2 & if S_l < S_{ls} \\ 1 & if S_l \geq S_{ls} \end{cases}$$

Gas relative permeability can be chosen as one of the following three forms, the second of which is due to Corey (1954)

$$k_{rg} = \begin{cases} 1 - k_{rl} \ if \ S_{gr} = 0 \ and \ RP(4) = RP(5) = 0 \\ \left(1 - \hat{S}\right)^2 \left(1 - \hat{S}^2\right) \ if \ S_{gr} > 0 \ and \ RP(4) > 0 \ and \ RP(5) = 0 \\ (1 - S^*)^2 (1 - S^{*\frac{2+\gamma}{\gamma}}, r = \dfrac{\lambda}{1-\lambda} \ if \ S_{gr} = 0 \ and \ RP(5) > 0 \end{cases}$$

subject to the restriction $0 \le k_{rl}, k_{rg} \le 1$

Here, $S^* = \dfrac{\left(S_l - S_{lr}\right)}{\left(S_{ls} - S_{lr}\right)}$, $\hat{S} = \dfrac{\left(S_l - S_{lr}\right)}{\left(1 - S_{lr} - S_{gr}\right)}$

Parameters: RP(1) = λ

RP(2) = S_{lr}

RP(3) = S_{ls}

RP(4) = S_{gr}

RP(5) = switching parameter

Notation: Parameter λ is m in van Genuchten's notation, with m = 1 - 1/n;
Parameter n is often written as β.

IRP = 8 Function of Verma et al. (1985)

$$k_{rl} = \hat{S}^3$$

$$k_{rg} = A + B\hat{S} + C\hat{S}^2$$

where $$\hat{S} = \frac{\left(S_l - S_{lr}\right)}{\left(S_{ls} - S_{lr}\right)}$$

Parameters as measured by Verma et al. (1985) for steam-water flow in an unconsolidated sand:

S_{lr} = RP(1) = 0.2

S_{ls} = RP(2) = 0.895

A = RP(3) = 1.259

B = RP(4) = -1.7615

C = RP(5) = 0.5089

IRP = 9, 10 ECM function (Pruess and Tsang, 1994)

These two options are the original effective continuum model (ECM), which use a threshold liquid saturation concept, defined as

$$S_{th} = \phi_m/(\phi_m + \phi_f)$$

where both ϕ_m and ϕ_f are void fractions or porosities for matrix and fractures respectively, defined in terms of the bulk volume of formation.

The only difference between IRP = 9 and = 10 is that option of IRP = 9 handles isotropic permeability cases and IRP = 10 handles anisotropic permeability scenarios. In general, the two ECM relative permeability functions need (1) matrix continuum and fracture continuum permeability and (2) a special capillary function (defined in ICP = 8 in Appendix D).

It is assumed that PER(i) and PERF(i), input in ROCKS, are absolute continuum permeability of matrix and fractures (i = 1, 2, 3), respectively, along the three principal axes or directions, as defined in CONNE. See the following table for parameter definition.

Table C.1. Definition of parameters for with ECM functions for IRP=10

IRP=	9	for ECM option in isotropic fracture systems.
IRP=	10	for ECM option in anisotropic fracture systems.
RP(1)=	M_m	of van Genuchten's function for matrix.
RP(2)=	S_{lr}	residual liquid saturation in matrix.
RP(3)=	M_f	of van Genuchten's function for fractures.
RP(4)=	S_{lr}	residual liquid saturation in fractures.
RP(5)=	k_f/k_m	ratio of fracture and matrix permeabilities, used only for isotropic properties of fracture-matrix systems.
RP(6)=	S_{th}	threshold liquid saturation.
RP(7)=	1- ϕ_f	f is fracture porosity.

IRP = 11 Generalized ECM function (Wu et al. 1996; Wu 2000)

This is a generalized ECM formulation, which relies only on thermodynamic equilibrium assumption for fracture and matrix systems (Wu, 2000). The generalized ECM relative permeability functions need (1) matrix continuum and fracture continuum permeability and (2) a special capillary function (defined in ICP = 9 in Appendix D). It is assumed that PER(i) and PERF(i), input in ROCKS, are absolute continuum permeability of matrix and fractures (i = 1, 2, 3), respectively, along the three principal axes or directions, as defined in CONNE. The following table defines the parameters for the ECM relative permeability function.

Table C.2. Definition of parameters for with ECM functions for IPR =11

IRP=	11	For generalized ECM option.
RP(1)=	M_m	Of van Genuchten's function for matrix.
RP(2)=	S_{lr}	Residual liquid saturation in matrix.
RP(3)=	M_f	Of van Genuchten's function for fractures.
RP(4)=	Slr	Residual liquid saturation in fractures.
RP(5)=	> 0 krg = 1.0 - krl <0 using Corey's function for krg.	
RP(6)=	S_{gr}	Residual gas saturation in matrix.
RP(7)=	ϕ_f	Fracture continuum porosity.

IRP = 12 Generalized Power Law

$$k_{rl} = \left(\frac{S_l - S_{l,min}}{S_{l,max-S_{l,min}}}\right)^{n_1}$$

$$k_{rg} = \left(\frac{S_g - S_{g,min}}{S_{g,max-S_{g,min}}}\right)^{n_g}$$

with $S_{l,min}$ = RP(1), Sl,max = RP(2), n1 =RP(3), Sg,min=RP(4), Sg,max = RP(5), ng=RP(6)

APPENDIX D. CAPILLARY PRESSURE FUNCTIONS

ICP = 1 Linear function

$$P_{cap} = \begin{cases} -CP(1) & for\ S_l \le CP(2) \\ 0 & for\ S_l \le CP(2) \\ -CP(1)\frac{CP(3)-S_L}{CP(3)-CP(2)} & for\ CP(2) < S_l < CP(3) \end{cases}$$

Restriction: CP(3) > CP(2).

ICP = 2 Function of Pickens et al. (1979)

$$P_{cap} = -P_0 \left\{ ln \left[\frac{A}{B} \left(1 + \sqrt{1 - \frac{B^2}{A^2}} \right) \right] \right\}^{\frac{1}{x}}$$

with

$A = (1 + S_l/S_{l0})(S_{l0} - S_{lr})/(S_{l0} + S_{lr})$

$B = 1 - S_l/S_{l0}$

where

P_0 = CP(1) S_{lr} = CP(2) S_{l0} = CP(3) x = CP(4)

Restrictions: $0 < CP(2) < 1 \leq CP(3)$; $CP(4) \neq 0$

ICP = 3 TRUST capillary pressure (Narasimhan et al., 1978)

$$P_{cap} = \begin{cases} -P_e - P_0 \left(\frac{1 - S_l}{S_l - S_{lr}} \right)^{\frac{1}{\eta}} & for\ S_l < 1 \\ 0 & for\ S_l < 1 \end{cases}$$

where

P_0 = CP(1) S_{lr} = CP(2) η = CP(3) P_e = CP(4)

Restrictions: $CP(2) \geq 0$; $CP(3) \neq 0$

ICP = 4 Milly's function (Milly, 1982)

$$P_{cap} = -97.783 \times 10^{A}$$

With

$$A = 2.26 \left(\frac{0.371}{S_l - S_{lr}} - 1 \right)^{1/4}$$

where S_{lr} = CP(1)

Restriction: $CP(1) \geq 0$.

ICP = 6 Leverett's function (Leverett, 1941; Udell and Fitch, 1985)

$$P_{cap} = -P_0 \sigma(T) f(S_l)$$

with

$\sigma(T)$ - surface tension of water (supplied internally in TOUGH2-EGS-MP)

$$f(S_l) = 1.417 (1 - S^*) - 2.120 (1 - S^*)^2 + 1.263 (1 - S^*)^3$$

where

$$S^* = (S_l - S_{lr})/(1 - S_{lr})$$

Parameters: $P_0 = CP(1)$ $S_{lr} = CP(2)$

Restriction: $0 \leq CP(2) < 1$

ICP = 7 van Genuchten function (van Genuchten, 1980)

$$P_{cap} = -P_0 \left[\left(S^* \right)^{-\frac{1}{\lambda}} - 1 \right]^{1-\lambda}$$

subject to the restriction

$$-P_{\max} \leq P_{cap} \leq 0$$

Here,

$$S^* = \left(S_l - S_{lr} \right) / \left(S_{ls} - S_{lr} \right)$$

Parameters: $CP(1) = \lambda = 1 - 1/n$

$CP(2) = S_{lr}$ (should be chosen smaller than the corresponding parameter in the relative permeability function; see note below.)

$CP(3) = 1/P_0$

$CP(4) = P_{max}$

$CP(5) = S_{ls}$

$CP(6) = \gamma$

Notation: Parameter λ is m in van Genuchten's notation, with $m = 1 - 1/n$; parameter n is often written as β.

Note on parameter choices: In van Genuchten's derivation (1980), the parameter S_{lr} for irreducible water saturation is the same in the relative permeability and capillary pressure functions. As a consequence, for $S_l \rightarrow S_{lr}$ we have $k_{rl} \rightarrow 0$ and $P_{cap} \rightarrow -\infty$, which is unphysical because it implies that the radii of capillary menisci go to zero as liquid phase is becoming immobile (discontinuous). In reality, no special capillary pressure effects are expected when liquid phase becomes discontinuous. Accordingly, we recommend to always choose a smaller S_{lr} for the capillary pressure as compared to the relative permeability function.

ICP = 8 ECM function (Pruess and Tsang, 1994)

This ECM capillary function should be used with Option IRP=9 or 10 of ECM relative permeability functions. Table D.1 lists the definition of the related parameters.

Table D.1. Definition of parameters for ICP=8 with ECM capillary pressure functions

ICP=	8	For effective continuum approach option.
CP(1)=	M	Of van Genuchten's function for matrix.
CP(3)=	S_{lr}	Residual liquid saturation in matrix.
CP(2)=	α	With units Pa^{-1}, van Genuchten's parameter for matrix.
CP(4)=	P_{cmax}	Maximum capillary pressure allowed.
CP(5)=	S_s	Satiated saturation in matrix.

CP(6)=	S_{th}	Threshold liquid saturation.
CP(7)=	δ	Parameter used to considering air entry effects.

ICP = 9 Generalized ECM function (Wu et al. 1996, Wu 2000)

The generalized ECM capillary function should be used only with Option IRP=11 of generalized ECM relative permeability functions. Table D.2 lists the definition of the related parameters.

Table D.2. Definition of parameters for ICP=9 with ECM capillary pressure functions

ICP=	9	For ECM option.
CP(1)=	M_m	Of van Genuchten's m for matrix.
CP(3)=	S_{lr}	Residual liquid saturation in matrix.
CP(2)=	α_m	With units Pa^{-1}, van Genuchten's parameter for matrix.
CP(4)=	P_{cmax}	Maximum capillary pressure allowed.
CP(5)=	S_{lr}	Residual liquid saturation in fractures.
CP(6)=	M_f	Of van Genuchten's m for fractures.
CP(7)=	α_f	With units Pa^{-1}, van Genuchten's parameter for fractures.